INVESTIGATION OF COLD ATMOSPHERIC PLASMA FOR WOUND CARE

By

ALVIN DINH NGO

Bachelor of Science in Aerospace Engineering
University of Oklahoma
Norman, Oklahoma
2015

Master of Science in Mechanical and Aerospace Engineering
Oklahoma State University
Stillwater, Oklahoma
2017

Submitted to the Faculty of the
Graduate College of the
Oklahoma State University
in partial fulfillment of
the requirements for
the Degree of
DOCTOR OF PHILOSOPHY
May, 2023

INVESTIGATION OF COLD ATMOSPHERIC PLASMA FOR WOUND CARE

Dissertation Approved:

Dr. Jamey D. Jacob

Dissertation Advisor

Dr. Arvind Santhanakrishnan

Dr. Brian Elbing

Dr. Akhilesh Ramachandran

ACKNOWLEDGMENTS

First and foremost, I would like to thank my parents, Nancy and Man. They were always very patient and accepting of everything I wanted to pursue. They have been and I'm sure will always be my number one enablers. Next I'd like to thank my dear sister Cynthia. She is single-handedly responsible for keeping me fed with delicious food when I visit home on weekends and led the charge for anti-stress activities.

Now I would like to thank my entire PhD committee: Dr. Jacob, Dr. Elbing, Dr. S, and Dr. Ramachandran. They put up with my last minute antics and gave valuable feedback on a very multidisciplinary and abstract topic. I'd like to extend a special thanks to Dr. Jacob for going above and beyond in guiding me throughout my 2 years doing my masters and 5+ years doing my PhD. He has given me significant insight into being an awesome leader, teacher, researcher, and engineer. I'd also like to extend a special thanks to Dr. Ramachandran for welcoming me into his lab and going above and beyond by staying late nights and working with me to reach deadlines.

I'd like to give additional thanks to four more professors: Dr. Ma, Dr. Madihally, Dr. Rizzi and Dr. Rudd. They provided invaluable consultation on subjects that I knew little about. They happily welcomed me into their labs and provided resources without any promise or return.

Next I'd like to thank a mentor and most importantly a friend, Kedar. The sheer breadth of knowledge this man has astounds me and he is not shy about sharing his genius. He guided me since day 1 of learning about plasma and is essentially the

Acknowledgments reflect the views of the author and are not endorsed by committee members or Oklahoma State University.

reason I stayed within this field. His passion for the subject has infected me and I'm glad it has. Fast forward 7 years and he is a close friend who I foresee having bonds with for decades to come.

There are three staff members at OSU that have given me a significant amount of their time for advice through the slog of various paperwork. Thank you Dr. Fore, Dr. Powers, and Ms. Motte. They notified me of amazing opportunities and always had my success in mind. Additionally, I'd like to thank 2 fellow students that I've met during my time here at OSU, Sai and Brittany. In fields that I would've been clueless without them, they not only guided me but worked hand-in-hand to produce valuable results. They are both amazing people that will go and do amazing things.

I'd like to extend a thanks to the HAL group under Dr. Jacob, USRI, IBMF (formerly NIMFABB), and OADDL for allowing me to utilize their resources as well as interact with their members. They have expanded my horizons in several fields and gave me the opportunity to meet some amazing people.

Finally, I'd like to thank the friends that have stuck by me throughout the rough times in my life. They helped me de-stress through eating delicious food, gaming late at night, traveling across the world, and simply just chatting. Thank you: Chris, Spenlee, Karami, Jordan, Johnson, Teddy and Sandro.

Acknowledgments reflect the views of the author and are not endorsed by committee members or Oklahoma State University.

Name: Alvin Dinh Ngo

Date of Degree: May 2023

Title of Study: INVESTIGATION OF COLD ATMOSPHERIC PLASMA FOR WOUND CARE

Major Field: MECHANICAL AND AEROSPACE ENGINEERING

Abstract:

Throughout the last decade, cold atmospheric plasma (CAP) has gained significant traction for aerospace and biomedical applications. The viability of CAP as a means for sterilization, and accordingly wound care, has made strides. There is a critical need for elucidation of the foundational mechanisms behind how CAP interacts with various cell types and surfaces to determine the pros, cons, and long-term viability of the technology for wound healing. In this study, a wound healing apparatus utilizing surface discharge actuators was designed and fabricated to perform laboratory testing. *Pseudomonas aeruginosa (P. aeruginosa)* and Methicillin-resistant *Staphylococcus aureus* (MRSA) were treated with CAP on plastic, glass, stainless steel, and aluminum and observed for differences in bacterial inactivation (BI) efficacy. BI testing resulted in stainless steel being more effective as a substrate for CAP treatment based on higher average absolute destruction of bacteria colonies. Two short studies on equine blood and mice skin were performed as a precursor and foundation for future studies that involve plasma x blood and plasma x skin interactions. Additionally, particle image velocimetry (PIV) was used to observe the flow field generated by the device for characterization and optimization of the flow. Several configurations and geometries, such as cylinders, threads, and meshes, were tested and observed for improvements in bacterial inactivation efficacy and mixing. The geometry and configuration of the plasma actuators were seen to have quantitative impacts in terms of BI efficacy and also showed high levels of form factor customizability of this technology. This study provides a wide breadth of preliminary research to lay the foundation for suggestions and recommendations for future research in CAP based wound care.

NOMENCLATURE

AC-SDBD – alternating current surface dielectric barrier discharge

ANOVA – analysis of variance

APPJ - atmospheric pressure plasma jet

BI – bacterial inactivation

CAD – computer-aided design

CA-MRSA – community-associated methicillin-resistant staphylococcus aureus

CAP – cold atmospheric plasma

CFU - colony forming unit

CLL - chronic lymphocytic leukemia

DBD – dielectric barrier discharge

DC – direct current

FTLE – finite-time lyapunov exponents

HBOT – hyperbaric oxygen therapy

HHPD – handheld plasma device

IACUC – institutional animal care and use committee

LCS – lagrangian coherent structures

MIC - minimum inhibitory concentration

MRSA – methicillin-resistant staphylococcus aureus

NCI – national cancer institute

NPWT – negative pressure wound therapy

NSF – national science foundation

OSU – oklahoma state university

PGS - plasma generated species

PIV - particle image velocimetry

PMMA – polymethyl methacrylate

PTFE – polytetrafluoroethylene

PVC – polyvinylchloride

PWH - plasma wound healing

RBC – red blood cell

RF – radiofrequency

RH - relative humidity

RMS – root mean squared

RNS - reactive nitrogen species

RONS - reactive oxygen and nitrogen species

ROS - reactive oxygen species

SAS – statistical analysis system

SDBD - surface dielectric barrier discharge

SE - standard error

SEP – solar electric propulsion

sUAS – small unmanned aerial system

TA – toxin-antitoxin

TEG – thromboelastography

UV – ultraviolet

VDBD – volumetric dielectric barrier discharge

VOC – volatile organic compound

WBC – white blood cell

ZNMF – zero net mass flux

TABLE OF CONTENTS

LIST OF TABLES

LIST OF FIGURES

CHAPTER I

INTRODUCTION

Wounds, medically defined by the NCI dictionary as a break in skin or body tissues caused by injury or surgical incision, are a common occurrence that range from kitchen cuts and simple surgeries to extreme physical abrasions and lacerations. There are several well-known and effective therapies for accelerating wound healing such as hyperbaric oxygen therapy (HBOT) and negative pressure wound therapy (NPWT). Unfortunately, the current state of the art in advanced therapies for wound healing suffers from being expensive and painful for the user, requiring large machinery, or necessitating a long treatment period (on the order of tens of minutes to hours) [168, 44]. For example, NPWT has concerns of causing excessive bleeding at the treatment site as well as pain for the patient [66, 92]. In a different example, a chronic wound developed due to pressure ulcers on bedridden geriatric patients is not easily treatable with the best solution most likely being preventative. Then there are problems with infected wounds that house chemically resistant bacteria that cause the wound to not reach the proper conditions to begin naturally wound healing and becomes a chronic wound [132]. Most advanced therapeutics are not used unless the problem is severe, and if the problem is severe in a specific way, the therapeutic runs into issues dealing with the problem. A more in-depth review of treatments and therapies for wound healing can be found elsewhere [166, 110, 58]. The main motivation behind this paper is a critical need for an inexpensive, non-invasive, and rapid treatment for the acceleration of wound healing to address the issues above.

1.1 Motivation

The motivation behind this wound healing study was heavily guided by a customer needs basis. In three separate interview focused studies funded by the National Science Foundation (NSF), relevant customer segments and important value propositions were determined for the interest of the design and development of a wound care device.

In Spring of 2019, 30 in-person interviews were performed on individuals consisting of surgeons, dentists, medical students, graduate students in veterinary medicine, and veterinary medicine professors to ascertain if there was any current real-world value in pursuing a next generation wound care device. The focus at this stage was to cast a wide net on potential consumers of a wound care device. The customer segments at this point were veterinary hospitals/clinics, human hospitals/clinics, dental offices/clinics, 3rd world applications, military applications, and surgeons. These interviews shed light on several important factors: 1. The ability to treat chemically resistant infections was desired but not currently critical, 2. Re-infection rates connected to surgeries were on the rise, and 3. The current process of reducing infections in specifically a thoracic surgical operation was to irrigate to dilute the bacteria down from a harmful load because the process is rapid and works reasonably well. Several surgeons mentioned that the concept of a cold plasma based wound healing device was a 'silver bullet' that needed to be more heavily researched before they bought into it. The main concern from both medical professionals and veterinary professionals stemmed from the notion that exposure of subjects to free radicals could harm the "good" cells of a subject or even induce cancer. The extreme end of utilizing the plasma-generated species of the wound care device over a long period of time would lead to decontamination and sterilization of the treated surface as seen by other studies [121]. Additionally, a major takeaway was that the human medicine market had several advanced therapeutics being used for wound healing purposes while the veterinary medicine market had very few. Veterinary professionals seemed more open

to an advanced therapeutic being introduced likely due to less stringent regulations. Thus, the decision was made to delve deeper into the veterinary sector.

In Fall of 2019, an entrepreneurial team was put together that included four business/marketing graduate students and two engineering graduate students to determine the acceptability of a wound care device in the current veterinary market. If the device was deemed feasible, the ending result would be a business plan detailing the devices motivation and finances. An additional 60 interviews were done with professionals in both the human medicine and veterinary medicine sectors as well as technical help from related subject professors at OSU. The team narrowed down the customer segment to specifically veterinarians and veterinary surgeons. Like the human medicine side, post-operative infections in dogs and cats were found to also be rising. In 2012, infection rates were at about 4.5%. As of 2019, this number increased to 8.7% [39]. Veterinary professionals valued the idea of lowering infection rates and accelerating recovery especially with a non-invasive, handheld, and low-cost device while also adding on an additional revenue stream for themselves (based on the developed business model). Form factors were discussed with interviewees to aid in the future design and fabrication of the wound care device. Major problems at the end of this study was the lack of a beachhead market and vague price estimations for a wound care device. Further design considerations from potential customers were obtained as well. The breakdown of interviews by customer segments from the 1st and 2nd phases are seen in Fig. I.1.

The final study in Spring of 2021 was a deep dive of 101 interviews specifically focused on individuals that work with, care for, or own animals as seen in Fig. I.2. The interviews were specifically designed to veil the wound care device itself and to only search for the 'need' that was wound care in veterinary medicine. These interviews ranged from certified veterinarians running clinics and pet owners to veterinary surgeons at teaching hospitals and ranch owners. The best fit for the cold plasma based

wound care device was found to be chronic wound management for small animals and surface leg wounds on non-sport equine. Rather than for small injuries and basic checkups, a significant amount of money was spent on a regular basis at veterinary clinics by pet owners for chronic wounds on small animals. Dr. Jeff Studer, veterinary medical teaching hospital director at OSU, says that "Wound management in small animal management is an expensive endeavor. All the highest bills that walk out are chronic wound cases. These cases are upwards of $20,000 because of serial anesthesia episodes." Equine are also especially susceptible to exacerbated damage from leg wounds. Dr. Daniel Burba, professor of equine surgery at OSU, mentions "Horse legs take forever to heal. The skin there is like a sock. Get me something that produces new skin cells. That'll save a lot of time and money." Additionally, Dr. Todd Holbrook, professor of equine internal medicine at OSU, states in reference to horse legs "Even as they're healing, they're prone to proud flesh. If you can control the granulation tissue growth, that would be groundbreaking." These accounts helped spur specific research ideas on CAP effects on granulation tissue growth and skin cells in general. Later in the study, specific types of wound patients were interviewed, e.g., burn, geriatric, and diabetic patients, as well as their care takers or nurses. Several patients discussed their dissatisfaction with current advanced therapeutics while nurses discussed the problems with bedridden patients and pressure ulcers. Chronic wounds are a large problem in hospitals simply because most patients do not have the luxury of moving about. They surmise that a technology that could speed up the recovery time of wounds could be something worth pursuing.

Some interesting additional finds from this study was the interest from show animal owners, e.g., zoos, aquariums, and fairs. Several studies have confirmed cold plasma's efficacy to inhibit scar formation [105, 17, 163]. Scars on show animals generally hold stigmas representing animal abuse and mistreatment even if the wounds and scars on these animals are from natural events like playing with each other. Show

animal owners value being able to aid these animals in healing properly so that scars are minimized to mitigate false rumors from spreading. Livestock owners, specifically cows, pigs, and sheep, usually did not require or even consider using any type of special wound treatment due to the resilience and infrequent injury of these animals. Sports animals, such as racehorses, that have been wounded are not commonly reintroduced back into competition after an injury and thus would not have a high demand for advanced therapeutics.

In summary, the three-phase interview focused study on whether or not there was a need for a wound care device showed there is significant interest in not only the veterinary medicine sector but also the human medicine sector. There are reservations specifically dealing with interaction of CAP with the 'good cells' vs 'bad cells' as well as possibly introducing cancerous elements. Though the cancerous elements are outside the scope of this specific study, the goals and objectives of the overall study is defined by a desire to provide a comfortable breadth of starting points for future experiments as well as following up on several already completed studies. To properly design a CAP based wound care device, user considerations were taken into account along with laboratory and bench testing ease-of-use. A comparison of advanced therapeutics mentioned in the introduction with estimated parameters for CAP based wound healing is displayed in Fig. I.3.

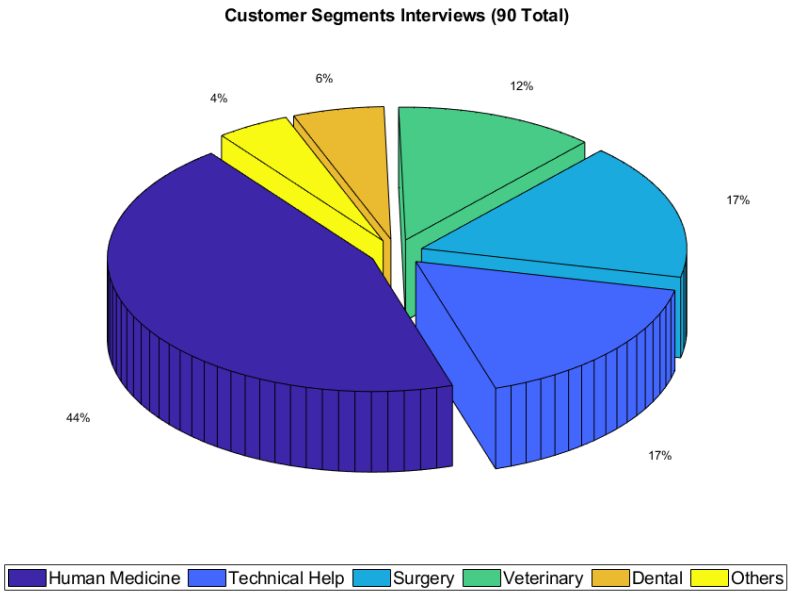

Figure I.1: Interviews categorized by customer segments for phase 1 and 2 of the interview study. 'Others' includes business related individuals.

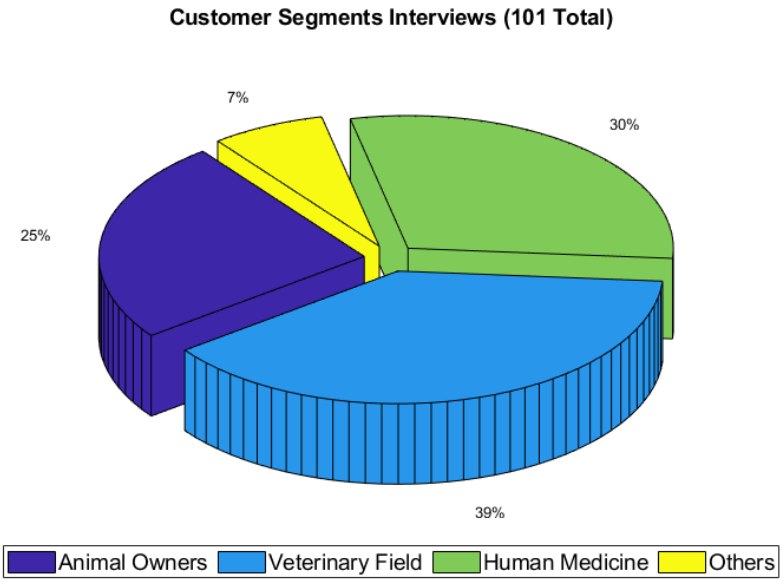

Figure I.2: Interviews categorized by customer segments for phase 3 of the interview study. 'Others' includes business related individuals.

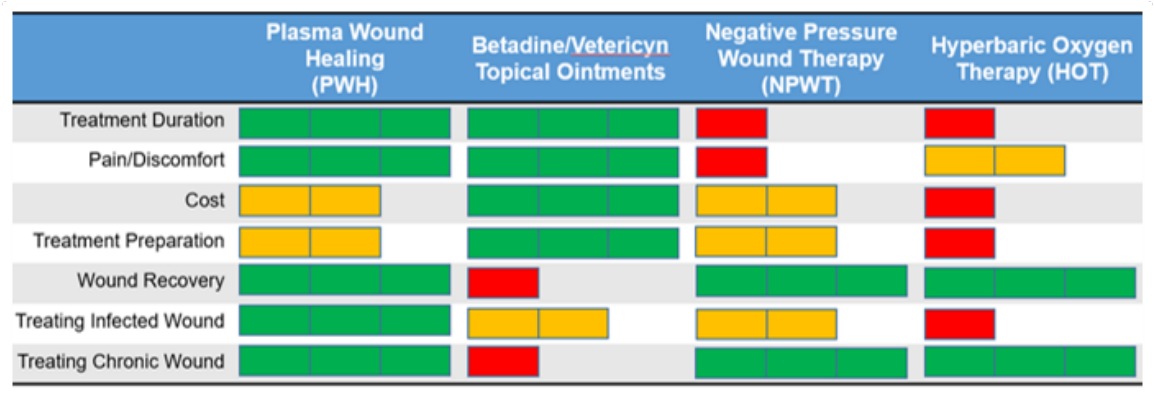

Figure I.3: Comparison of current advanced therapeutics and plasma wound healing (PWH) across several valuable parameters for users. Values are relative to one another and PWH outcomes are estimations.

1.2 Goals and Objectives

What separates this work from previous works is the usage of an open AC-SDBD system specifically for wound healing capabilities. The highest level goal of this study is to determine whether surface discharge is suitable for wound healing. This goal is understandably not achievable in one PhD Dissertation. Rather, the main goal of this study is to elucidate some of the mechanisms necessary for cold plasma wound healing and investigate SDBD actuators for plasma generation and application as a wound healing therapeutic. These are both broad goals that are detailed through several distinct objectives below:

- Investigation of CAP interactions with commonly used inanimate substrates
- Observation of CAP interactions with organic surfaces such as skin
- Observation of CAP interactions with blood
- Evaluation of feasible geometries and configuration for an SDBD based wound care device

Meeting these objectives will provide an adequate entryway into other critical studies for utilizing surface discharge for wound healing that will be expanded on in Chapter V. Three objectives use bacterial inactivation as a primary tool to evaluate interactions and one objective uses flow visualization to characterize configurations. These objectives were developed using previous related projects with surface discharge and have developed into several publications (printed and in-review) in plasma specific journals, conferences, and papers.

1.3 Outline

This dissertation has been organized into five chapters. Chapter I provides an introduction that begins with the motivation behind the study and segues into the high level goals, specific achievable goals, and objectives of the individual projects. Chapter II provides a comprehensive background for the reader to understand the reasoning behind the upcoming experimental designs through an comprehensive review of cold plasma, SDBD, wound healing, amongst other related topics. Chapters III and IV cover a wide range of specific topics pertaining to the design, testing, and improvement of an SDBD system for wound healing. These chapters are based on written articles that have been either published, submitted, or are in preparation for submission.

Chapter III leads with the biological testing of various inanimate substrates with *P. aeruginosa* and MRSA. The latter portion of Chapter III delves into a mixture of biological specimen samples, specifically mice skin, as well as the first portion of a plasma-blood interaction experiment. This chapter will lay a strong foundation for future studies towards whether surface discharge is applicable to wound healing.

Chapter IV exhibits the experimentation of geometries and configurations for a feasible wound healing device form factor. Cylinders, threads, and meshes, their respective flow fields, and some bacterial inactivation efficacy is discussed here. The chapter ends with a short mixing analysis.

Chapter V provides the overall conclusion of the findings of the previous chapters and discusses paths moving forward as well as recommendations and suggestions for future work.

CHAPTER II

Background

2.1 Introduction

Chronologically, plasma was the first state of matter. As the Universe was created through the well-known phenomenon known as 'the Big Bang', the first dregs of existence as we know it began in the form of plasma due to everything being very hot. Eventually things started to cool down and gases, liquids, and eventually solids began to form [37]. As fundamental to nature as plasma is, the average college campus habitué does not in fact know much if anything at all about plasma, distinctly described as plasma (physics). In an informal survey of approximately 100 on-campus students at Oklahoma State University (OSU) in 2017, only 7 people were able to give a single fact about plasma with 3 of them knowing significantly more. Plasma is usually not included in fundamental physics curriculum, yet it exists throughout everyone's daily life by making up most of the Sun, being created through lightning, and even illuminating rooms as fluorescent light bulbs. This seems to be changing as a similar survey at OSU in 2022 yielded 20 individuals that knew of either a fact about plasma or a device that utilizes plasma. Knowledge of plasma is growing rapidly as well as its applications. As the feasibility of cold plasma technology becomes more researched, so does the opportunities for additional research. Nowadays, plasma is mentioned in school curriculum as the fourth state of matter and there are even specific programs dedicated to nurturing its proliferation.

The growth of plasma applications, specifically non-thermal plasma, has been

noticeable in the aerospace and biomedical industry. Though the idea itself is not novel, being initiated as early as the 1950s, biomedical applications have been gaining more traction especially within the last two decades [43]. Biomedical technology is on the rise for not only improved efficiency and efficacy, but rather novel and radical changes that can treat and cure things previously not remediable. Plasma medicine itself has exploded in potentially feasible applications within the last decade and have contenders for sterilization, cancer applications, pharmacology, and plasma-aided wound healing [88].

2.2 Plasma Characteristics

2.2.1 Degree of Ionization

The first design decision in this work is which overarching plasma type to utilize for intended research applications. Plasma is commonly separated into two schools: hot (thermal) plasma and cold (non-thermal) plasma. There are also known ultra-cold plasma that blur the lines further, but these are pushing the limits of physics and require techniques like photoionizing laser-cooled atoms near their ionization thresholds. These will not be discussed here but can be referred to in *Killian et al* [77]. An important means of distinguishing between plasma types is their degree of ionization with the base definition of ionization being at least one electron is not bound to an atom or molecule. In general, phases of matter are characterized by the expression of molecular motion, usually through heat. In the case of plasma, heat is expressed by separate electron and ion motions [37]. Gases begin to disobey the kinetic theory of gas and functions as plasma once a specific threshold of ionization is reached, and the phase change officially occurs, which varies significantly from weakly ionized plasma to completely ionized plasma [43]. Rather than the usual Brownian motion seen in gases, the energized particles are more or less heavily affected by coulomb forces. It has been shown that unique phenomena occur even at low ionization states. A gas can achieve electrical conductivity equal to that of a fully ionized gas with as little as 1% ionization [65]. From this we can see the generalization that plasma is fundamentally an ionized gas.

2.2.2 Methods of Generating Plasma

With the advancement of laboratory technology and techniques comes many different unnatural or man-made ways to generate plasma. The main principle behind generating plasma is the Townsend discharge/avalanche mechanism. In a system with a significant electric field and a source of free electrons, when the free electrons are accelerated by an electric field, they collide with gas molecules. These molecules in turn release an electron that accelerates and follow the same path as their counterparts. A multiplicative avalanche occurs due to the chain reaction. This allows for electric conduction through the gas [170]. The number of collisions due to electrons grows exponentially at first and eventually reaches the physical upper limit pf the ionization avalanche known as the Raether limit.

In the above system a cathode and anode are assumed to generate the electric field. The quasi-constant voltage between these electrodes is equal to the breakdown voltage required to achieve the self-sustaining avalanche. The breakdown voltage is defined as the minimum voltage required to cause an insulator to experience electrical breakdown thus becoming conductive [103]. Plasma is characterized in many different ways by distinguishing between thermal/non-thermal discharges, high/low pressure discharges, electrode/electrodeless discharges, self-sustained/non-self-sustained discharges, and even DC/non-DC discharges [43]. In general however, an important factor in feasible applications for industrial usage is a manageable operating temperature. With plasma, the electron temperature may be high (10,000-100,000K), but the heavy particle temperature could be as low as 300-1000K [151].

Below is a non-comprehensive list of commonly used means to generate plasma each with their own popular applications.

Corona Discharge: Corona discharge is a type of atmospheric-pressure cold discharge that is characterized by its weak luminous appearance on sharp points, edges, and thin wires. This discharge is always non-uniform with the electrons moving from one electrode to another due to sufficiently high energy levels due to the surrounding electric field. Ionization of surrounding gas molecules and atoms occur due to the electron acceleration and pass through [131]. Typically this type of discharge operates on the order of kV as well as higher pressures (atmospheric or higher). Corona discharge has several applications in for sterilization and volatile organic compound (VOC) destruction [173, 146].

Glow Discharge: Glow discharge is the most investigated and thus best understood non-thermal plasma generation method. Glow discharge operates at a low gas pressure and is named because of the illumination it gives off. Neon and fluorescent lamps as well as plasma-screen televisions all use glow discharge to function. It is commonly used for analytical chemistry, spectroscopy, and surface modification (sputtering) [32, 18, 69].

Microwave Discharge: Microwave discharge is characterized by a centimeter-range electromagnetic waves interacting with plasma. In general these systems will be high pressure and optic based. Though usually high powered, there is a low-power microwave microplasma version that utilizes argon and air discharges for bio-MEMS sterilization and small-scale biomaterial processing [25, 139, 28].

Radiofrequency Discharge: RF discharges are commonly used in tissue engineering and electronics due to the high-precision surface treatment that it provides [12, 8]. RF discharges are characterized as strongly non-equilibrium and cold at low pressures. The upper and lower limits of RF frequencies are due to system

sized wavelengths and frequencies of ionization and ion transfer. Around 13.6 MHz is a common frequency in industrial use [43].

Arc Discharge: Arc discharges are characterized by high gas temperatures (on the order of 10,000 K) and in general are self-sustaining DC discharges. These high temperatures are associated with medical applications like surgical cauterization and ablation [85, 34] however recent studies have shown applications towards improving germination and combustion assistance [133, 61]. There are many different types of arc discharges with nuances that may be applied to specific applications, e.g. vacuum arcs, high-pressure arc discharges (0.1-0.5 atm), low-pressure arc discharges [43].

Silent Discharge: Sometimes considered a combination of glow and corona discharge, the silent discharge is named so because it was created by attempting to create a corona discharge that avoids spark formation (which generally also includes local shock waves and noise) [43]. Also named the dielectric barrier discharge, this type of plasma generation is the main subject of this work. This discharge is characterized by a dielectric barrier that stops current and spark formation. Initially thought of to preclude DC operation because of the usual operating frequencies, 0.05-500 kHz, that has been circumvented as seen in recent works [36, 148]. Silent discharge is widely used for ozone generation as well as other biological/medical applications [176, 121, 13, 45, 95].

2.2.3 Paschen's Law

For this work in particular, there is a focus on cold plasma generation techniques. Cold plasma is a partially ionized gas comprising of electrons, ions, photons, and reactive neutrals [145]. Friedrich Paschen discovered an equation in 1889 that is commonly used in discussions of breakdown voltage to start discharges and generate plasma. This equation is known as Paschen's law, eq. 2.2.1, where V_B is the breakdown voltage, p is the pressure, d is the electrode gap distance, A is the saturation ionization in the gas, B is a relationship between excitation and ionization energies, and γ_{se} is the secondary-electron-emission coefficient [94].

$$V_B = \frac{Bpd}{\ln(Apd) - \ln[\ln(1 + \frac{1}{\gamma_{se}})]} \tag{2.2.1}$$

Paschen's law describes the voltage necessary to start a discharge between two electrodes in a specified gas as a function of pressure and electrode gap distance. Paschen curves are made and referenced as guidelines for generating these discharges in specific gases and at specific pressures. Certain interesting relationships were discovered that pertained to the minimum distance and required voltages to forcefully cause arcing. A commonly used example is that in air at 1 atm, the minimum distance for voltage breakdown is 7.5 μm and 327 V. Yet, increasing the gaps width or even making it narrower would cause the arcing to cease [24]. Paschen's law can be taken further and discussed in terms of mean free path l. This is the average distance between a molecule and its collision with another molecule. This concept is vital in the avalanche based mechanism that plasma requires for generation. Mean free path has an inversely proportional relationship with pressure, given a constant temperature. More collisions results in lower electron energy causing ionization of a molecule to be more difficult. Thus, a lower-pressure gas would cause less collisions, keeping the energy high and making ionization, or the generation of plasma, easier.

This concept will come into play more in the future studies section.

For the cases described throughout this work, currents are of the milliamps mA magnitude and voltages are in the kilovolts kV magnitude. Additionally, all of the experiments and scenarios will be at atmospheric pressure because this work uses cold atmospheric plasma, CAP. The surface discharges described in the next section require a high voltage and consequently a low current.

2.3 Dielectric Barrier Discharge

The dielectric barrier discharge (DBD) can be generated in a volume (VDBD) or on a surface (SDBD). Both generation types have their pros and cons that dictate which is more efficient at certain applications that overlap e.g. ozone generation and bacterial/viral inactivation [176, 125]. VDBD utilizes some type of gas as the medium for the discharge to form in. This creates interesting and unique plasma-generated species to form. SDBD generates plasma across a surface, the dielectric, which in turn interacts with adjacent gases. The plasma itself is generated separate from the gas but used to convert the gas as a secondary effect. Due to the gas being converted directly in VDBD, biomedical applications initially utilized VDBD. SDBDs on the other hand are generated across a surface through microdischarges resulting a more homogeneous plasma. Though there are specific applications in which VDBD is essentially the only option there are several key differences between the two types that push SDBD as a more feasible option.

2.3.1 Power Consumption

Energy and power consumption is an important factor in engineering a device for biomedical applications. Cost inefficiencies can be a significant obstacle for biomedical devices to be successful. DBDs in general utilize a high voltage (kV) and accordingly low current levels (mA). Due to the relatively large voltages, a key factor to observe is the relationship between power consumption and increasing operating voltage, Eq. 2.3.1 [83].

$$P_A = f(V)^x \tag{2.3.1}$$

Several groups have reported an exponent value between 2 and 3 or approximately 7/2 for surface discharges and this was again confirmed by Kriegseis through analyzing Lissajous figures and comparing to experimental data sets [83, 38, 83, 115].

Older studies of volume discharges in other gases and configurations also show higher exponents. Since then, the power law has been characterized to a greater extent, specifically for surface discharge actuators, Eq. 2.3.2 [165]. This expression includes correlations to frequency, actuator length, dielectric material and thickness, and notably voltage. From this equation and experimental data with it, we can still see that approximation are accurate.

$$P = f\frac{\epsilon_0\epsilon_r L(W_0 + c_1\frac{V_{pp}-V_0}{2})}{d}V_0(V_{pp} - V_0) \tag{2.3.2}$$

Gibalov looked at ozone generation versus power consumption between multiple VDBD and SDBD configurations [47]. It was shown that ozone generation in air and oxygen was comparable between the two methods, but they had different energy densities at different phases of their respective discharges. A look at homogeneous micro-discharges and streamer generation is brought into question here. In general, streamer generation is energy translated into unwanted heat and light. Streamer appearance in SDBD is less likely with the proposed surface discharge arrangement when compared to VDBD generated streamers, especially in electronegative gases [47].

Though intuitively volume discharge would take more energy to function because of having to jump the gap (the gas), there are certain novel configurations that are being developed to circumvent this power consumption con. One example is with Xu's wire-to-wire DBD configuration which utilizes a gas gap jump making it a volume discharge, but the resulting power consumption and resulting power yields are efficient and close to that of surface discharges [172]. In general however, volume discharges have higher power consumption versus surface discharges mainly due to streamer generation and differing energy density timelines.

2.3.2 Induced Body Force

A unique property of the surface discharge is its inherent induced body force. This body force is generated due to the entrainment of adjacent gas due to momentum that is transferred into the gas from coupling between the electric field and the plasma-generated [29, 162, 153]. This property is what allows DBD plasma actuators to be utilized as a flow control device for aerospace applications. The plasma actuators function as all-electric flow control devices that utilize no hydraulics or moving parts. They react quickly, are light weight, and have a form factor that is potentially thin allowing for flush aerodynamics designs. The self-limiting nature of surface discharge actuators also positively affects its industrialization. As the electrons gradually accumulate on the dielectric surface, the potential difference is reduced and eventually quenches additional plasma formation [162]. Adjacent gases are accelerated due to ion collisions resulting in a net body force that can be directed depending on the configuration.

Many studies have been done to observe this wall jet phenomenon and characterize it through various flow visualization techniques such as particle image velocimetry (PIV) and smoke flow visualization [129, 164]. Post and Whalley showed that a shear layer is created that rolls up to form a vortical structure. Multiple spirals form around the center of this vortex. The direction of flow suggets that the entrainment is replenished by the adjacent gas directly above the actuator. Eventually more vorticity is formed nearby the initial vortex to maintain the no-slip boundary condition, along the wall. This vorticity then joins the larger vortex [164, 4]. The momentum steadily increases at a linear rate until it reaches a steady state velocity which suggests that there is a constant force behind the entrained fluid.

Several groups have utilized this mechanism for novel concepts such as plasma synthetic jets, plasma spark jets, and plasma vortex generators [135, 55, 119]. The plasma synthetic jets of Santhanakrishnan's work became a stepping stone eventually

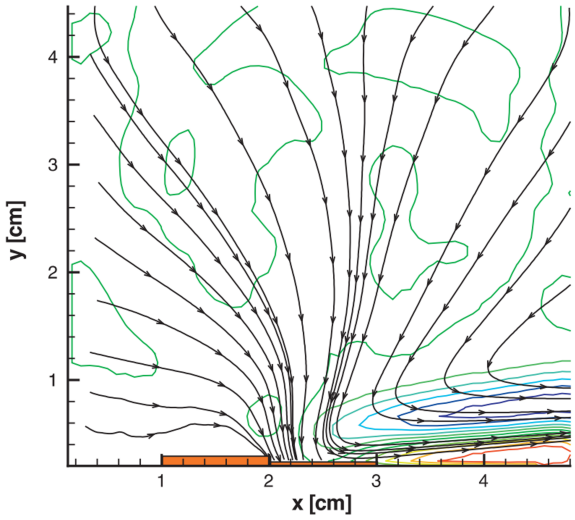

Figure II.1: Single SDBD actuator in quiescent flow. Streamlines are present [135].

leading to aerodynamic control through plasma jet vectoring. Bolitho utilized the zero net mass flux (ZNMF) nature of single DBD plasma actuators in various arrangements to control the direction of the plasma jet. Additionally, asymmetrically varying the strength of continue surface discharge produced a controllable jet stream that was affected by pulsing frequency and duty cycle [19].

2.3.3 Design Options and Capabilities

The surface dielectric barrier discharge (SDBD) actuator, also shortened as surface discharge actuator, can be highly flexible in design. As previously stated, a surface discharge actuator is simply two electrodes that are separated by some type of dielectric material. Due to the simplicity of the require materials and formation, several design options are made available that can be chosen based on the application warranted such as: electrode encapsulation, electrode symmetry, gas medium/environment, durability/malleability, dielectric constant, material thickness, electrode gap distance, and touchability

Electrode Encapsulation: A commonly used design option is to encapsulate one electrode with any type of insulation material. The better the material is at sealing off the electrode, the better the encapsulation effect is. Electrical tape, or polyvinylchloride (PVC), is frequently used for encapsulation because it can stretch, stick, and insulate well. Encapsulation reduces power consumption on that side of the dielectric material and forces the generation of plasma to be on the opposite side, Fig. II.2. Encapsulation is utilized for uni-direction flow manipulation where having species generated and flow on both sides is not beneficial.

Electrode Symmetry: SDBD actuator configurations are often times split into two categories: asymmetric, Fig. II.2, and symmetric, Fig. II.3, electrode configurations. The difference is in the positioning of the electrodes either being directly on top of one another or in a staggered configuration. The asymmetric configuration produces its body force in one direction at a higher magnitude rather than in both direction at a lower magnitude. This higher induced body force can be used to deliver plasma-generated species a further distance and/or deliver the short lived species to surfaces that would not be exposed as much.

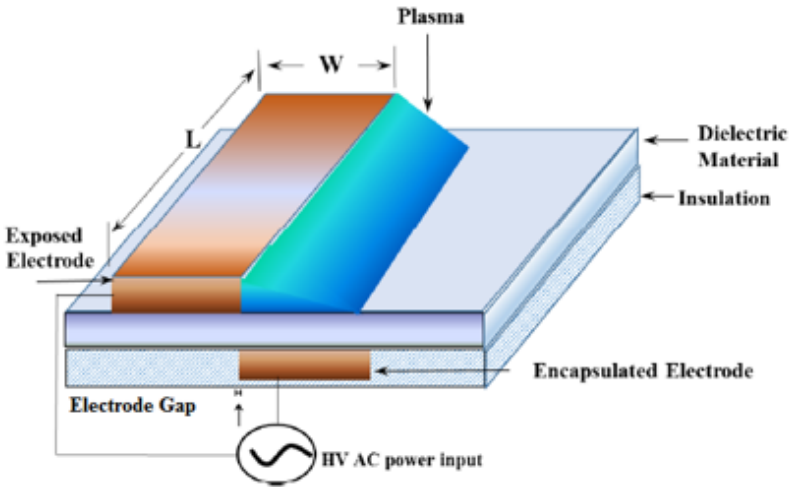

Figure II.2: Schematic of a single asymmetric SDBD actuator.

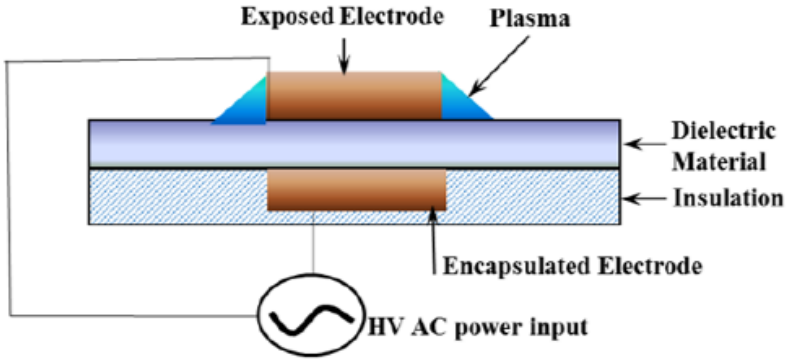

Figure II.3: Schematic of a single symmetric SDBD actuator.

This results in higher bacterial inactivation efficacy [154]. In other aerospace specific applications, asymmetric configurations are used to create larger arrays that additively combine their force magnitudes.

Gas Medium/Environment: As previously touched on, the gas medium that is exposed to the discharge actuator alters the plasma-generated species that form [149]. Depending on the application, specific gases may be used for specific reasons. Example gases are air, argon, neon, oxygen, helium, and nitrogen as well as various combination of the aforementioned, such as argon-helium and argon-oxygen [161, 50, 121]. Certain reactive species cause higher levels of oxidation, corrosion, bacterial inactivation, or even wound healing [46, 16, 121, 56]. In

addition to this, the temperature and pressure of the system also affects which species are more prevalent. Certain applications prefer reactive nitrogen species (RNS) and thus having a higher temperature environment would promote the chemical reaction towards a higher concentration of RNS [21, 109]. However, the flip side to this is that higher temperatures generate nitrogen species which cause corrosion in certain metals and alloys that would normally not be as quick to deteriorate but occurs because of the higher concentrations. For this work, atmospheric air will be the standard for the gas medium because of the easy accessibility, simple aftermath, and still effective species generation.

Durability/Malleability: The dielectric material, electrode material, and even insulation material make a difference not only in the flow produced but the reactive species produced. The material hardness and flexibility then has a direct affect on what the application can be used for. For wearing applications, such as a cuff for wound healing, a malleable actuator would be beneficial. For aerospace application where cross sectional area and weight matter a great deal for efficiency and aerodynamics, a material that is more efficient at conduction per unit area as well as can be engineered to fit on a wing would be beneficial.

Examples of dielectric materials commonly used for various biomedical and aerospace applications are kapton (polymide film), polytetrafluoroethylene (PTFE or Teflon), alumina (Al_2O_3 or aluminum oxide), quartz (SiO_2 or silicon dioxide), FR-4 (fiberglass with epoxy resin), and polymethyl methacrylate (PMMA or acrylic) [114, 118, 141, 116, 178, 60]. Previous studies by the author along with others have shown that the material has significant effects on the produced flow magnitude, spread, and power/voltage consumption and requirements. Additionally, these materials come in various forms from a solid malleable sheet to a hardened ceramic. For some applications, the generation of streamers is beneficial (excess voltage/power to generate streamers in the form of excess light

Material	Dielectric Constant
Kapton	3.4-3.5
Teflon	2.1
Alumina	9.8
Quartz	5.0
FR-4	3.8-4.8

Table II.1: Table of commonly used dielectric materials in actuators and their respective dielectric constants.

and heat). In these cases, a hardened ceramic would help increase the lifespan of the actuator and allow for the actuator to handle the higher heat buildup of the streamers.

Dielectric Constant: The dielectric constant of the material indicates the materials ability to store electrical energy. It is mathematically expressed as the ratio between the material's permittivity to its permittivity of free space (capacitance of the material to the capacitance of a capacitor with air as the dielectric). Functionally, dielectric materials poorly conduct electricity. Instead they store electric charge. Dielectric materials are commonly used to increase a capacitor's capacitance. Several variables, like temperature and pressure of the system, frequency of the passing voltage, thickness of the sample material, and even the structural weave of the material has been shown to affect the dielectric constant even between samples of itself. Possessing a higher dielectric constant has been shown to exhibit an decreased DC flashover voltage [1]. Altering the dielectric constant specifically has displayed the ability to manipulate plasma light emissions in the form of plasma uniformity and streaming size/spread [116, 82, 177]. As dielectric constant increases, the streamer propagation speed, streamer length, discharge energy, and gas heating increase. Essentially, as dielectric constant increases, the plasma regime shifts from uniform to streamers which expends energy through heat, light, and size of the streamer.

Material Thickness: The material thickness plays a role in several ways. The first is to aid in rigidity and durability of the actuator. The second is to alter the point of plasma generation. Increasing the dielectric material thickness consequently increases the electrode gap distance as well [116]. This increases the required voltage and thus power required to generate the plasma. Fundamentally, the electrons have a larger gap to close with their jump. This forces the generation of streamers. Certain applications that prefer this would be better off without a surface substrate allowing the electrons to just jump through the air. This allows the electrons to freely collide with air molecules [171]. Increasing the material thickness would also naturally increase the weight of the actuator and make customization more difficult. With a thinner material thickness, the actuator runs the risk of arcing through the dielectric and short circuiting the actuator and not generating plasma.

Electrode Gap Distance: This is a parameter that affects the regime of surface discharge created: uniform versus streamer. It is the physical distance between electrodes. This is affected by the material thickness as well as electrode configuration and placement. A uniform plasma regime is generally more coveted for a larger plasma surface area and thus larger gas to plasma species conversion rate. This also requires less power and lower breakthrough voltage. This regime leans towards biomedical applications. A streamer regime utilizes energy to produce heat and light and has interesting effects on the flow field with higher maximum values and different spreads than uniform plasma. This regime comes at the cost of higher power consumption and increased breakthrough voltage [116]. This regime leans towards flow control applications, surface modification applications, and some biomedical applications.

Touchability: This design option is usually utilized for biomedical applications and refers to being able to touch the 'plasma'. Plasma is simply just ionized gas and cold plasma has a low bulk temperature (still high electron temperature), but this allows for humans to be able to touch plasma without having thermal or other skin damage [140, 10, 89]. Howvever, the electrode that generates the plasma has high voltage current flowing through it, thus touching it would be quite shocking. This is circumvented by combining the function of the dielectric material needed to generate the plasma with the function of an insulator. The plasma can form along the intersections but the electrodes are covered from direct contact. This will be shown and discussed in a later chapter. Touchability is important for discussions involving plasma system direct contact with users in the form of clothing or wearable systems. Examples of these are dust repelling layers and wound healing sleeves/cuffs.

2.4 Plasma Applications

With the numerous plasma generation methods each with their own unique characteristics, there are accordingly a plethora of industrial applications, many of which have been previously mentioned. This section details some of the more common uses of SDBDs as well as the budding fields that have shown significant growth or future promise.

2.4.1 Aerospace Applications

The main contribution that surface discharge lends to aerospace applications is by utilizing the induced body force it inherently generates. There are exceptions like the sterilization/decontamination of aircraft and spacecraft using cold plasma, but that would also fall under the category of biomedical applications. The induced force is relatively low, but comes in the form of non-moving parts and when customized properly can have a small form factor and use relatively low power. Technology utilizing the induced body force are restricted in size for certain applications and limited by portable energy in the form of batteries or mobile power supplies. Being so, as technology advances and energy storage becomes more efficient, it is feasible to assume that the proliferation of plasma based force will occur. Though the main focus of this paper is not aerospace applications, certain principles for engineering design are taken from aerospace application research results and some results of this paper are applicable to aerospace applications.

Flow Control: Flow control is the main usage of cold plasma in aerospace applications [19, 29, 54, 55, 114, 119, 153, 162]. The ability to rapidly reattach flow on command with no mechanical parts (non-moving) on a wing creates several interesting opportunities for aircraft wing development. Plasma actuators in this scenario would function similarly to flight control surfaces but without re-

quiring pneumatic operations or risking mechanical failure. Electrical failure increases in frequency however. There is also risks of sparking that could be hazardous. The low force nature of cold plasma inherent flow is just enough to provide the reattachment of flow across a wing. Reattaching flow in specific situations pushes stall to a different point (angle of attack). This allows for aircraft to behave differently at previous points of stall. In addition to this, having separated flow behind the wing reduces lift and causes large pressure drag. The quick actuation speed is also a large plus for aircraft maneuvering.

Primary Propulsion: This application can be seen in two different ways: 1. propulsion on Earth for very small objects, such as small unmanned aerial systems (sUAS) or 2. propulsion in space where a small bit of force goes a long way. The first application is less used because current portable energy storage is still bulky and plasma generation efficiency is not good enough to where the power consumption would be efficient over a long period of time (on the order of hours). Add to this the problem of the output force being relatively low compared to the vehicle and that payload weight is a coveted parameter of sUAS creates a large problem for cold plasma primary propulsion to overcome. Xu developed the 'solid-state propulsion aircraft' that drafted significant attention because the aircraft flew distances up to 45 m of powered flight. Eventually the fixed-wing aircraft would glide but the impressive 8-9 s of steady flight drew a lot of attention [171]. This propulsion utilized ionic wind which has been shown to yield higher velocity magnitudes versus surface discharge.

The second application is seen relatively commonly due to being the only reasonable solution for its proposed problem: deep space flight. With deep-space missions having ΔV's of thousands of m/s, it is essential that spacecraft be able to propel themselves with specialized system. After a deep-space mission utilizes chemical propulsion to overcome Earth's gravitation, solar electric propulsion

(SEP) steps in to do the heavy lifting. In space where there is little to no resistance, solar or air, a small force but high impulse is invaluable for moving around. SEP engines are known for having low force on the order of millinewtons mN and high specific impulse I_{sp} on the order of thousands of seconds. In the same vein, cold plasma could be utilized in a similar fashion in which electrodes could be used to generate an electric field that accelerates masses to produce thrust though this concept has not been proven or developed. Cold plasma is limited in its usage as a primary means of propulsion simply because of its inefficiencies in terms of power in versus power out.

2.4.2 Biomedical Applications

Plasma has had deep connections to the medical field since its inception in 1928 by Irving Langmuir [22]. Its main attractive feature in this role is that it can hold a high concentration of energetic and chemically active species at low temperatures, even room temperature, and pressures. This opens up the possibility for many possible biomedical applications. Initially, applications were mainly indirect in that plasma was used to generate a product and that product was then used for a specific job. With certain actuator configurations, touching the actuators become possible and a more direct usage of cold plasma became a reality. Cold plasma is useful for many different biomedical applications because of the cocktail of products that it creates: reactive oxygen species (ROS), reactive nitrogen species (RNS), charged ions, ultraviolet light, and heat [121]. This paper will refer to the majority of these as plasma-generated species. Most biomedical applications utilize these species in some shape or form usually with a dose dependence, meaning the effect changes according to how long the treatment is or how concentrated the species are. Surface discharge has an additional boon in plasma-generated species usage in that the inherent induced force can be used to essentially deliver the species to a surface for treatment. The species are light

enough that the relatively low force works effectively for transport. Some applications only utilize certain plasma-generated species. Thus, more research is being put into the control of which species are formed and in what concentration so that specific dosages can be used to achieve specific effects.

Sterilization: Currently, one of the most common applications of not only surface discharge but cold plasma as a whole is decontamination and to a higher extent sterilization. Cold plasma has been known to cause microbial inactivation and now many studies have been performed to observe the effects of specific plasma-generated species for the inactivation of all sorts of cells (bacterial [154, 121, 117, 128, 177], viral [40, 169, 106], spores [93, 97, 158], biofilms [179, 49, 62]). Though each component of the plasma cocktail has some hand in microbial inactivation, the main culprit for sterilization is ozone O_3. Super oxides [68, 123] and super nitrites [21, 143] play a significant role but are too short lived to really push towards microbial death. Ultraviolet light has always had a part in sterilization [84, 99], but has problems with shadowing, penetration, and possibly causing cancer. Heat when increased significantly will obvious cause cell death. Charged ions have been known to accumulate on the surface of microbes to cause cell death [26, 11]. But out of all of these species ozone can be created in larger quantities, last for longer periods of time (requiring less refreshing of plasma-generated species), and still effectively performed microbial inactivation [121, 78, 157, 2]. This technology has been proven by a significant amount of research and is now in the stages of improving efficiency and industrialization.

Wound Healing: Wound healing is commonly broken down into four phases that cold plasma interferes with/promotes activation in: hemostasis [3, 175, 86], inflammatory [113, 101, 5], proliferation [113, 156, 15], and remodeling phase [113, 156, 35, 79]. All of these applications affect one another in the rebuilding of a wound. Cold plasma also affects each phase concurrently. Initial studies

show that very short exposure to plasma-generated species can cause the coagulation of blood, redox stimulation, production of collagen, and induces the expression of key genes for wound healing response. In addition to this, further treatment dosage can lead to the disinfection of chemically resistant bacteria [121]. Though this work does not specifically target these phases in wound healing, it provides additional background for understanding why and how cold plasma affects wound healing as well as pathways to develop an efficient system to deploy it.

MISC: Cold plasma has also been seen to positively affect the fight against cancer [74, 75, 137, 104, 53]. Plasma treatment has been shown to selectively attack cancer cells without damaging normal cells and significantly lower tumor size. The effects are good enough that there is lasting partial remission from clinical patients [104]. The cause for the shrinking of tumors seems to be the oxidative and nitrosative stress that the plasma-generated species cause the neoplastic tissue to go through [53]. Other methods of treating cancer such as ionizing radiation and chemotherapies use similar tactics of oxidative/nitrosative stress mechanisms. This is because the mechanism is physical so there is little to no resistance that can build up from it. As cold plasma technology matures, the efficiency and specificity of treatment will also improve and continue to push towards becoming a viable means of treating cancer.

2.5 SDBD Design Choices

For the majority of the experiments involved throughout this paper, certain design decisions were made due to previous personal experiments as well as literature.

2.5.1 Asymmetric vs. Symmetric

From works such as *Timmons et al* it seems likely that asymmetric surface discharge is the way to go to fully utilize the induced flow that it provides [154]. An asymmetric configuration allows for simple actuator serial configuration (side-by-side) with the electric fields additively pushing outward from the actuator. Additionally, asymmetric configurations are seen to produce higher velocity magnitude per amount of power consumed.

2.5.2 Dielectric Material

Teflon provides a suitable base for the electrodes in this actuator design. It is malleable when thin but with thicknesses in the tens of millimeters it can become a rigid surface. It is relatively lightweight, works well as the dielectric for plasma generation (looking at dielectric constant), and is not too expensive. The material can also have adhesive stick to it for various supplementary applications like adding in heat sinks.

2.5.3 Geometric Design Considerations

For the initial design considerations, the actuator was designed to be close to a square so that the electric field generated would be relatively uniform and the plasma species would be delivered uniformly as well. The housing device has a hole in the bottom piece to allow for plasma-generated species to flow through once carried by the induced flow. The initial design also utilizes changeable stilts to allow for freely changing the distance between the surface sample and actuator.

2.5.4 Extra Considerations:

User Interface, Gas Medium, and Lab Testing

The housing device was created to snuggly hold the actuator but allow easy actuator replacement. There is a designed handle bar for easy placement of the device. The top is open to allow for heat ventilation. With laboratory testing in mind, the actuators were designed to provide symmetric flow. The power supply and transformer used can run off of a standard US wall outlet allowing for universal use. The connections were made to be plugs for easy disconnects and reconnects.

Atmospheric air was chosen as the gas medium because it is simple to attain and the species conversion is relatively well known. Additionally when the species live their half-life, they naturally return back into atmospheric air. An Arduino was used to interface with the power supply to easily control the pulse rate and duty cycle. Fully autonomous treatment was also feasible.

CHAPTER III

CAP Interaction with Substrates

3.1 Introduction

Resistance to antimicrobial agents pose major challenges to treating infectious diseases and results in significant risks to human and animal health. Bacterial strains may be innately resistant to certain antimicrobial agents or they can acquire resistance by genetic mutations or lateral transfer of resistance genes from other bacteria [42, 48, 174]. By the year 2050, it is estimated that 10 million lives will be lost each year resulting from infections with resistant bacteria and the economic losses are projected to be up to a trillion dollars [31].

Infection by resistant bacteria can be acquired from different sources. The impact of nosocomial infections resulting from multidrug resistant bacteria has been widely studied. Some of the common bacterial species causing nosocomial infections include *Escherichia coli, Staphylococcus spp., Enterococcus spp., Pseudomonas spp.* etc. [30]. Many of these bacteria have shown resistance towards common antiseptic treatments and are able to persist in the environment on surfaces such as chairs, tables, and other equipment thereby increasing risk of patient exposure in a hospital setting [30, 81]. Out of every one hundred patients hospitalized, seven patients in developed countries and ten patients in developing countries acquire nosocomial infections [76]. There is a critical need for novel strategies that efficiently destroy these organisms without inducing the development of resistant phenotypes.

Cold atmospheric plasma (CAP), or non-thermal plasma produced at atmospheric

pressure, has demonstrated utility in both surface decontamination and airflow control in the past two decades [6, 67, 70, 108, 127, 156]. CAP can be generated through several methods. Surface dielectric barrier discharge (SDBD) is one of the simplest means where plasma is generated between two asymmetrically placed electrodes and at least one of these electrodes is covered by a dielectric material (embedded). The main advantages of SDBD over other plasma generation methods are the low power requirements, customizability (design and scalability), lack of gas flow requirement, and most importantly a corona discharge-like ability for localized airflow induction. An asymmetric design of SDBD imparts momentum into the gas adjacent to the exposed electrode as a result of the electric field coupling with the surrounding gas. The gas is entrained and an effective "induced flow" is produced. In gaseous mediums including atmospheric air, CAP induces the generation of free radicals, charged particles, and ultraviolet (UV) light. These are attributed as the major players contributing to bacterial inactivation observed in previous studies [121]. Bacterial cellular damage results from high oxidative stress imposed on treated cells as a result of free radical actions, as well as electrostatic interactions of charged particles across the bacterial cell wall. Ultimately the cells die due to the constant barrage of accumulating reactive species while being unable to maintain lipid, protein, and DNA repair [155].

3.2 Plasma-Assisted Decontamination

Free radicals such as reactive oxygen species (ROS) and reactive nitrogen species (RNS) are chemically unique compounds, usually produced in a normal cell during the electron transport chain in oxidative phosphorylation for ATP production [41]. Reactive oxygen and nitrogen species (RONS) are usually scavenged by cellular systems [180].

Some of the commonly produced free radicals inside the cell include superoxide (O_2^-), hydroxyl radical ($^{\cdot}OH$), singlet oxygen ($^1O_2$), hydrogen peroxide (H_2O_2), ozone

(O_3), and nitric oxide (NO) [59, 159]. These free radicals, upon interaction with peptidoglycan or the lipopolysaccharides, initiate a cascade of events that may result in the breakdown of C-O bonds, thus resulting in destabilization of the cell. In most cases, this destabilization can result in variations in osmotic pressures inside the cell and subsequently in cell death. *Han et al.* reported cell shrinkage in gram-positive bacteria before cell death indicating that the cells are at higher stress levels [59]. This method of chemical interaction-based destruction of bacterial cell walls has been accepted as the primary method of bacterial destruction during and after plasma treatment. Additionally, *Pai et al.* reported that ROS have been more effective than RNS in bacterial inactivation [121].

There were a few studies that indicated that RONS are produced outside the cell and are imbibed/absorbed into the cell as a result of the weakened cell walls [59, 121]. ROS mediates various cellular events such as cell death, cell senescence, etc. [159, 23, 41, 98]. Oxidative stress occurs when cells begin to accumulate free radicals beyond the scavenging potential of the cell. Toxin-antitoxin (TA) system is one of the many known mechanisms of cell death in bacteria [150]. When the accumulation is beyond a 'point of no return', bacterial cells which had entered bacteriostasis for cellular repair activates enzymatic pathways. This results in cell membrane damage in gram-negative bacteria and damage to cellular components in gram-positive bacteria along with final DNA fragmentation and membrane alterations leading to bacterial cell death [59]. Besides the TA mediated cell death, there are various other pathways, such as peptidoglycan-hydrolase pathways, CidA/LrgA, Bcl-2 family mediated pathways, that can also induce bacterial cell death [150, 14].

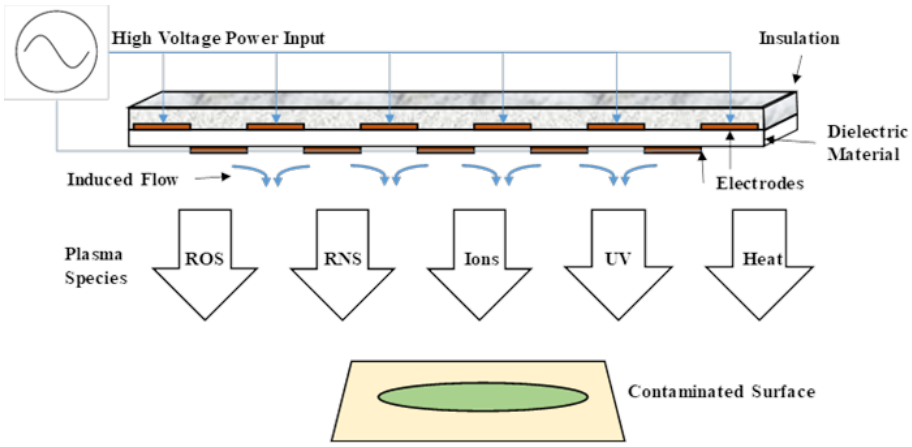

Figure III.1: Schematic representation of an SDBD plasma actuator system for surface decontamination detailing plasma-generated products.

3.3 Plasma System Design

As described in Chapter II, SDBD actuators involved two electrodes that are separated by a dielectric material (Fig. III.1). To fully utilize the inherent induced body force from SDBDs, actuators in this study were designed in an asymmetric configuration in which the electrodes were offset by a set distance. The control of induced air flow in an SDBD system was influenced by geometric changes such as altering the 3D structure of the dielectric material, increasing the electrode gap distance, altering the dielectric material and/or its thickness, and altering the electrode configuration [116]. Additionally, increasing the number of electrodes altered plasma volume and induced flow intensity [120].

The SDBD platform can be designed as an open or closed plasma system. An open system has the benefits of continuous airflow for cooling and a higher limit on free radical conversions while a closed system has the benefit of increased contact and dwell time of the free radicals with the treatment surface. Although an exhaustive amount of research has been reported for induced flow control from SDBD, their biomedical applications remain largely unexplored [29, 54, 152].

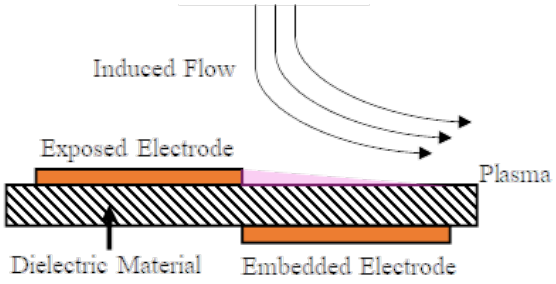

Figure III.2: Schematic representation of a single asymmetric SDBD actuator showing the induced flow location and direction.

The induced flow of SDBD actuators functioned as an effective delivery mechanism for the plasma-generated free radicals to reach contaminated surfaces [121]. By optimizing the plasma actuator geometric configurations, the plasma-produced free radicals are impelled towards a surface in a relatively power-efficient manner, when compared to volumetric DBD (VDBD). Although VDBD has been utilized for bacterial inactivation, it requires higher power input, a gas flow, and is highly limited in effective treatment area. VDBD lacks the natural means of species delivery that SDBD possesses, namely the induced fluid body flow. The true potential of SDBD is realized through the manipulation and utilization of the induced flow (Fig. III.2).

The handheld plasma device (HHPD) was developed with user ergonomics and ease of use in mind. Figure III.3 illustrated a computer aided design (CAD) schematic of the prototype used in this study. Main features to noted are its center-of-mass balanced handle, the open top ventilation, and adjustable snap-on stilts. The open top is necessary for heat buildup relief through dissipation.

Figure III.4a illustrates a simple flow chart of the components necessary for the HHPD. A simple Arduino code was run on an Arduino Uno to allow for an adjustable duty cycle and automatically control rest periods between runs. A PVM400 transformer (Information Unlimited, NH, USA) was used as the transformer to step up the voltage for plasma generation. Both the transformer and the Arduino utilized standard AC wall outlet power.

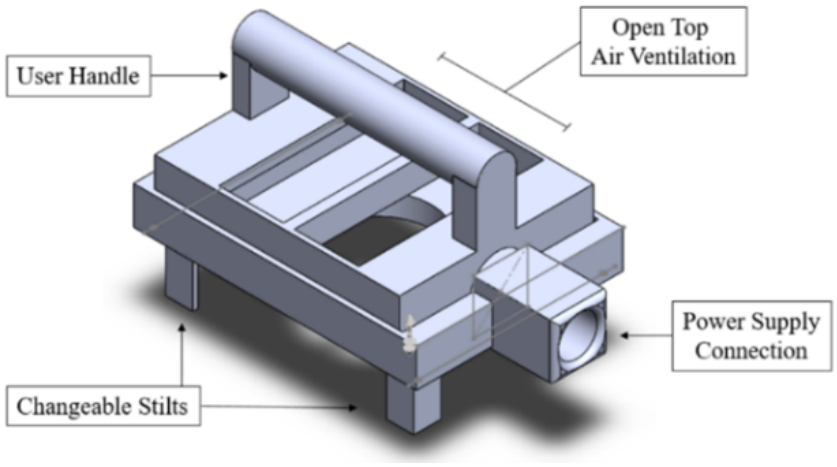

Figure III.3: CAD model of the handheld prototype.

The device shell was fabricated using a FormLabs 2 3D printer (FormLabs, MA, USA). Regular FormLabs black resin was used to print the device. The device was printed in two sections: top and bottom. The plasma actuator fit tightly into the bottom piece. Four raised edges in the corners prevented direct contact between the generated plasma and the housing device. The top piece snapped into place across the top side of the actuator with open air sections in marked places to allow for heat dissipation.

The custom designed actuators consisted of 5 exposed rows of copper electrodes arranged in a side-by-side configuration to create a net induced body force facing perpendicularly away from the actuator surface. The copper electrodes were covered with a solder mask to prevent external damages to the electrodes, e.g., scratches, debris, etc. Teflon at a thickness of 0.15 cm was used as the dielectric material. The actuator dimensions were 8.85×10.15 cm^2. Each actuator was tested for consistent performance across multiple runs of 5 surface treatment sessions.

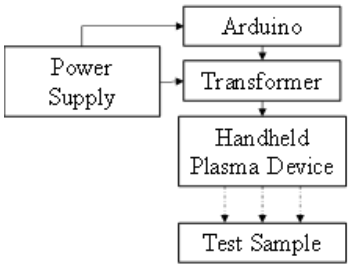

(a) Flow chart of handheld plasma device.

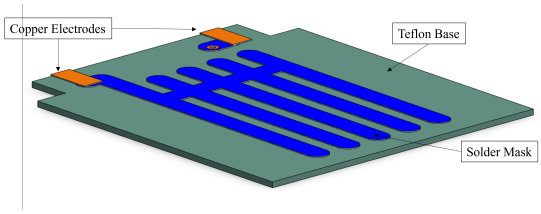

(b) Isometric view of actuator CAD model.

Figure III.4: Connection flow chart of handheld plasma device (a) and actuator illustration (b)

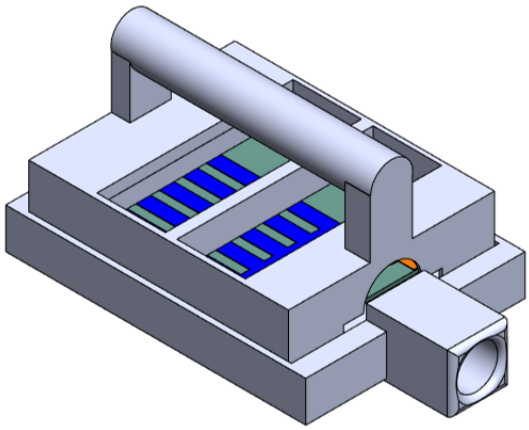

(a) Isometric view of handheld plasma device CAD model.

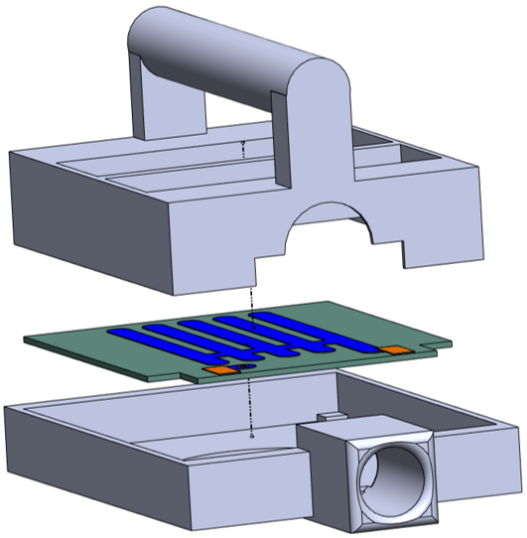

(b) Exploded view of handheld plasma device CAD model.

Figure III.5: CAD models of the surface discharge plasma system.

3.4 Surface Discharge Effects on Inanimate Substrates

3.4.1 Experimental Variables

- *Bacterial Inactivation Treatment Surfaces*: Surfaces such as stainless steel (metal tabs), hard plastic (microscope cover slips), glass (glass slides) and aluminum (aluminum foil) were plasma treated using the HHPD. Blood agar media was also tested and treated simultaneously.

- *Bacteria Treated*: Bacterial isolates of *S. aureus* and *P. aeruginosa*, obtained from clinical samples, were used for the study.

3.4.2 Bacteria Used for Treatment

Staphylococcus aureus is a ubiquitous gram-positive pathogen that is responsible for numerous infections in mammals. *S. aureus* can also be found as part of the normal flora of humans and animals [41]. This organism has been reported to survive on different organic surfaces for extended periods of time and is also capable of nosocomial transmission [81, 126]. *S. aureus* is also known to acquire antibiotic resistance. Due to their ubiquitous presence, *S. aureus* can be found on open wounds and may complicate healing. There have been numerous reports of Community-Associated Methicillin Resistant *Staphylococcus aureus* (CA-MRSA) on wounds and open surfaces in the United States demonstrating the importance of *S. aureus* in human beings, animals, and in the environment [111]. Antibiotic resistance in *S. aureus* is a major issue faced by healthcare professionals. More recently, *S. aureus* has been reported to exhibit evolving resistance to ionizing radiations such as UV rays, which can complicate disinfection strategies in healthcare systems [144].

Pseudomonas aeruginosa is a gram-negative organism and is ubiquitous in presence similar to *S. aureus*. *P. aeruginosa* has been isolated from wounds, ear and other superficial infections [160]. Various strains of *P. aeruginosa* have been recorded to

harbor intrinsic resistance to multiple classes of antimicrobial drugs [96]. Similar to *S. aureus*, *P. aeruginosa* is capable of persisting in its native environment for a long time as well as nosocomial transmission [64]. Both *S. aureus* and *P. aeruginosa* were resistent to multiple classes of antimicrobials.

3.4.3 Methods and Procedure

Glass slides, plastic cover slips, aluminum foil, stainless-steel tablets (metal tabs), and 5% sheep blood agar were prepared for bacterial inoculation. Bacterial suspensions were applied to the different substrate surfaces and exposed to plasma treatment. After plasma treatment of inanimate surfaces, the surfaces were washed with buffer which was then collected and cultured on 5% sheep blood agar plates for CFU determination. The blood plate substrates were incubated directly after plasma treatment. All experiments were performed in triplicate.

Bacterial suspensions were prepared in 1 $\times$ phosphate buffered saline (PBS) at concentrations ranging from 10^9 CFU/mL to 1 CFU/mL. 10 μL of these bacterial suspensions were then added to the different substrate surfaces and allowed to dry in a 37°C incubator for 20-30 minutes. The substrates were then plasma treated using the HHPD at a distance of 1 inch. The pulsing parameters of the HHPD were coded so that surfaces would be treated for 2.5 minutes followed by a 1-minute break and then a second treatment for 2.5 minutes, summing to a total of 5 minutes of treatment time.

Following plasma treatment, the treated surfaces and control untreated surfaces (inoculated with same number of bacteria) were washed in 50 μL of 1 $\times$ PBS and plated for culture. After incubation for 18-24 hours, the untreated control and treated plates were compared to determine the presence of bacterial growth. The concentration of the bacterial suspension at which zero bacterial growth was observed was used to calculate the log reduction.

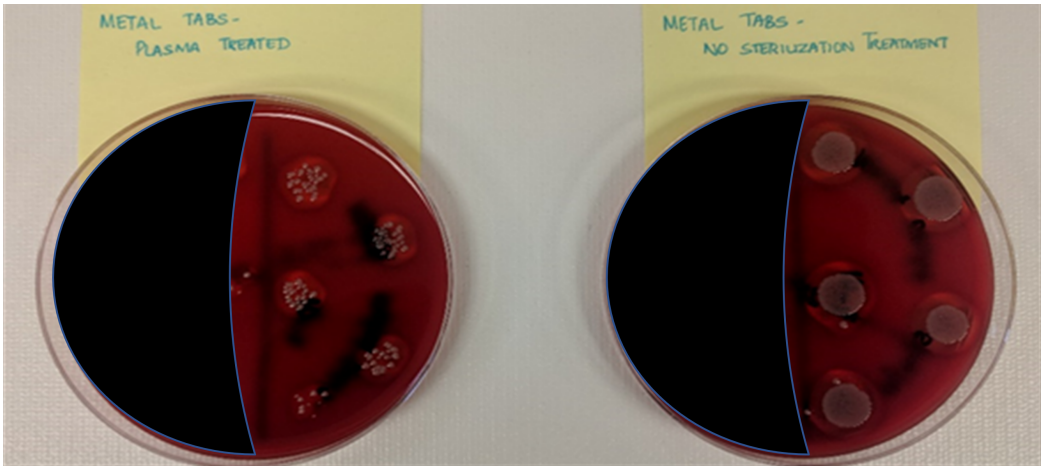

Figure III.6: A picture of the plating and growth of metal tab treated and untreated samples.

3.4.4 Results and Discussion

Controlled plasma exposure was accomplished using the SDBD platform designed specifically for this study. An example of the effects of plasma treatment is shown in Figure III.6. Each of the five growth spots on the plate represents bacterial growth from 10 μL of sample. Based on the number of colonies, it can be seen that the bacterial count in the culture plate (5% sheep blood) with the treated sample was much lower than in the culture plate with the untreated sample. In the plate with the untreated sample, as expected, there was a very large number of bacteria and their individual colonies merged together to form one big circle. In the plate with the treated sample, there was a lower number of bacteria and their growth can be appreciated as individual colonies.

The overall reduction in bacterial count is shown in Figs. III.7 and III.8. The results for *P. aeruginosa* (Fig. III.8) represents only 2 sets of data. Data from the third experiment could not be used because of sample contamination with other bacterial species. Plasma was most effective on blood agar media attaining an average of 5-log reduction for both bacterial species tested. After plasma treatment the color of blood agar media was found to darken, however based on separate experiments

this was found not to affect bacterial growth (data not shown). The error bars in Fig. III.7 are representative of the mean ± standard error of each experimental set, calculated with Eq. 3.4.1 where σ is the standard deviation and N is the number of samples.

$$SE = \frac{\sigma}{\sqrt{N}} \tag{3.4.1}$$

Plasma was more effective in destruction of *P. aeruginosa* on all inanimate surfaces tested when compared with *S. aureus*. There was an average of 4-log reduction in CFUs of *S. aureus* and *P. aeruginosa* on stainless steel surfaces. On aluminum foil and glass slides, there was an average of 1.5-log reduction in CFUs of *S. aureus* and 3-log reduction in CFUs of *P. aeruginosa*. On hard plastic, there was an average of 2-log reduction in CFUs of *S. aureus* and 3-log reduction in CFUs of *P. aeruginosa*. Since SE could not be calculated for *P. aeruginosa* because only 2 sets of data were recovered, the error bars in Fig. III.8 represent the confidence calculated from the average of error in Fig. III.7.

For this study, cold plasma treatment with the proposed surface discharge system yielded better results on *P. aeruginosa* as compared to *S. aureus* in terms of cell log reduction. As previously mentioned in Chapter II, gram-positive bacteria have a thick peptidoglycan layer and no outer lipid membrane while gram-negative bacteria have a thin peptidoglycan layer and an outer lipid membrane. *Han et al.* reported that there are different inactivation mechanisms that affect gram-positive vs gram-negative bacteria [59]. Gram-positive showed intracellular damage with little envelope damage while gram-negative displayed cell leakage and DNA damage. *Lee et al.* reported that certain gram-negative bacteria exhibit more significant morphological changes [90]. Several studies reported a dose dependent (usually time based) reaction to plasma treatment that is also dependent on the bacteria specific phenotype [100, 90, 122]. The results of this study agrees with previous reports showing that gram-negative

bacteria (*P. aeruginosa*) are more affected by plasma treatment versus gram-positive bacteria (*S. aureus*).

In general, this study displayed a clear difference between bacterial inactivation (BI) on metal tabs (stainless steel) versus plastics/glass/aluminum foil. It is known that for some materials, plasma treatment (for example microwave-induced argon) alters the composition and roughness of the material surface [87, 63, 167]. The contact angle, wettability, and thus the hydrophilicity are all parameters that change depending on plasma exposure duration. Other studies have observed that higher relative humidity (RH) results in increased inactivation of bacteria when exposed to cold plasma [124, 107].

Similar to these previous studies the results of the current study (observed for metal tabs) also suggested that there may be a correlation between the change in surface adhesion (lower surface contact angle therefore higher surface energy) and BI. This could be because of a local increase in RH or specific increases in efficiency of other plasma-based mechanisms that affect BI. Though there are many confounding factors that still need to be isolated, there is a suggestive track that for simple gram-positive/gram-negative bacteria, this plasma treatment is effective for BI.

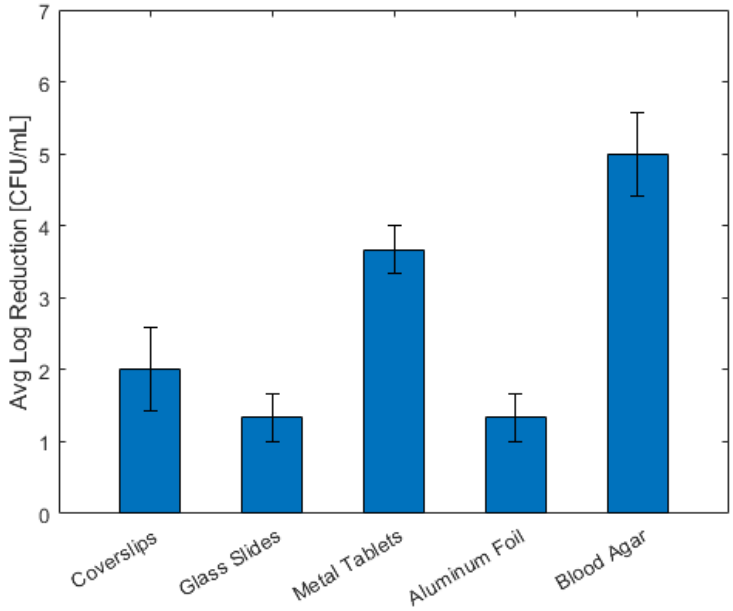

Figure III.7: Log reduction of *S. aureus* on various substrates after plasma treatment. The standard error from three runs are also depicted.

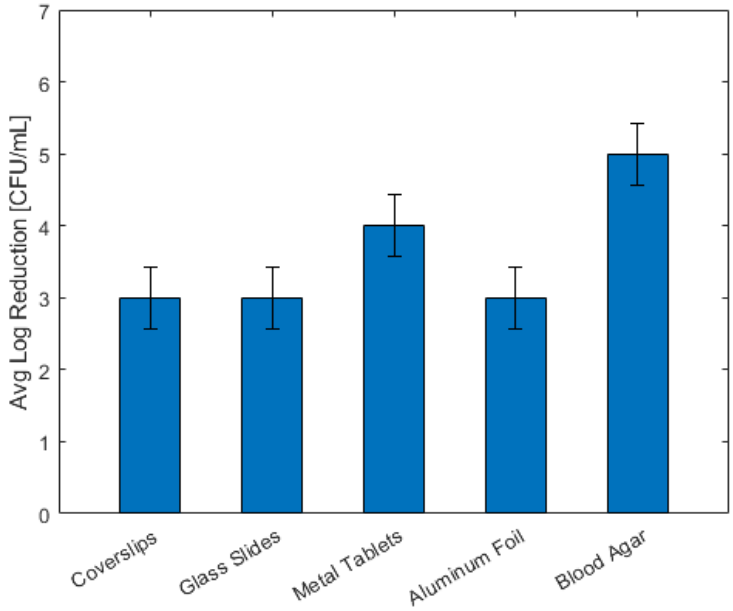

Figure III.8: Log reduction of *P. aeruginosa* on various substrates after plasma treatment. Averages are calculated with only 2 sets of data. The error bars represent an estimation of the confidence based upon the previous test as shown in III.7.

3.5 Surface Discharge Effects on Mice Skin

Understanding the effects of plasma on inanimate objects provides valuable efficiency data, however an animal model would be useful in evaluating its applicability for biological/clinical applications, such as wound healing. In this study a mouse model was used to investigate any negative effect of CAP on healthy skin. All studies were performed in accordance with approved protocols from the Institutional Animal Care and Use Committee (IACUC).

3.5.1 Experiment Design

Six to seven week old C57BL/6 albino laboratory mice from Jackson Laboratories were obtained for the study. Mice were sedated using isoflurane inhalant anesthesia or injectable anesthesia using a ketamine mixture. The right and left lateral sides of the abdomen area of the mice were shaved.

The same handheld open plasma system that was used in the substrate treatment study was used for this mice skin study, Fig. III.9a. New actuators were used for each experiment. The right side was treated with plasma for 5 minutes with a 1-minute break after 2.5 minutes, similar to the treatment procedure used for the inorganic surfaces study. The left side served as the negative control. Following treatment, the mice were euthanized and the shaved regions of the skin from both sides were immediately excised out and transferred into 10% neutral-buffered formalin for histological examination.

3.5.2 Results and Discussion

The study on mice was conducted to evaluate any adverse effects plasma treatment may induce on skin (Figs. III.11a and III.11b). No observable thermal/electrical damage was detected following plasma treatment.

Histological examination of plasma-treated skin, performed by a board certified

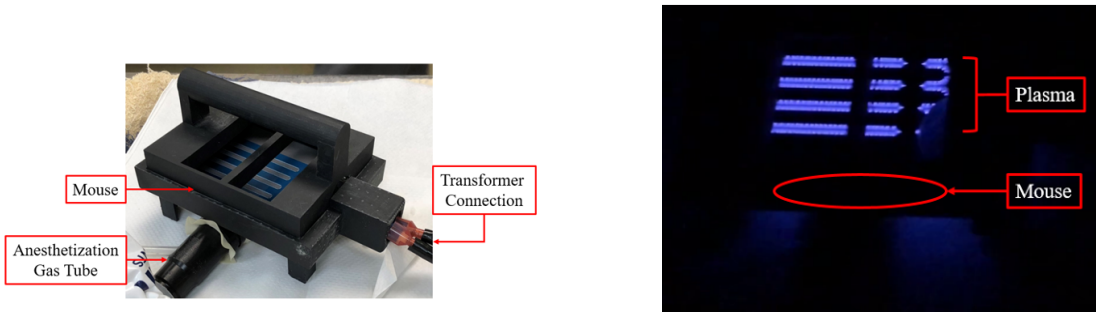

(a) Mouse experiment setup. (b) Plasma on.

Figure III.9: Plasma treatment on mice skin.

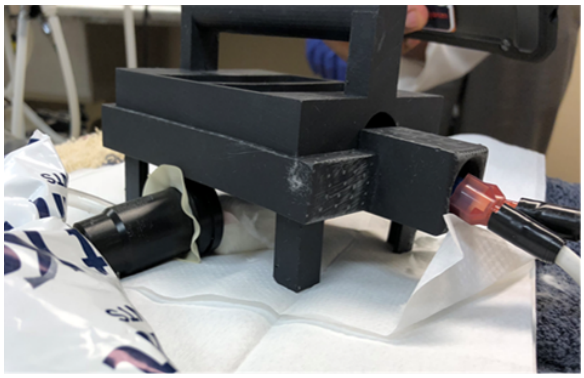

Figure III.10: Side view of the plasma treatment on mouse skin experiment.

pathologist, did not reveal any evidence of thermal damage or inflammation. There were no observable histologic difference between treated and untreated mouse skin. However, damage to skin following plasma treatment has been reported by other researchers [80, 147, 72]. These studies used other types of cold plasma (helium plasma jet and atmospheric pressure plasma jets).

Though the effects of plasma on wounds is still relatively unexplored, it can be inferred that this plasma treatment is apparently safe for use on intact skin.

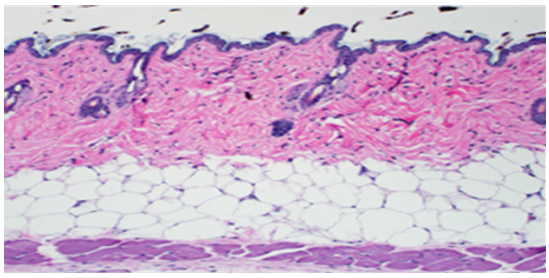

(a) Untreated mice skin (left abdomen).

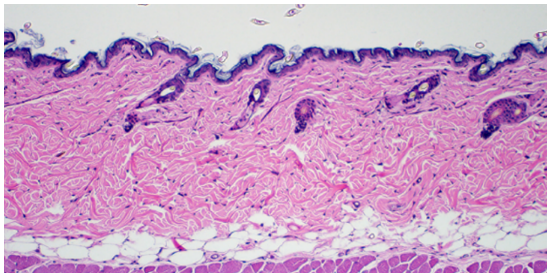

(b) Treated mice skin (right abdomen).

Figure III.11: No observable histologic difference between treated and untreated mouse skin.

3.6 Plasma System Temperature Study

An important final product for this project was to obtain reasonable improvements for future devices based off of in-lab testing of the device in a near appropriate environment. During the previously discussed inanimate substrates test, temperatures were recorded during the treatment of the samples. This was to determine the pulsing duration and whether a break-time was required.

3.6.1 Methods and Procedure

Due to the semi-closed state of the system, heat dissipation from the plasma actuator radiated to the sample and back to the actuator. The actuator itself was brought to the highest level of uniform plasma (right before reaching the streamer regime) to improve bacterial inactivation. This also increased the energy dissipation from the actuator in the forms of heat and light. The temperature was recorded using a infrared thermal imaging camera on both the actuator and treatment surface before testing, immediately after the first wave of pulses, and after the second wave of pulses.

3.6.2 Results and Discussion

An example of the thermal imaging of the HHPD is shown in Fig. III.12. The image showed that the temperature displays 109°C on the surface of the actuator.

However this temperature is not indicative of what the temperature on the substrate is. Radiated heat does reach the treatment surface but through the relationship seen in Equation 3.6.1. With a few centimeters of separation, the heat felt reduces down to reasonable levels that do not thermally hurt samples (below 60°C). The temperature was observed to continuously rise upon each actuator pulse until a peak point was reached upon turning off the actuator for a temperature rest (Fig. III.13). The plot displayed a drop of temperature during actuator off moments and a rise in temperature during 'on' moments. The temperature decreased at a slower pace than the pace increased as represented by the lower negative slow vs positive slopes in most cases. Similar results and trends were seen in other materials. At the end of the treatment, the peak of temperature was reached at around 60°C. This temperature, though not severely thermally damaging, could be reduced using methods such as airflow through the device or heat sinks on the actuator. Though the device already provided some airflow itself due to the inherent body force from the actuator, more airflow could move the higher temperature air and replace it with cooling air. The pitfall here is that there could be a loss in plasma-generated species though some studies suggested that refreshed species could be beneficial for microbial inactivation. The addition of heat sinks required critical thinking. Most heat sinks are conductive and so would cause arcing on the actuator. The highest temperature points as seen in Fig. III.12 is directly on the electrodes. To combat this, ceramic or non-electrical conducting heat sinks were used. Inefficiencies here needed to be dealt with because of possible arcing problems.

$$q = \sigma T^4 A \tag{3.6.1}$$

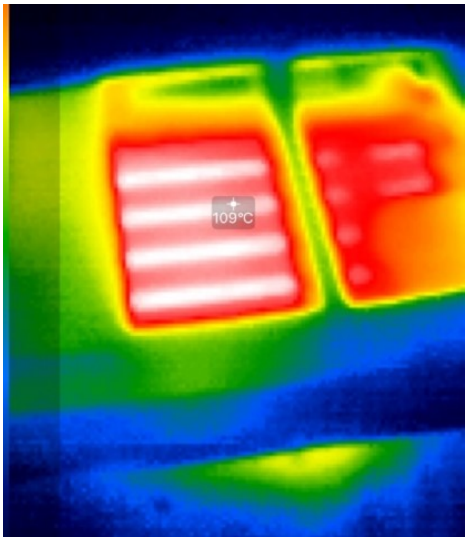

Figure III.12: Infrared thermal imaging of the handheld plasma device in operation.

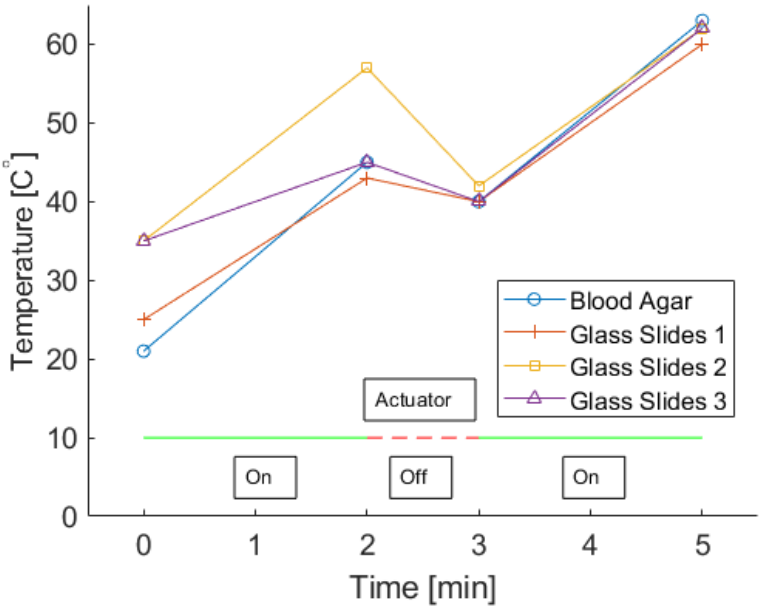

Figure III.13: Temperature profiles of blood agar and glass slides during plasma treatments.

3.7 Surface Discharge Effects on Equine Blood

Surface discharge effects on living cells is critical for understanding whether cold plasma can be utilized for wound healing. Various studies have shown that there are coagulation effects on blood post plasma treatment [102, 33, 175], but more research is needed to observe specifically what happens to certain blood cell types especially using surface discharge. In the following experiment, equine blood is treated with cold plasma through surface discharge. The goal will be an overhead view at the effects of plasma treatment on red blood cells (RBC), white blood cells (WBC), and platelets.

3.7.1 Experiment Design

The same handheld open surface discharge plasma system was used to treat equine blood samples. The blood had anti-coagulant in it to prevent it from coagulating immediately upon being drawn. The blood was donated from the veterinary school at Oklahoma State University by Drs. Todd Holbrook and Theresa Rizzi. For this experiment, the blood smears were made and treated with the plasma device pulsing at 500 ms on/off. The treatments were 0 (control), 1, 2, and 5 minutes long. Time segments of 1 and 2 minutes were chosen because they mimic short term treatment time to promote wound healing capabilities as described in Chapter II. The time segment of 5 minutes was chosen because a longer term effect would provide valuable insight into pushing the boundary of dosage and seeing whether decontamination-like effects would start occurring. Each trial used a different blood smear because staining of the blood smear would be performed posttreatment. Two distances were tested as an additional variable: 0 and 1 inch away from the surface (plus device offset). The device sat directly above the blood smear.

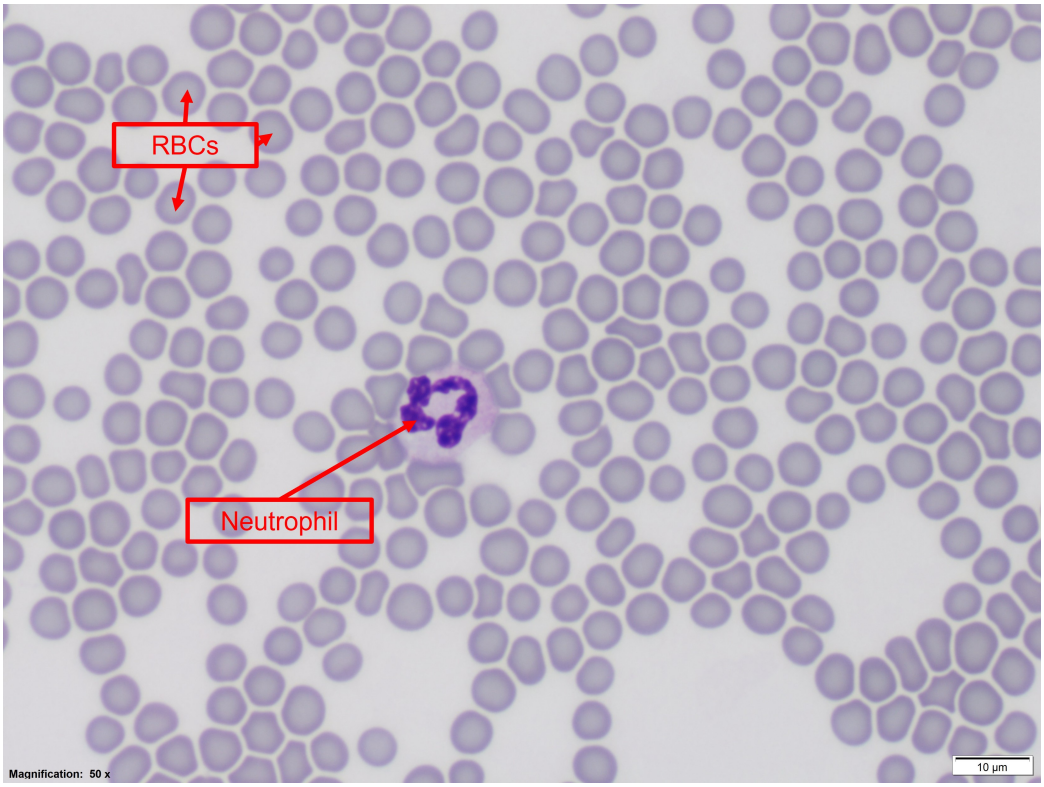

Figure III.14: Image of untreated blood smear with no plasma exposure. Magnification at 100x.

3.7.2 Results and Discussion

An image of a non-plasma treated blood smear is shown in Fig. III.14.

There was no difference in cell morphology following plasma treatment of the two distances evaluated. At minute 1, Fig. III.15, and 2, Fig.III.16, of plasma treatment, there were little to no changes in cell morphology of RBC, WBC, and platelets. At 5 minutes of plasma treatment, morphological changes were evident (Fig. III.17), which could be due to oxidative stress.

No significant changes in structure of the WBCs were observed during any of the time points (Fig. III.18).

Lastly, changes in platelets were observed by the 5 minute mark (Fig. III.19). It is unusual to see multiple platelets in one viewing window at 100x magnification as shown in Fig. III.19. Possible platelet activation following 5 minutes of treatment

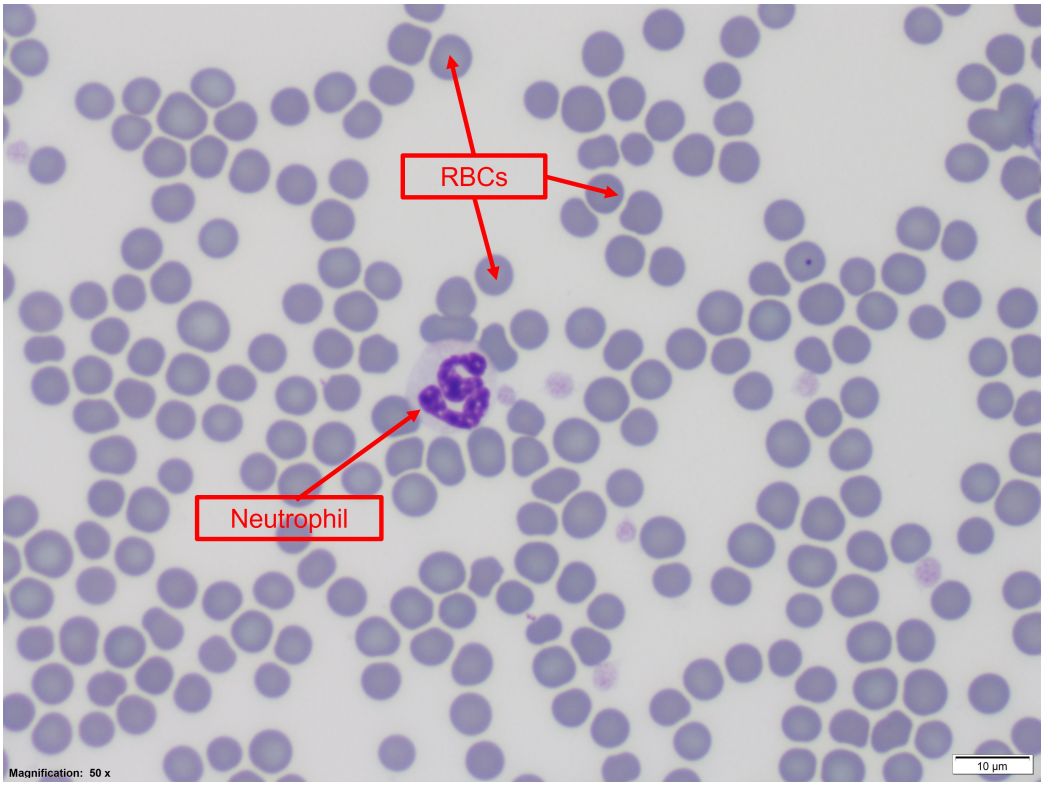

Figure III.15: Image of treated blood smear after one minute of exposure. Magnification at 100x..

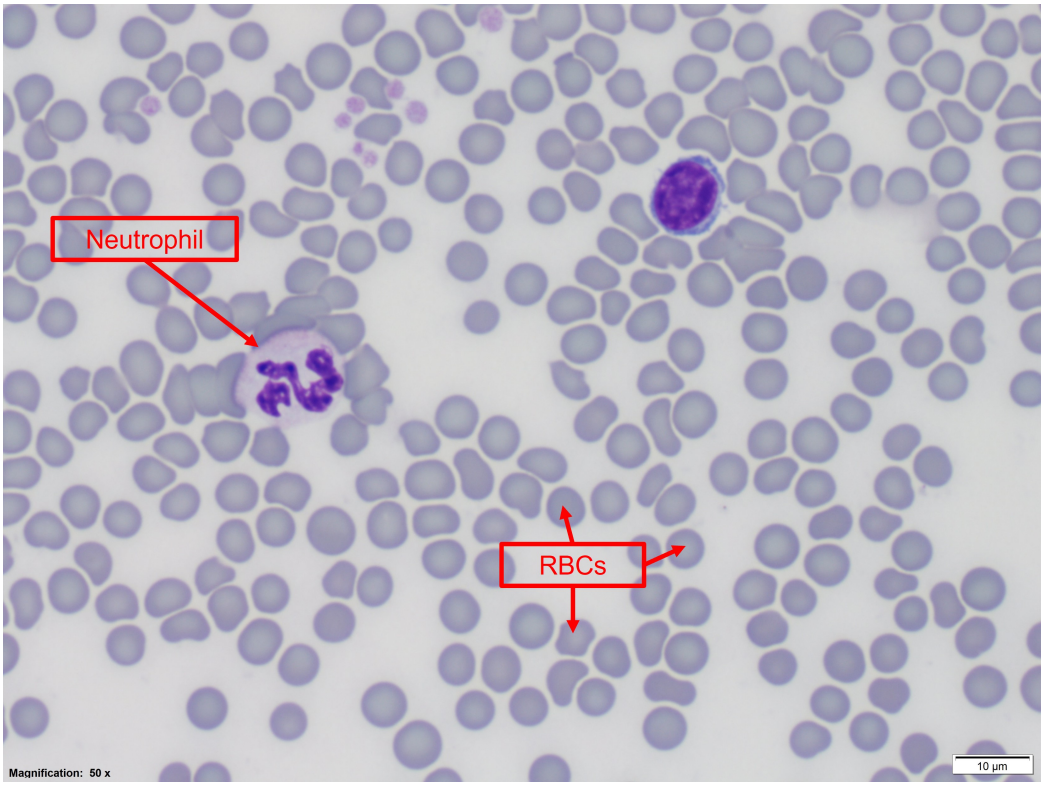

Figure III.16: Image of treated blood smear after two minutes of exposure. Magnification at 100x.

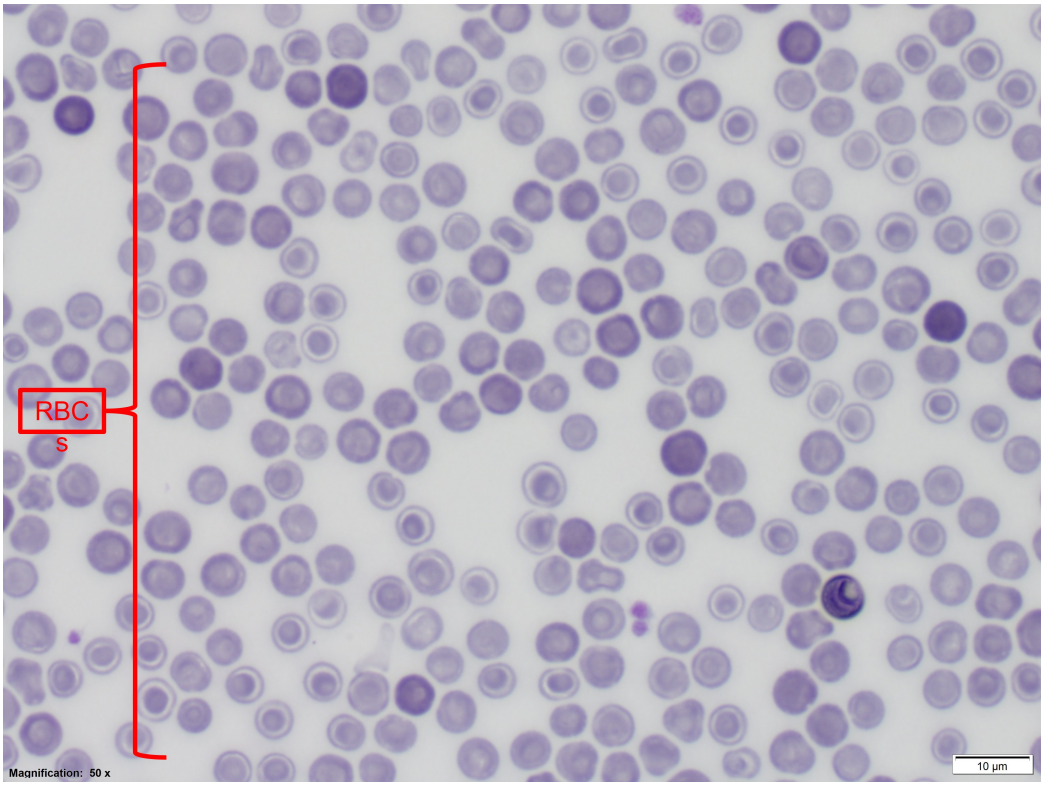

Figure III.17: Image of treated blood smear after five minutes of exposure. Magnification at 100x.

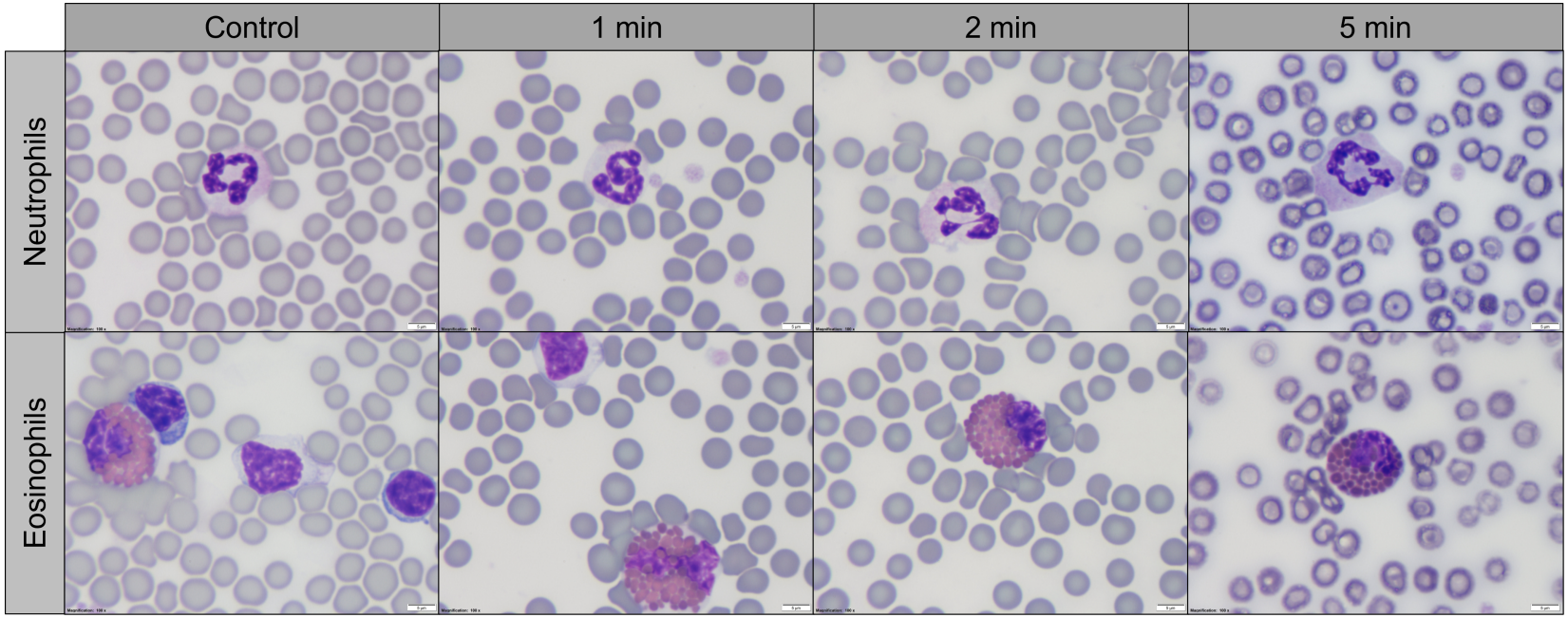

Figure III.18: Comparison of neutrophils and eosinophils with increasing plasma exposure. Magnification at 100x.

Figure III.19: Aggregating platelets after 5 minutes of plasma treatment.

was also observed (Fig. III.20).

Yan et al. reported that rapid *in vitro* blood coagulation from a plasma-induced agglomerated layer of blood that was thick and dense and composed of broken platelets [175]. They concluded that cold plasma was effective for stanching bleeding from a surgical incisions in rats. *Golpour et al.* reported that the mean number of RBC, WBC, platelets, and hemoglobin concentration remained similar between plasma treated and untreated whole blood samples of chronic lymphocytic leukemia patients [51]. They observed an increase in lipid peroxidation and RNS deposition in the whole blood of both CLL patients and healthy subjects. *Schmidt et al.* reported that plasma-treated skin increased the disaggregation of cells in the stratum corneum which led to increased tissue oxygenation, oxidation of SC-lipids, and restricted penetration of the model drug they used (curcumin) [138]. This study was centered around skin barrier regulation. These previous studies give interesting insights and confirm and/or give context for the results found in the blood study presented here. Future studies that isolate and observe blood cell functionality following plasma treatment can help in better understanding the results observed in the current study.

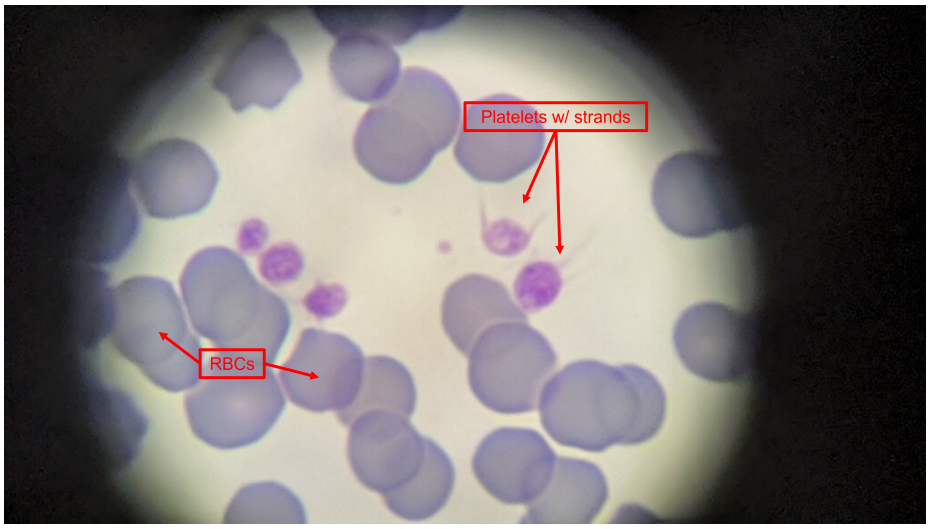

Figure III.20: Possible platelet activation and aggregation after 5 minutes of plasma treatment. Note the streams extending from the platelets.

3.8 Summary

Cold plasma is a novel technique that can revolutionize healthcare system across the globe. Continued advancements in this technology, we are tapping into an unknown source with strong potential for use in disinfection, sterilization, surface decontamination, and wound treatments. With further testing, plasma can be optimized for decontamination of all types of surfaces, including skin. Unlike antimicrobial drugs, plasma treatment is not likely to induce antimicrobial resistance traits in bacteria due to it employing cellular destruction through the multiple physical pathways that result in loss of cell wall integrity [59].

This study described a handheld open type model for localized sterilization which can be used on both animate and inanimate objects. The effectiveness of an open model plasma system at bacterial destruction was demonstrated in this study. Various surfaces tested indicated at least a 3-log reduction in bacterial load. Efficacy of plasma treatment varied across different surfaces and across bacterial species tested. Stainless steel and hard plastic showed the highest efficacy for bacterial inactivation. Inactivation of bacteria on aluminum foil and glass slides were successful; however,

efficiency was lower compared to metal surfaces. Plasma treatment was found to more effectively inactivate *P. aeruginosa*, a gram-negative bacterial when compared to *S. aureus*, a gram-positive bacteria.

A pilot study performed on mice to evaluate thermal and physical effects of plasma treatment on skin was promising and did not reveal any significant histological changes.

Similarly not much effect was noticed following short term plasma treatment on blood samples. However, prolonged treatment at 5 minutes induced morphological changes to the cellular structure that could have a negative impact.

To further optimize device performance thermal imaging techniques were used for the identification of heat buildup locations and appropriate positioning of heat sinks. This helped in lowering the radiative heat to the testing surface and maintaining it below 60°C.

CHAPTER IV

Configurations of Plasma Actuators

4.1 Introduction

The easily customizable nature of SDBD actuators allows for the construction of various geometries and configurations to improve the efficacy of desired parameters. In the following chapter, three specific configurations will be discussed: cylinder, thread, and mesh. The goal of this investigation into configuration changes is to determine whether certain configurations will have a better effect for wound healing by altering the flow field and thus changing the literal direction and quality of species (through mixing) of the plasma-generated species. A brief dive into quantifying mixing will be towards the end.

4.2 Designs Considered

To determine what is necessary, we needed to find out what was possible. Brainstorming to determine feasible designs and their applications occurred.

Plasma Wand: This design is based on surface treatments from a distance, Fig. IV.1. The actuator sat in the top piece of the device with the electrodes leading down the handle. The handle had the ability to be designed to be longer or shorter. The design was made for situations in which one could either not reach the surface or is required to be far from the surface. In general, other plasma wand designs utilized a plasma jet as the plasma generation method. The top

piece of the design ended up being flimsy when 3D printed and the application was not commonly needed.

Plasma Activated Water: This design was common for indirect biomedical applications from sterilization to cancer treatment. The idea was to generate species in a separate container and bubble the species through the water. The surface area of the bubbles allowed the generated species to affect the water and effectively activate it. Though the application was completely necessary, the actual activation of the water proved to be difficult. The pH of the water was measured to observe changes in species to no avail. Longer bubbling time or a completely different method were considerations.

MISC: Handheld plasma device and plasma spirals were also considered for more complex designs, Figs. IV.2 and IV.3. The handheld device was a combination between the wand design and the current benchtop-sitting-on-a-surface design. The spiral design theoretically helped induce vorticies to mix the plasma-generated species.

The design settled on for this study was the cylinder. This was because the design is simple to create, and could still provide valuable insight into parameters that could affect future geometric changes. The idea behind delving into cylinders was to better understand the role of species mixing for microbial inactivation/wound healing.

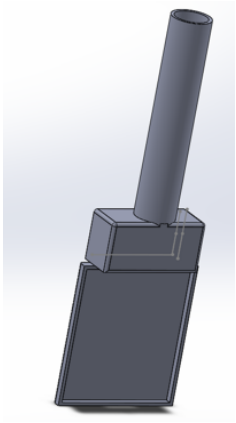

Figure IV.1: CAD model of a plasma wand design.

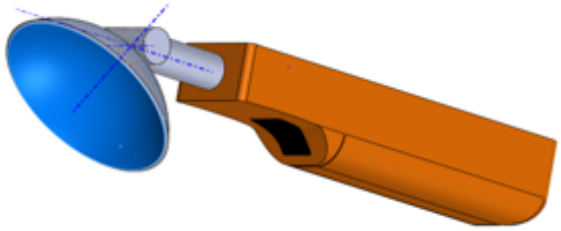

Figure IV.2: CAD model of a handheld plasma design.

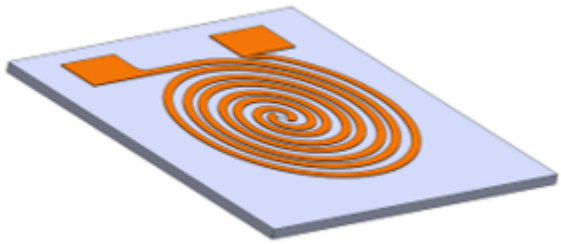

Figure IV.3: CAD model of a plasma spiral design.

4.3 Cylinders

In the first study, SDBD was used to evaluate cylindrical plasma actuators for inactivation of *Salmonella enterica*. A cylindrical SDBD configuration was evaluated to determine if the inherent induced body force could be leveraged to impel plasma species, such as reactive oxygen and nitrogen species (RONS), as an apparatus to sterilize surfaces. The cylindrical structure is evaluated in this study to observe whether an increase in mixing is possible to efficiently distribute the plasma species, thereby improving bacterial inactivation efficiency.

4.3.1 Actuator Material and Design

The cylindrical actuators used in this experiment were created using thin Teflon sheets, viewfoil made from polyester, and copper tape for the electrodes. The viewfoil was critical to this experiment to allow laser light to penetrate the cylinder. Half the cylinder was viewfoil, while the other half was Teflon to act as the dielectric for the surface discharge actuator. The actuators were relatively circular with a diameter of around 1 inch. The actuators were constructed in an asymmetric configuration to allow for stronger induced flow. Each actuator configuration is displayed at the start of each electrode configuration PIV analysis, respectively. In the PIV experiment and the biological experiment, ambient air was used as the gas medium.

The electronics powering the actuator consisted of a minimax70 transformer (Information Unlimited, Amherst, NH, USA) running at 7 kV and 10 mA and a 4.8V 2000 mAh battery pack (Tenergy, Fremont, CA, USA), as seen in Fig. IV.4. The transformer utilizes a five-stage multiplier and can easily generate 30 kV at 0.5 mA with the output at 25-35 kHz. The power going into the actuator is high-voltage AC.

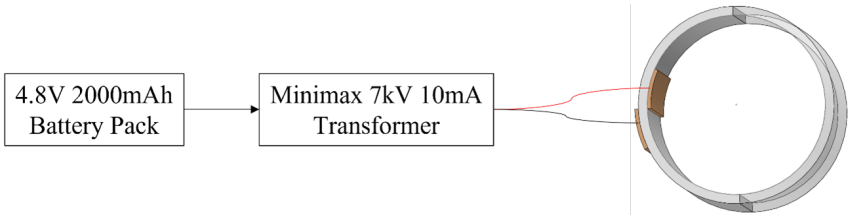

Figure IV.4: Flowchart of the electronics setup for the actuator.

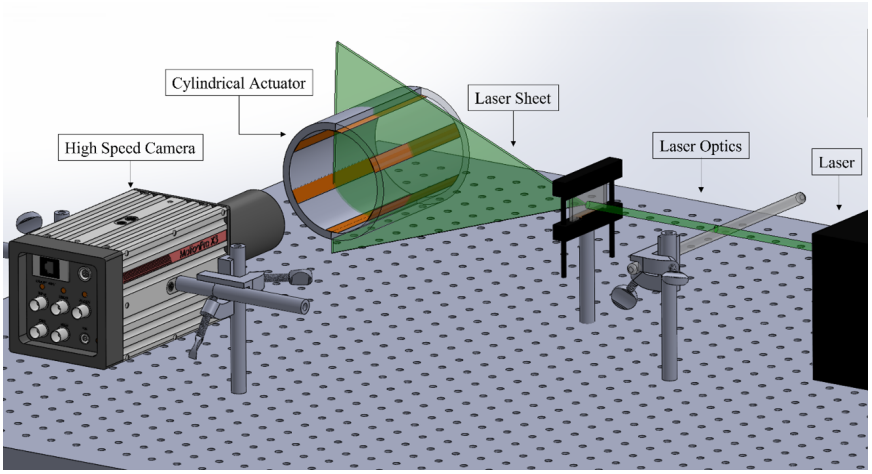

Figure IV.5: PIV setup schematic.

4.3.2 Particle Image Velocimetry Setup

Particle image velocimetry (PIV) is a commonly used analytical technique used to evaluate bulk fluid velocity profiles. In this experiment, the PIV setup utilized a Big Sky Laser Ultra Duel Nd:YAG laser that was connected to a pulse generator along with a high-speed Motion Pro X3 camera, as seen in Fig. IV.5. A Taitech DG-100 timing control unit was used to control a Quantum Composers Plus 9518 pulse generator for laser/camera alignment. A Tektronix TDS 2014B oscilloscope was connected between the pulse generator and the lasers to monitor pulse delays. A laser optical setup that consisted of a cylindrical rod and a mixture of convex and concave lenses was used to obtain a <2 mm laser sheet thickness. A ChauvetDJ Hurricane 700 fog generator was used to seed the air for PIV measurements. The time delay, dt, used for this specific experiment was 500 μs.

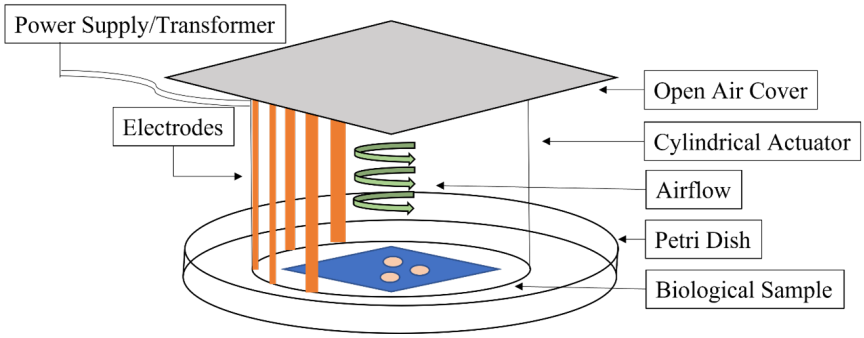

Figure IV.6: Schematic of the biological experiment setup.

4.3.3 Biological Experiment Setup

For the bacterial inactivation section of this experiment, each cylinder configuration was used as a tube that enclosed a biological sample. The cylinders were rotated sideways and sat flat over the sample in a way to not touch the sample. A plastic cover was used to cover the open end of the cylinder. The entire setup was performed in a biosafety cabinet in a Petri dish. The setup is seen in Fig. IV.6.

4.3.4 Results and Discussion

Particle Image Velocimetry

Particle image velocimetry (PIV) analysis was used to evaluate the bulk fluid velocity profiles and mixing parameters within cylindrical SDBD plasma actuators with one, two, three, and six electrode arrays. The aim of PIV analysis was to determine the extent to which the actuators were capable of inducing airflow mixing. Since plasma-generated reactive species are known to have biocidal effects, an increase in airflow velocity and mixing capability would theoretically result in improved delivery of reactive species to contaminated surfaces, resulting in increased efficiency for surface decontamination applications. Although SDBD actuators can be constructed and arranged into any three-dimensional structure, a cylindrical structure was used in this study to allow the optimal evaluation of airflow mixing capabilities since no edges or corners are present to influence the airflow dynamics. Additionally, the number of

electrodes was varied from between one and six to evaluate the effects of increased plasma volume on the airflow velocity and mixing capabilities. The higher resolution in lower electrode numbers (one, two, and three electrodes) was to observe minute differences between each, while the larger electrode number of six was utilized to observe the upper limit of mixing. To compare the amount of mixing between the various electrode arrangements, several parameters were examined, including vorticity, streamlines, velocity magnitude, and root mean squared (RMS) velocity fluctuation.

For the one-electrode actuators, a strong single vortex was generated near the actuator that entrained only the flow close to the walls (Fig. IV.7a). Note that the actuator is positioned in the same location across all plots and their respective schematic. A highly concentrated vortex was clearly visible near the location of the actuator interface where the plasma-induced wall jet is generated (Fig. IV.7c). As expected, this was also the location of maximum particle velocity (Fig. IV.7) and velocity fluctuation (Fig. IV.7d), indicating a higher degree of mixing.

When two-electrode actuators were used, the flow properties were more uniform within the entire cylindrical region (Fig. IV.8). However, unlike the single small, strong vortex close to the electrode in the one-electrode arrangement (Fig. IV.7c), two larger but comparatively weaker vortices were observed in the two-electrode arrangement (Fig. IV.8c).

Accordingly, when three electrodes were used, three vortices were observed—two of which were considerably smaller than the third (Fig. IV.9). The largest vortex at the center of the cylinder is presumed to influence the plasma-produced particles and redistribute them throughout the cross-section of the flow (Fig. IV.9c). This characteristic results in a more uniform distribution of plasma-generated reactive species and more efficient surface decontamination potential.

The jump to six electrodes continued this trend with the most complete redistribution of particles in the flow (Fig. IV.10). An increase in electrodes also comes

with an increase in locations for the induced flow to originate from. Characteristically, more electrodes contribute to an increase in plasma surface area and volume, resulting in a higher concentration of reactive species in the flow.

These results suggested that increasing the number of electrodes and strategic positioning of the electrodes allows greater circulation and promotes better distribution of the induced airflow. Increasing the number of electrodes resulted in increased airflow uniformity and greater airflow mixing within the entire cylindrical region (Figs. IV.10a to IV.10d). This increased airflow uniformity may be attributed to the coupling of the flow of two adjacent opposite-acting actuators that result in a plasma jet directed perpendicularly to the surface. Increased mixing was primarily observed at the point of convergence of streamlines where the two vortices met (Figs. IV.8c and IV.9c). Thus, a higher number of vortices resulted in increased velocity variation and improved mixing tendencies (Fig. IV.10c).

Further analysis of the flow field without a cylindrical enclosure revealed that the flow is perpendicular to the cylindrical actuator surface and the vortices are a result of the obstruction formed by the remainder of the cylindrical enclosure formed by the transparent shell. These results suggested that increasing the number of electrodes and strategic positioning of the electrodes allows for an increased circulation and optimal mixing of the flow.

Bacterial Inactivation by Cylindrical SDBD Actuators

All four SDBD actuator arrangements, utilizing one, two, three, and six electrodes, reduced Salmonella enterica populations on the inoculated coverslips after four minutes of treatment. Average log CFU mL^{-1} reductions of Salmonella cells were 1.30, 1.54, 1.81, and 2.28 for the one-, two-, three-, and six-electrode actuator arrangements, respectively (Fig. IV.11). The average bacterial log reductions for the one-, three-, and six-electrode arrangements were significantly different from each other, while the log

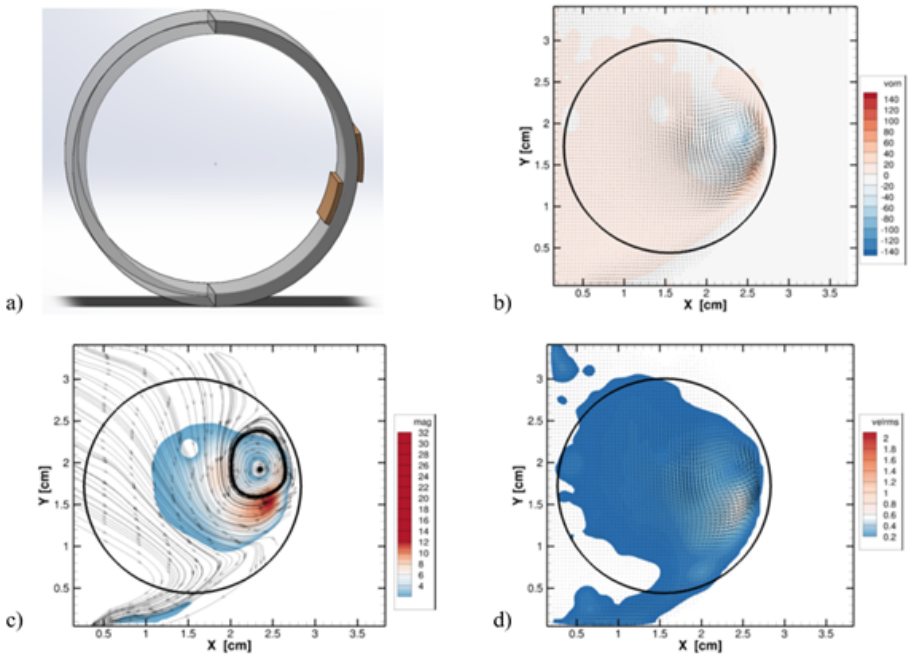

Figure IV.7: (a) Schematic of one electrode (1E) actuator (not to scale), (b) 1E vorticity plot, (c) 1E streamline and velocity magnitude plot, and (d) 1E RMS velocity plot.

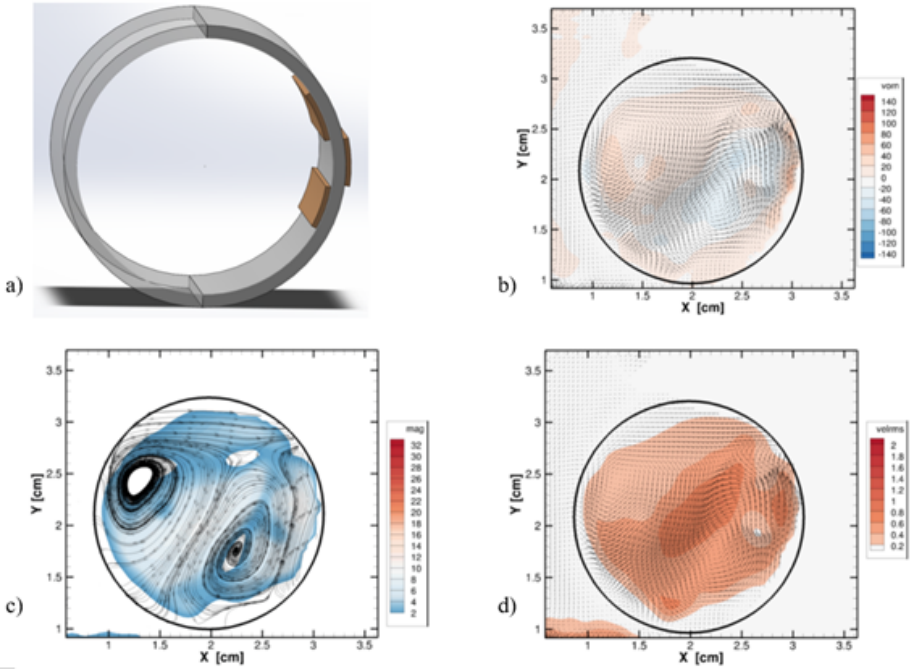

Figure IV.8: (a) Schematic of one electrode (2E) actuator (not to scale), (b) 2E vorticity plot, (c) 2E streamline and velocity magnitude plot, and (d) 2E RMS velocity plot.

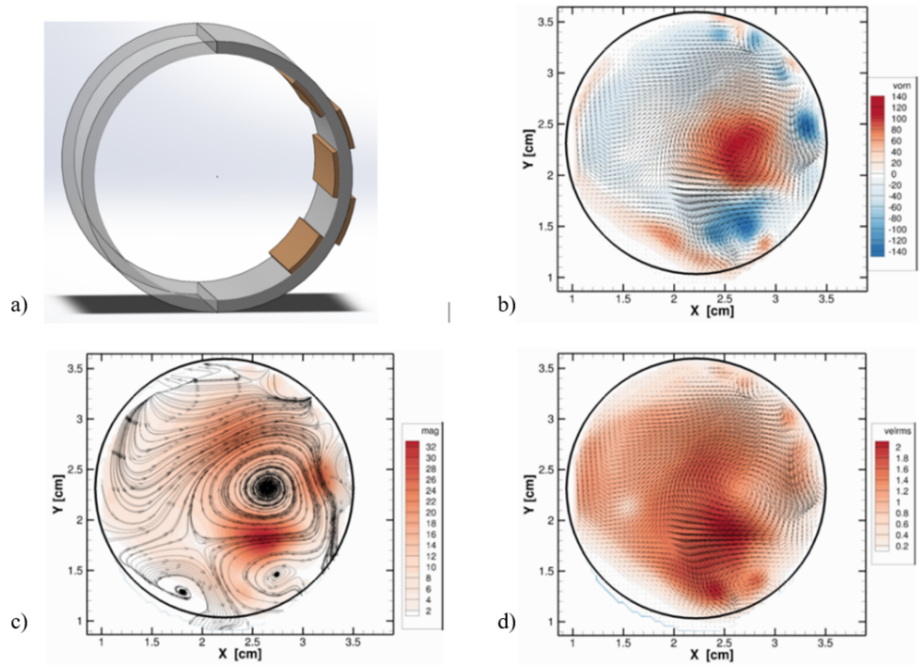

Figure IV.9: (a) Schematic of one electrode (3E) actuator (not to scale), (b) 3E vorticity plot, (c) 3E streamline and velocity magnitude plot, and (d) 3E RMS velocity plot.

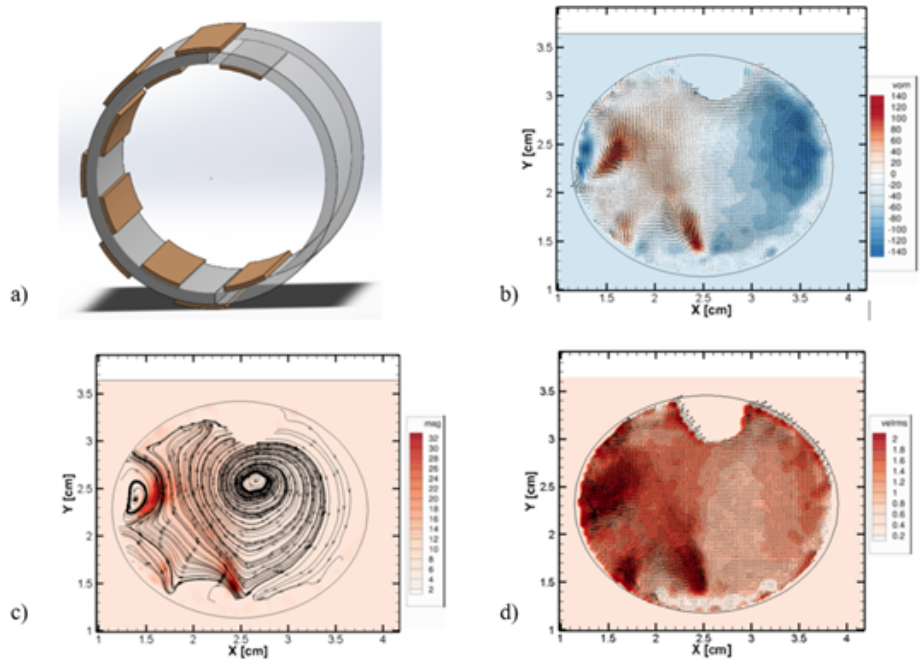

Figure IV.10: (a) Schematic of one electrode (6E) actuator (not to scale), (b) 6E vorticity plot, (c) 6E streamline and velocity magnitude plot, and (d) 6E RMS velocity plot.

reduction from the two-electrode arrangement was only significantly different from the six-electrode arrangement ($p \leq 0.05$). These data confirmed that the increase in induced airflow of SDBD actuators with increased numbers of electrodes correlates with increased bacterial inactivation. These results suggested that improved particle velocity, increased airflow mixing, and increased plasma volume resulted in increased surface decontamination efficiency. It should be noted that bacterial-inoculated coverslips were treated in line with the airflow and particle motion in this study. It is suspected that an increased bacterial reduction efficiency would have been observed if inoculated coverslips were placed perpendicular to the airflow and particle motion. A perpendicular orientation of contaminated substrate to plasma-induced airflow would allow a more direct bombardment of plasma-produced reactive species and would maximize the cell-damaging effects of these particles for surface decontamination applications.

A five-strain mixture of *Salmonella enterica* subspecies *enterica* (serovars Enteritidis, Typhimurium, Javiana, Seftenburg, and Poona) was used for inoculation of sterile glass coverslips, which were then placed in the center of cylindrical SDBD actuators with one, two, three, and six electrodes and treated for 4 min. Bacterial strains were grown aerobically overnight with shaking (250 rpm) at 37 °C in 5 mL tryptic soy broth (TSB, Difco, Sparks, MD, USA). The bacterial concentration of each overnight liquid culture was determined by serially diluting the culture in 0.1% (w/v) sterile peptone (Difco, Sparks, MD, USA) and plating in duplicate on tryptic soy agar (TSA, Difco, Sparks, MD, USA), incubated overnight at 37 °C.

To prepare the inocula, 1 mL of each liquid culture was centrifuged at 9000×g for 3 min and resuspended in 1 mL of 0.1% (w/v) sterile peptone before being combined with all other strains. In addition, 100 µL of the bacterial suspension (approximately 10^7 CFU) was used as inoculum and spotted in 20-25 spots (between 10^5 and 10^6 CFU/spot) onto single sterile 22×22 mm glass coverslips and dried in a biosafety

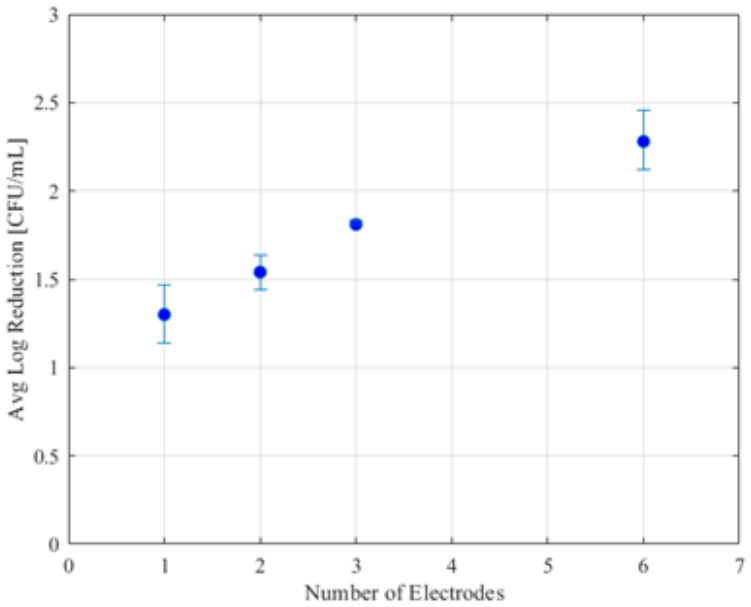

Figure IV.11: Average log reduction (CFU mL^{-1}) of Salmonella cells inoculated onto glass coverslips placed within SDBD actuators with one, two, three, and six electrodes and treated for four minutes.

cabinet for 90 min prior to cold plasma treatment. Immediately after cold plasma treatment, treated and untreated control inoculated coverslips were washed by vortexing for 30 s in 10 mL 0.1% (w/v) sterile peptone in 50 mL conical tubes. The wash fluid was ten-fold serially diluted in 0.1% peptone, and 100 μL of appropriate dilutions was plated in duplicate on TSA and incubated overnight at 37 °C.

Three biological repeats containing two replicates of each treatment were conducted. Log reductions due to plasma treatment were calculated by comparing the numbers of recovered cells from treated samples and untreated controls. Statistical difference was calculated between treated samples and untreated controls from plate counts by using analysis of variance (ANOVA) with SAS (Statistical Analysis System. Inst. Inc., Cary, NC, USA). A significant difference was defined at $p \leq 0.05$.

Mixing Analysis

The flow field data from the PIV measurements were taken an Lagrangian coherent structures (LCS) analysis was performed on it. A Matlab code written by the Dabiri Lab at the California Institute of Technology was used to perform the analysis [142]. Finite-Time Lyapunov Exponents (FTLE) are essentially a quantification of the separation of a flow. This was used as the output for the LCS analysis. The cylinder flow fields from the previous sections were used to calculate FTLE values across different number of electrodes. The flow fields gave a point with (x,y) coordinates along with their respective (u,v) velocities. Different mesh sizes were used to quickly calculate FTLE value or to thoroughly calculate them depending on resources.

Figures IV.12 and IV.13 are similar but it is clear that certain data is lost or found upon increasing mesh size. For the comparison analysis, a mesh size of 200x200 was used. Figure IV.14 showed that there is a linear increase in FTLE as the number of electrodes increases with the exception of 1E. As mentioned, FTLE quantified the separation at specific points based off of a time series of data inputted. When summing up all amounts of separation, 6E was found to have the most separation with 1E near it. It is possible that the differences were not appreciable for the effects on BI, additional testing is necessary. It is also possible that separation did not perfectly equate to mixing the species. Finally, there is the possibility that mixing did not have any effect on BI and the increase in BI found before was purely from plasma volume increase and thus higher species conversion.

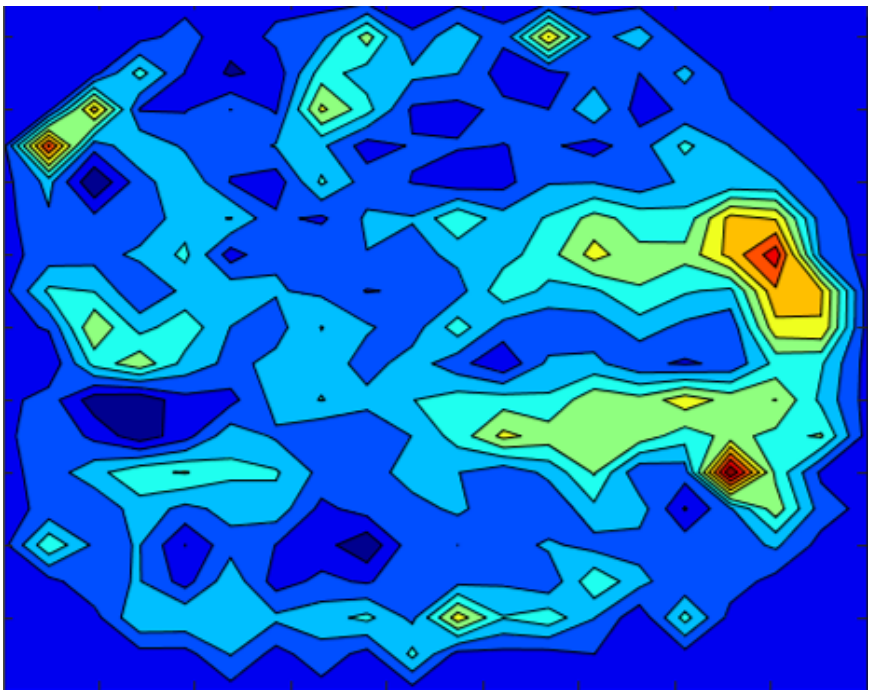

Figure IV.12: Contour plot showing FTLE values for 3E at a mesh size of 20x20.

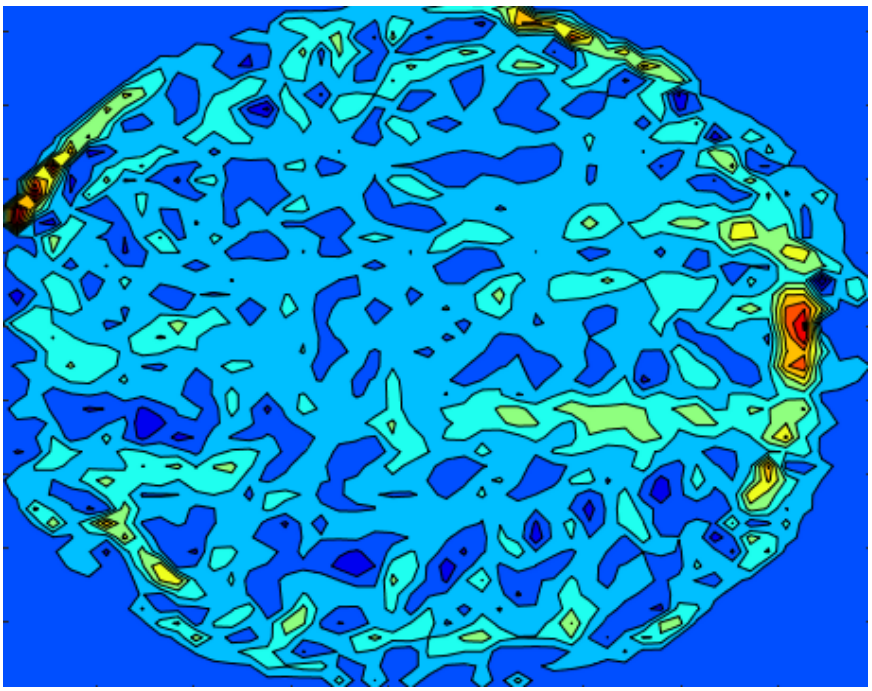

Figure IV.13: Contour plot showing FTLE values for 3E at a mesh size of 50x50.

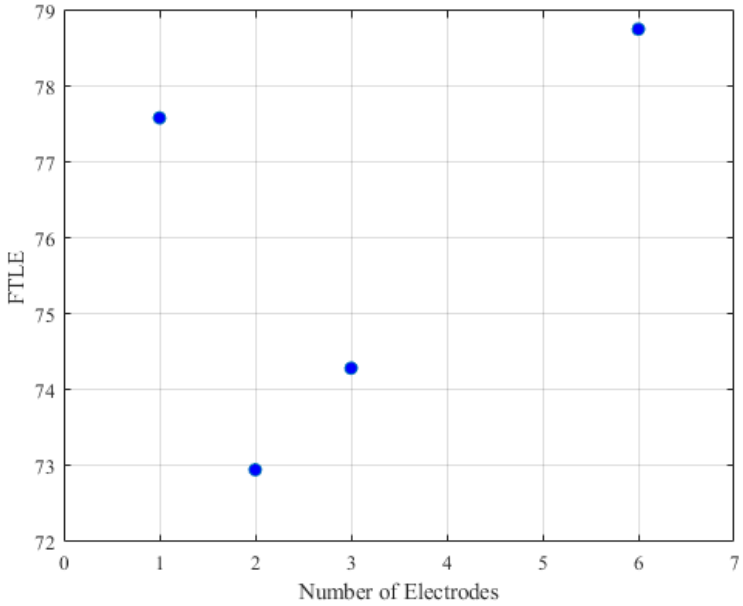

Figure IV.14: Plot of FTLE vs. number of electrodes.

4.4 Plasma Thread and Mesh

An interesting configuration that utilizes the uniqueness of surface discharge and its 'touchability' is the plasma thread and mesh design. The following section discusses preliminary experiments in characterizing these designs because of their potential for future biomedical applications.

4.4.1 Plasma Thread and Mesh Design

This study was based off a design in which two Teflon covered metal wires are twisted into a helical configuration, Fig. IV.15a. A line of intersection was twisted along the length of the wire. This is where plasma was formed. Further, the mesh design was created by weaving one strand of wire perpendicularly into another, rounding back after a set distance, creating many intersection points, Fig. IV.15b. For this project, 3×3 in^2 sized meshes were created. The final configuration design was modeled after a possible wound healing or dust mitigation application. By taking 3 sets of 3×3 in^2 mesh pieces, a cuff was formed, Figs. IV.16 and IV.24. The cylindrical design

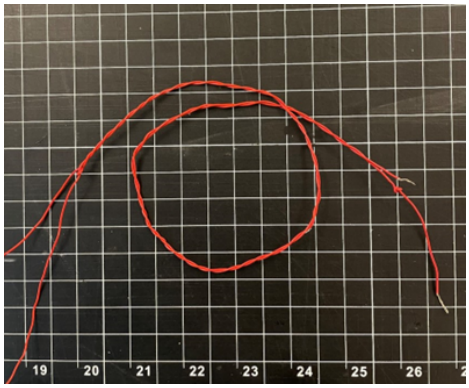

(a) Picture of the plasma helical thread.

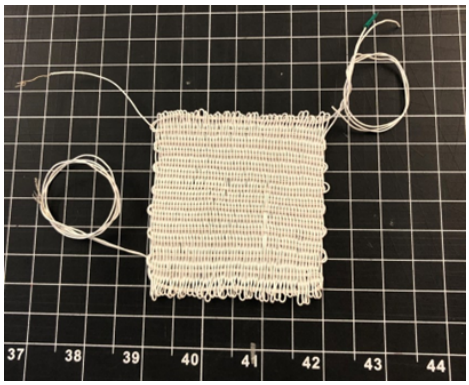

(b) Picture of the plasma mesh.

Figure IV.15: SDBD helical threads made from Teflon covered copper wires (left) and SDBD plasma mesh woven from Teflon covered copper wires (right).

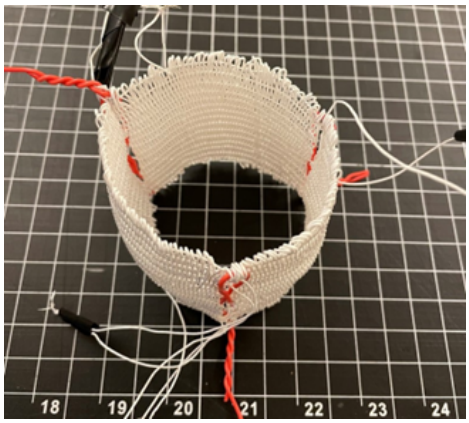

(a) Plasma Mesh 'Cuff' (Top View)

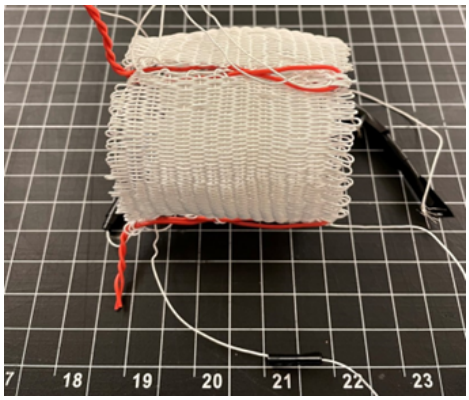

(b) Plasma Mesh 'Cuff (Side View)

Figure IV.16: Mockup of a 'cuff' design for wound healing or dust mitigation application.

was large enough to fit an average sized arm inside. The Teflon allowed for directly touching the mesh without being in danger of electrical shock.

4.4.2 Experiment Setup

All experiments were performed at the Oklahoma State University Advanced Technology Research Center in the Hydrodynamics and Aerodynamics Laboratory. The following setup was on an optics table with several grounds connected for safety. The setup for this experiment was a simple PIV arrangement consisting of a dual-pulsed Nd:YAG laser, a high speed camera, a pulse generator to synchronize between

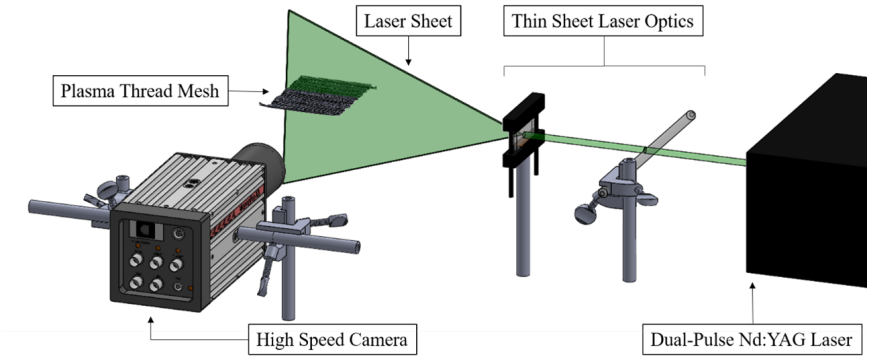

Figure IV.17: PIV setup for flow visualization around a plasma thread mesh.

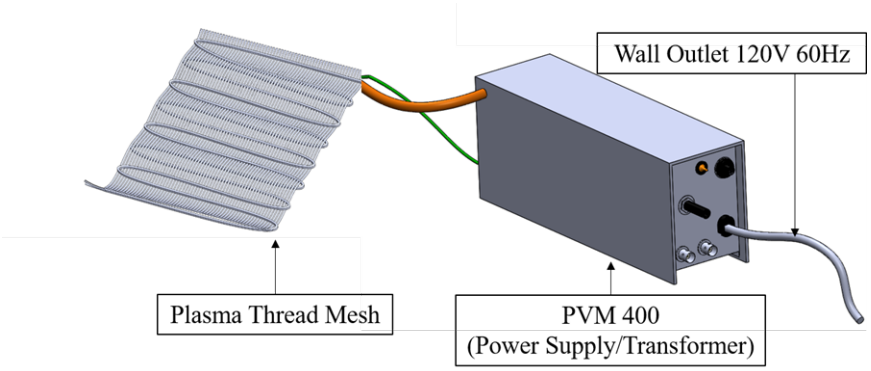

Figure IV.18: Schematic of the plasma mesh electronics setup.

the laser and camera, an optical setup to create and focus the laser sheet, and the plasma system, Fig. IV.17. The plasma system included a power supply/transformer combination, a microcontroller for duty cycle and frequency control, and the plasma actuator itself, Fig. IV.18. The high voltage transformer was an off-the-shelf plasma power supply from Information Unlimited, NH. With a microcontroller, the duty cycle was controllable, but was kept at a constant 'on' throughout this experiment.

4.4.3 Experiment Procedure

Due to the goal of the experiment mainly being qualitative and baseline feasibility, the procedure was relatively simple but repetitive. Each plasma configuration was tested at relatively similar primary side voltages until a uniform plasma distribution is seen on the actuator. The primary and secondary side voltages and currents were

measured. Initial tests started at a 100% duty cycle for simplicity. Each actuator had several PIV data sets to confirm findings. The procedure was performed as followed:

1. Turned on the plasma and reach a steady and uniform state. Noted the voltage and current on both the secondary and primary side of the plasma system upon reaching this point.

2. Held at this position for 30 seconds to allow for the flow to stabilize. Note, previous tests showed that the primary side voltage will steadily decrease over time.

3. Began the high-speed camera recording.

4. Performed PIV analysis.

5. Repeated steps 1-4 for several trials and take note of voltage and current changes.

6. Repeated steps 1-5 for each actuator configuration and mesh orientation.

4.4.4 Results and Discussion

In each of the following PIV result analyses and discussion, the laser sheet entered the frame from the right side, thus illuminating more seeding particles on that side. The camera was perpendicular to the one plane illuminated by the laser sheet. The circular aperture of the camera was visible in all the following images. The laser pulses were phase locked with the camera capture to ensure images at each laser pulse. The duty cycle of the plasma actuators were not phase locked in this case because they were not pulsed but kept running throughout the entire data capture sequence. Various locations have been masked out due to bright reflections generating arbitrary data. Due to the low velocity nature of the flows here, the time delay between laser pulses (and thus camera snapshots) dt was approximately 1000 ms. The PIV analysis was

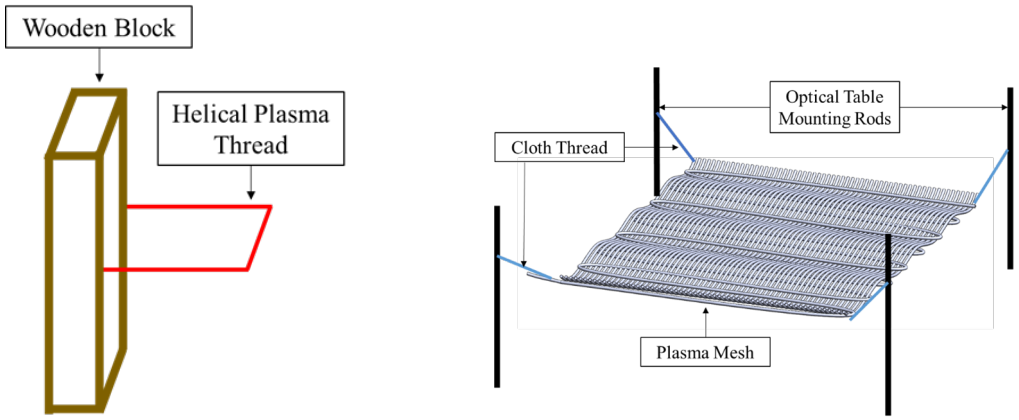

(a) Thread setup schematic. (b) Mesh setup schematic.

Figure IV.19: Low interference PIV setups for mounting the thread and mesh, respectively.

run with interrogation windows of 32×32 for the first pass and 24×24 for the second pass. Minimal amounts of pre- and post- processing was performed. The coloring scale of the vectors were arbitrarily maximized between the lowest and highest recorded values to better display visual differences in pixel displacement.

Plasma Thread

The first configuration was the plasma thread. In the results below, the plasma thread helix was mounted on a wooden block and viewed along the length of the helix, Fig. IV.19a. At each section of the helix was a different flow field cross section. In the plane viewed here, the flow is observed to flow upward directly adjacent above the helix. From this point, the flow began to form a vortex that flows clockwise upward and to the right of the helix, Fig. IV.20b. The flow strength was seen to be higher, closer to the helix while weakening away from the helix. The possibility that this was an artifact of the camera aperture should be noted. Initial thoughts were that the helix would form a vortex centered on the helix itself, but it was possible mounting setup affected the position of this vortex. Looking only at the raw footage, the vortex seemed to be in the same location the entire way along the helix, Fig. IV.20a. In all 3 trials performed on the plasma thread, the results were similar in that a vortex

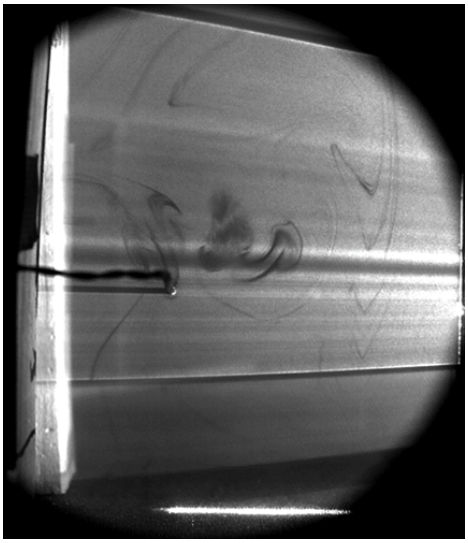

(a) Raw camera image of the flow.

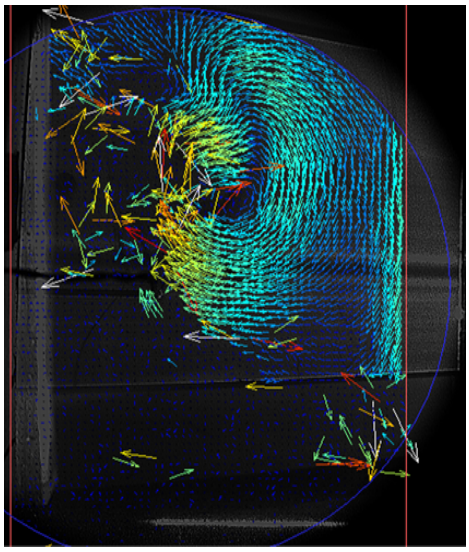

(b) PIV image of the instantaneous velocity field.

Figure IV.20: Raw image and vector field of the plasma thread flow field.

formed in a similar location with similar intensities. The average velocity field of the experiment displayed a milder version of the instantaneous velocity field, but similar trends and slightly lower vortex core, Fig. IV.21. Further investigation is required, but if the vortex location was controlled, this was a particularly useful find.

Plasma Mesh

The second configuration was the plasma mesh, Figs. IV.22 and IV.23. In the results below, each corner of the plasma mesh was mounted to an optical mounting rod directly inserted into an optical table, Fig. IV.19b. The mesh was mounted using cloth threads to prevent the conduction of current. The first notable trend was that there is an overall upward flow, Fig. IV.22a. The raw footage showed that flow is pulled in from the top right, top left, and bottom of the image. The flows on the topside of the mesh were moving faster than the flows below. All the flow was then forced directly upward with various fluctuations due to colliding flows, Fig. IV.22b. Vortices rolling up along the intersection points of the mesh were also visible in the raw footage and periodically show up in the PIV analysis. There is one section that

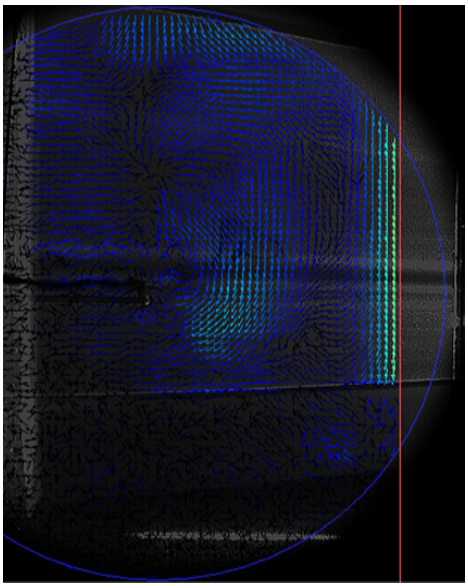

Figure IV.21: Average velocity field.

appeared unnaturally darker than the rest near the middle of the PIV analysis frame where the flow should look symmetric. This looked to be an artifact of the laser sheet coming in from the right of the frame and even when average over many frames still holds steady, Fig. IV.23b.

Plasma Cuff

The third configuration was the plasma cuff, Fig. IV.16. The plasma meshes were all connected in series thus requiring three times more power for the same level of plasma uniformity as the plasma mesh above. The cuff was also mounted in a similar method to the mesh so that it would be suspended. It should be noted that the plasma here in this image is safe to the touch and in these short duration experiments did not produce large amounts of heat. Unfortunately, the plan for this analysis was to utilize the light passing through the small holes in the mesh for PIV analysis, but there were not enough light particles. Streaks were visible in the raw image that illuminated the particles in the air/laser sheet, but there were not enough for a proper PIV analysis, Fig. IV.24a. In the future works section, a technique was described to attain this

(a) Raw camera image of the flow.

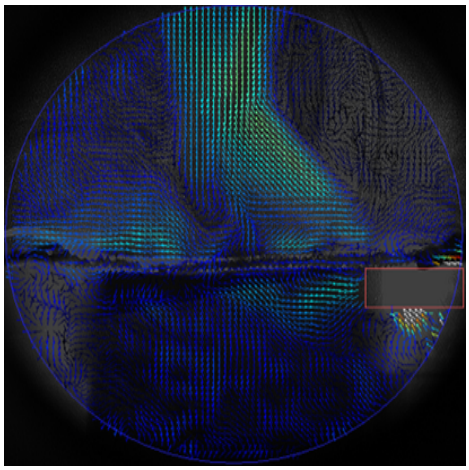

(b) PIV image of the instantaneous velocity field.

Figure IV.22: Raw image and vector field of the plasma thread flow field.

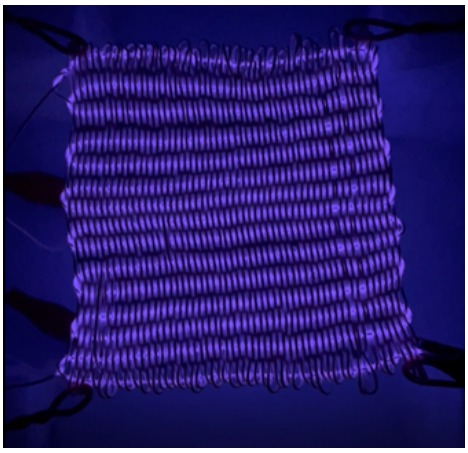

(a) Raw image of the mesh actuator 'on'.

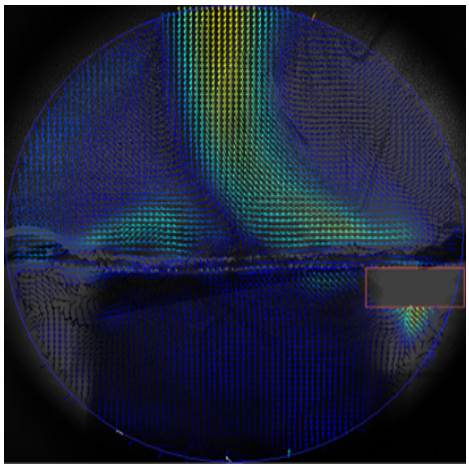

(b) PIV image of the average velocity field.

Figure IV.23: Images of an actuating and average velocity PIV images for the plasma mesh.

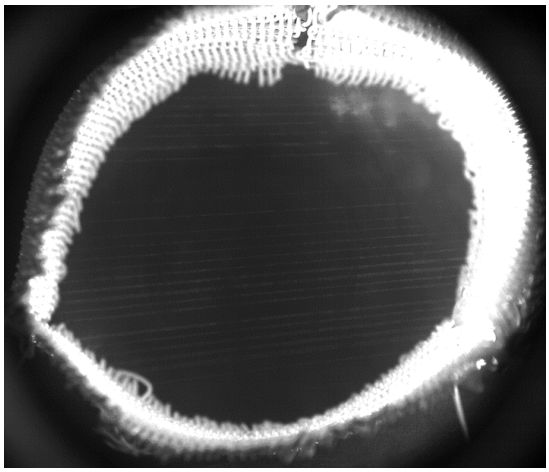

(a) Raw camera image of the plasma cuff prior to PIV testing.

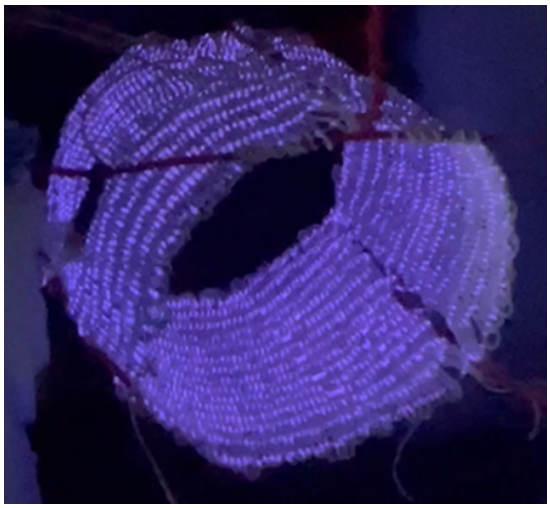

(b) Plasma cuff actuator on.

Figure IV.24: Plasma cuff actuated on and in position for PIV testing.

data at a later point in time.

4.5 Summary

4.5.1 Cylinders

In summary, using a cylindrical SDBD actuator, a correlation between an increase in the number of electrodes and an increase in the degree of mixing was observed. The increase in electrodes provides more wall locations for airflow to be entrained. Velocity fluctuations increased as well, which demonstrated a higher degree of particle redistribution within the airflow. The total number of vortices perceived within the cylindrical structure increased with more electrodes. The area between vortical structures caused the highest fluctuation in velocities, which potentially indicated mixing. Additionally, the increase in electrodes yielded an increase in total plasma surface area, which is observed to correlate with an increase in bacterial inactivation. More plasma species were generated by the higher plasma volume, and the bacterial inactivation efficiency of these species were enhanced due to the higher particle redistribution rate. A relative decrease in power per plasma surface area in the actuators

with more electrodes was not observed to play a role in plasma-based decontamination but needed to be analyzed for changes in the type of dominant species produced when higher power regimes are used. Increased power only produced streamers and heat in this study, which may not be beneficial for actuator longevity.

A cartoon schematic was illustrated below to summarize expected vortices from certain cylindrical electrode configurations (Fig. IV.25). In the case of an odd number of exposed electrodes, the imperfections in the electrodes have one side dominant, thus altered the positions of the expected vortices. In future studies, cylindrical structures could be further explored in cases of electrodes all the way around the cylinder with the jet vectors, all directed inward along with various combinations of laid along the wall to accelerate or interrupt the flow. In this study, in which a cylindrical configuration with an increased number of electrodes was used, a higher efficiency SDBD actuator in terms of degree of airflow mixing was possible for bacterial inactivation. Potential applications of these findings spanned multiple disciplines for surface decontamination of complex structures.

Finally, there were essentially 3 pieces affecting this current analysis: 1. electrodes or in essence plasma volume, 2. mixing (FTLE), and 3. microbial or specifically bacterial inactivation (or in our case the log reduction). The BI analysis resulted in a relationship between between plasma volume and BI efficacy. Note that there were differences in effects on mixing due to actuator geometry/position of the electrodes. The LCS plot displayed prior shows a relationship between plasma volume and mixing. And finally, the last portion should be a relationship between mixing and BI efficacy. This last portion should ideally be independent of volume. This analysis showed that there are several parameters that could be held static or varied in several different configurations to observe the combination or individual contributions of each. There was also positioning that definitely plays a complex role because of the 6E actuator covering half the entire actuator while the 1E only covers about 1/6

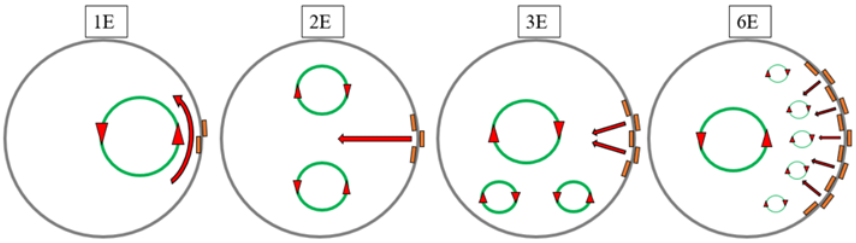

Figure IV.25: Cartoon schematic of expected vortices from one, two, three, and six electrode cylindrical actuators.

of that. Understanding this, there were several proposed works that stem from this analysis that will be discussed in the future works section.

4.5.2 Plasma Thread

One novel usage of the plasma thread in which it was designed for was to decontaminate subjects in tubes. By vortexing a test tube with a plasma helix in it, the reactive species would be able to sterilize or decontaminate seasonings or spices (smaller particulates in the order of 0.1-0.5mm) in tubes while utilizing the induced air flow generated by the helix to fill up the entire tube, leaving no stagnant points. The PIV results here showed that the vortex is indeed strongest near the helix, but the air affected extends out a sizeable range. This opens the possibility of using the thread as pillars/nodes within a structure to release and convert the air at those points into plasma species for decontamination. Note, for each experiment the resulting air vortex was above and adjacent to the thread rather than directly around it. This may be due to buoyancy effects as along with the semi-closed nature of the system. Though the system was partially isolated along the sides and the top, the bottom had a small opening that might have affected the results, though consistently. There have been several studies that discuss running into buoyancy effects created due to the heat dissipation from the plasma system [7, 71]. Though these plasma systems are not the same as the one here, there was no reason to not suspect similar effects due similar experimental conditions.

In the future, further tests on different cross sections of the helix as well as other custom configurations of the helix, such as a helix of the helix, could be explored for further complex geometrical flow fields. A setup in which the system was truly isolated would aid in confirming why the resulting vortex was not directly on the helix. Additionally, the temperature of the helix and the surrounding air could provide useful data in analyzing whether buoyancy effects were at play, though previous works suggest this as a real possibility. The thread is also small enough that it could slip into locations that many other plasma configurations cannot, such as endoscopes and other medical devices that are difficult to sterilize. Additionally, further analysis of the current data set in the form of derived quantities could be performed. This plasma thread was made with just two strands of Teflon covered copper thread. Having 2 sets of pairs wrapped around one another as well as having them counter rotating and adjacent could provide useful applications.

4.5.3 Plasma Mesh

From the results above it is evident that the flow is biased towards one side. We hypothesized that reversing the polarity of the current could alter this. The mesh in and of itself had many different forms, but one potential application was as a dust mitigation tool. By having something like this on a desirable surface, one actuation would repel charged particles away from the surface. Additionally, there are more complex methods of weaving that would allow for possible changes to the flow field such as having a 2:1 ratio for the positive:negative electrodes. This could bias the flow and allow for a controllable tilt in the flow field.

Pushing this concept further, by having multiple actuator setups in the same mesh, each controlled independently, it could be possible to have flow moving in one direction and immediately reverse the flow by changing the threads being powered. The flexibility of this technology is not simply in its geometry but also in its electrical

configuration. Further tests are required in to determine the charge polarity effects as well as the concept of thread power control. Similarly, to the plasma thread data, derived quantities such as total momentum flux at specific cross sections could be calculated based off the PIV data.

As with the plasma thread, buoyancy effects might have effected the plasma mesh as well. With the current configuration, it was difficult to tell if this is the case, but a piece of mesh that is side mounted and temperature readings would aid in properly isolating and characterize these conditions. There was also a consistent dark spot that could possibly be air that is rotating out of the frame that the PIV is consistently not picking up. Taking slices of the PIV at different positions into and out of the page would aid this or 3D PIV. The obvious usage of the mesh would be in 3D shapes like the plasma cuff.

4.5.4 Plasma Cuff

To successfully perform PIV analysis on the cuff, the laser sheet must be allowed to pass through the cuff. To do this, one of two methods could be used. Two smaller 1.5x3 in^2 sections could be mounted separately allowing the sheet to be squeezed in between them or the same cuff but with 2 cuffs side by side could be used. A clear, non-conductive material could be used to maintain the cylindrical shape of the actuator on the inside such as view foil.

Being designed as clothing, the plasma cuff is the closest to being a high-tech realistic application. The current limitations are portable power supplies that are efficient enough to not be cumbersome to carry but can still produce enough energy to power SDBDs. Additionally, the biological effects on bacteria, viruses, and cells in general are still thoroughly being researched. The parameters used to control the induced flow generated by the SDBD are also still being properly and fully characterized. If optimized for power miniaturization, safety, and consistency, this technology could

yield next level benefits for not just the biomedical industry but for many aerospace applications as well.

CHAPTER V

Closing

In this chapter we will summarize the results and findings of the two main chapters describing experiments, Chapter III and IV. Conclusions will be drawn and suggestions will be given after the summary. The aforementioned experiments have all been performed to determine the feasibility of an asymmetrically arranged SDBD actuator plasma system for wound care applications.

5.1 Summary and Conclusions

In Chapter I, we defined four objectives housed under an large plasma-system based goal within an overarching, ambitious goal for mankind. With enough time and effort in the form of several more studies involving cold plasma based wound care, the fabrication of a plasma system for wound care could be feasible. There are still requirements such as the assessment of good versus bad traits of PGS on good cells, a more in-depth analysis and isolation of confounding factors found in plasma treatment of live cells, and a dose dependent study for the control of these PGS. On an individual level, this paper served as a foundation for three different aspects of cold plasma wound care: 1. CAP interactions with various inanimate subtrates, 2. CAP interactions with organic substrates, 3. CAP interaction with blood, and 3. the evaluation of several geometries to improve the efficacy of plasma treatment for the proposed biological objectives.

In Chapter III, we utilized previously obtained design parameters to engineer

an open air asymmetrically arranged SDBD actuator plasma system. There were three sections to this chapter: inanimate substrates, mice skin, and blood. Testing procedures were adapted from previous experiments. The actuator was designed in Eagle and ordered. The housing unit for the actuator was 3D printed with Formlabs resin. All three experiments utilized the same plasma system. The results of the inanimate substrates experiment was that for *S. aureus* metal tabs had the highest average log reduction, followed by coverslips, and finally glass slides being similar to aluminum foil. Similar results were seen for *P. aeruginosa* but with on average higher log reduction. These results suggest that metal tabs, or stainless steel in this case specifically, works well as a substrate for more effective decontamination/sterilization plasma treatment. We have guesses that this increase in BI efficacy has to do with the plasma treatment effectively altering the substrate and causing it to become an inhospitable location microbes to proliferate. Additionally, MRSA is more resistant to decontamination plasma treatment when compared to *P. aeruginosa*. This is a consistent find with other studies and has to do with the gram-positive/gram-negative nature of the bacteria. We can say that a solid foundation has been defined for future studies that involve physical surface changes due to plasma and bacterial inactivation due to plasma. Objective 1 has been satisfied with the investigation of CAP and inanimate substrates.

Next we plasma treated mice skin and to see if there would be thermal or other physical damages. Our results were that there were no histological changes to the outer layer of the skin. We also looked at surface temperature changes on the inanimate substrates and determined that after a 5 minute plasma treatment the surface would reach a peak of 60°C. We can conclude that with our time frame, plasma treatment does not cause thermal damage to skin. With the observation of an organic substrate, we round off our substrates study with a preliminary experiment that works towards a wound healing model (possible murine model). This also satisfies

Objective 2.

Next we plasma treated anti-coagulated equine blood to observe its effects on the different blood cells: RBC, WBC, and platelets. The plasma system was the same as the previous 2 experiments, treatment regime was only observed at 0, 1, 2, and 5 minutes. This was because of the staining method needed to freeze the blood cells posttreatment. Additionally different treatment heights was tested, 0 and 1 inch from the surface. The results showed the treatment height did not change cell morphology or behavior. Additionally, no changes happened at 1 or 2 minutes of plasma treatment. By 5 minutes however, RBCs had begun experiencing oxidative stress and many were deemed irreparable to the point they would not function any longer. The neutrophils and eosinophils were essentially unchanged even when compared to the control at 0 minutes of exposure time. The platelets began aggregating and possible activating. We can conclude that plasma does indeed have an effect on blood morphology and behavior. When looking at specific cells, RBCs lose function earlier than WBCs which could potentially be a boon towards wound healing. Damaging WBCs could be a strike when it comes to wound care. As for the change in platelet behavior, plasma treatment has been known to induce coagulation. This could very well align with that theory. Overall, treatment on blood does not discount it as a possible pro in wound healing. The observation of blood is a critical part of understanding CAP for wound care. The initial observations have been made and overall judgments are given. This experiment satisfies initial requirements for Objective 3.

In Chapter IV, we performed several characterization experiments on different, potentially useful, geometries and configurations. We specifically worked on cylinders, threads, meshes, and cuffs. PIV analysis was combined with BI testing and an LCS analysis to determine whether cylinders yielded positive results towards BI efficacy. Though the study resulted in being inconclusive, it paved the way for the next cycle of testing to tie up loose ends. There is a possible co-dependency between plasma

volume, mixing, and BI. The results of the initial PIV test on cylinders was that 1E produced the highest magnitude velocity with one large vortex while 6E produce many small vortices with low magnitude velocities.

BI testing indicated that as the number of electrodes increased, so did the BI efficacy. Previous other previous works we know that there has been a relationship established between plasma volume and BI. This is because a larger plasma volume (even if it is at a lower intensity) converts more plasma species which results in increase BI efficacy. However, due to there being an element of mixing due to the actuator positions and the geometry of the actuator, there is inconclusive evidence that mixing could have played a role.

An LCS analysis was performed on the cylinder's velocity flow field PIV data. This resulted in linearly increasing FTLE numbers for electrodes 2, 3, and 6. 1E however, was an exception that had almost as high of an FTLE as 6E. We hypothesize that this is because there are no competing flows in 1E so the air inside the cylinder just spins quickly (highest velocity magnitude) around and around causing a large deal of separation to occur overall. We suggest from this that FTLE is proportional to the number of electrodes save for the special case of 1E.

Lastly, PIV tests were done on the plasma thread, mesh and cuff. The cuff tests were incomplete because of seeding issues, but the thread and mesh show expected results. The thread generated a vortex a little way adjacent to it with fairly high magnitude. The mesh functioned as many surface discharge actuator in series and gather all the flow and pushed it in one summed direction. The BI and mixing analysis of cylindrical actuators amongst other geometries starts the dive into possibly more efficient geometries and configurations for an SDBD based wound care device, thus satisfying Objective 4.

Overall, the four defined objectives have been given foundations for further elaboration through additional future studies/experiments or have been satisfied for an

initial investigation. Progress has been made towards the overall goal of a cold plasma based wound care device, but certain steps will be necessary to continue the development of this technology.

5.2 Future Work Suggestions

5.2.1 Research Suggestions

From the work described above, there are many different pathways to pursue.

Substrates: It is clear that substrates alter the BI efficacy of plasma treatment. The next step would be either 1. test different substrates but of the same material, e.g. different types of stainless steel, or 2. determine why a certain material is more or less effective based off of parametric guesses. Plasma treatment is sometimes used for surface modification [57, 73, 27]. Various parameters like contact angle and deposition of materials could be reasons for increased BI efficacy. These are also conjointly related to humidity, pressure, and temperature. These involve changing the PGS created and control of what is and is not affected. A study that surrounds observing the materials pre- and post-treatment from an electron microscopy stand point would provide an effective foundation into characterizing changes in contact angle/material deposition.

It should be noted that wood was attempted as a substrate but the inoculation of a wet bacteria sample made recovery on the wood difficult and inconsistent. Wood is a commonly found substrate that should be explored for its effects as a substrate. The attempt was performed with and without drying the wood post-inoculation. Aside from wood, other new generation materials should be tested as well such as titanium, gold, platinum, cobalt chrome, copper, or even magnesium-based materials. The wear down of these materials should also be a point to consider. After multiple treatments, how is the material affected in terms of BI efficacy?

Additionally, as mentioned in the discussion of Chapter III, there are several direct means of improving the experiment. Although utilizing log reduction was a quick method of determining cell count, it is an estimation of powers of 10

bacteria colonies. Because of this, a better method for counting cells should be used if the resources were available for a more detailed bacteria count. This would prevent the problem of having 0 SE appear in the case of *P. aeruginosa* for the substrates experiment allowing for more accurate portrayal of cell death due to plasma treatment. The experiment described here was not a dosage dependent study, which would significantly improve the usefulness of the data. Temperature was an after product of the treatment that was only controlled to a minor extent. Future studies should attempt to further mitigate temperature effects due to its effects on the species generated, the movement of the species, and the possible hazard to the sample/subjects.

Wound Model: Moving forward from mice skin would be a skin wound or some type of wound model. Although a live wound model is preferred and required eventually, a preliminary wound model in the form of just epithelial cells would suffice for initial tests with surface discharge [91, 136]. Several studies by other authors have shown the effectiveness of murine models for demonstrating the effectiveness of wound care related technologies. Thus it is suggested that a murine model would be a great stepping stone towards equine models and eventually human models.

The wound models would start with a simple separated layer of cells that would be observed over a period of time for cell migration. A dose dependent study could be done on this simple model and slowly upgraded in terms of cell layer thickness. The migration rate could be compared pre- and posttreatment to estimate the efficacy of CAP for healing breaks in skin. This study could be pushed further by "infecting" the model with bacteria and observing the cell migration pre- and posttreatment as a representation of an infected wound. Here, the decontamination aspect of CAP could be quantified and determined to be supportive or resistive of wound healing. For each increase in complexity

of wound models, epithelial cell models → murine models → feline/porcine models → equine/bovine models → human models, the effects of cells migration would be a strong place to start because of the lesser invasive nature of skin experiments versus the other phases of wound healing. The bacteria used to "infect" the model could also be slowly upgraded in terms of its ability to mutate and become chemically resistant. The degree to which CAP is effective on chemically resistant infections is theorized and proven to a certain extent, but not well quantified and if characterized could prove to be monumental for CAP based treatments.

To improve the mice skin study itself, a controlled look at the bacteria on the skin pre- and post-treatment would be enlightening. The main issue before was that there was a significant amount of uncontrolled bacteria already present on the skin. In an improved study, a set amount could be placed on a certain location, treated with plasma, and recovered posttreatment. Additionally, a time sensitive study, or dosage dependent study, would prove very useful to observe changes to the skin in more extreme conditions over time.

Blood: With the main subject of wound healing in mind, testing whether the different blood cells still function post plasma treatment would be an interesting first step. Isolating the specific blood cell types and treating them individually and testing their function afterwards could yield valuable results [9, 112, 130, 134]. By individually looking at how CAP treatment affects red blood cells, white blood cells, and platelets, the total effectiveness of CAP for wound healing especially in terms of blood interactions could be quantified. The degree of platelet aggregation and activation as well as the amount of remaining functionality of white blood cells posttreatment would be pivotal in the development of a CAP wound care device. Quantifying and consequently answering the question of

whether CAP does more harm than good would provide a solid foundation for future technology funding and development.

Next, testing the coagulation rate of blood post plasma treatment would give a more quantifiable answer to whether plasma is good for coagulation or not. This could be done through thromboelastography (TEG) [20, 52]. Determining the rate of coagulation and whether it is feasible to control its rate would help determine what applications are feasible. A steep increase in coagulation rate could be useful in time sensitive scenarios such as war-time triage, 3rd world country applications, etc. Applications in which the treatment would need to be quick and effective to multiple samples would be the target here.

Cylinders: Continuing with the discussion that was started in the cylinder's results section, to properly close out and understand the relationship between the three components (plasma volume, mixing, and BI), a few more steps need to be completed.

1. Do an experiment in which mixing is taken out of the equation with a force stronger than the actuator and observe the relationship between plasma volume and BI efficacy. This will fundamentally be the same as a BI efficacy test on any geometry because the cylindrical shape was only present to induce mixing. This experiment will essentially be the control and baseline, but should be proven none-the-less.
2. Do an experiment with similar plasma volumes but control the mixing with an outside source, could be a fan or some rotating object. Increment the mixing speed to observe the relationship between mixing and BI efficacy. A larger mixing force would effectively eliminate the interference of the smaller mixing due to the actuators.
3. Do an investigation into whether the cylinder itself provides an adequate

amount of mixing to warrant its design versus other geometries that provide more erratic mixing e.g. a box. This parameter is abstract but would determine if increasing locations of stagnation within a similar volume of space would affect the BI efficacy.

4. Do an investigation into other curved structures with added benefits e.g. a cone for added directional control of the species. This experiment will have several difficult to control parameters, but one parameter to toggle could be the distance from the testing surface.

5. Do a comprehensive study on plasma intensity versus BI efficacy. This can be done by utilizing previous methods such as OIA [116]. By measuring the optical output of the actuator, they can be quantitatively compared with their BI efficacy.

These experiments will complete the triangle that is 1. number of electrodes has a correlation to an increase in mixing, 2. mixing has a correlation to BI efficacy, and 3. number of electrodes has a correlation to BI efficacy.

Thread, Mesh, and Cuff: These three geometries have promise for biomedical applications. For future work, all three of them could be tested for specific scenarios of either BI efficacy or promoting some type of wound healing.

By configuring pairs of thread to be co/counter-rotating there are several applications that can be tested and then up-scaled. Adding single strands to adjust the polarity also adds an avenue that could alter the electric field and thus the flow field generated. Connecting the thread to a free spinning wheel would allow for possibly more decontamination in powders/smaller particulates.

The mesh has several aerospace applications centered around dust mitigation. The technology involves utilizing electron charges so experiments pertaining to polarity control and electric field strength and direction would benefit this study.

Weaving the mesh with a 2-to-1 ratio of threads or even creating different weave patterns could change the resulting electric field. A circular pattern versus a rectangular stitch pattern could result in varying control of the electric field.

For the cuff, a PIV analysis on it would be interesting to see. It is possible that the species will be self contained and pushed inward towards the wearer if the outside is encapsulated. Developing a cuff large enough for wound models would be a large step in developing this technology and preparing it for wound model testing.

5.2.2 Design Consideration Suggestions

For design considerations, there are several suggestions that arose from the experiments above. For many of the tests, heat build on the actuator was a problem. Even if the radiative heat was not enough to cause damage to surface samples, the actuator would have to be replaced often because of damage to itself. A housing device with more more airflow and heat sinks on the actuator would help keep the actuator cooler for prolonged use. In addition to this, the electrode wires were too close to each other and caused losses in energy when plasma was formed between the wires in unwanted places. So, two separate channels made for each electrode would be beneficial in keeping excess plasma generation to a minimum V.1.

Redesigns of the bottom piece of the hand held device could come in handy especially for benchtop testing. A changeable bottom piece means most useful shapes can be 3D printed for the device. A cone for directing species or a space for exactly the height needed is possible Fig. V.2.

Additionally, a large and potentially wearable plasma cuff Fig. V.3. The cuff should be woven together from the start rather than made serially with mesh pieces. This is for aesthetics and seamless power connection.

As for housing device material, actuator material, or leveling material, The hous-

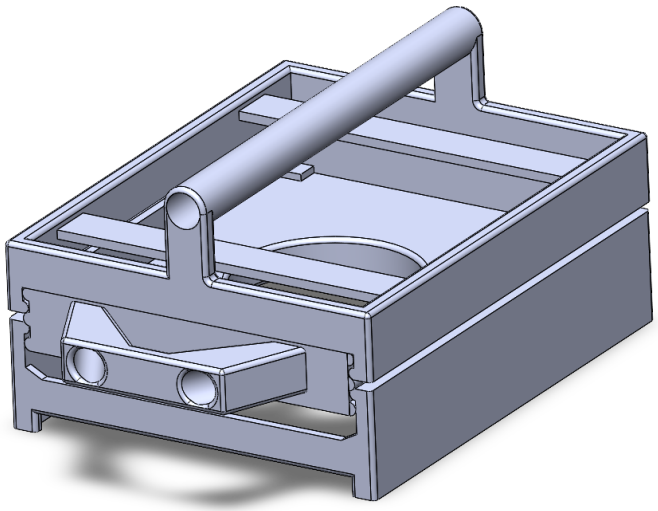

Figure V.1: Adjusted version of the handheld plasma device that aids in keeping temperature and excess plasma generation down.

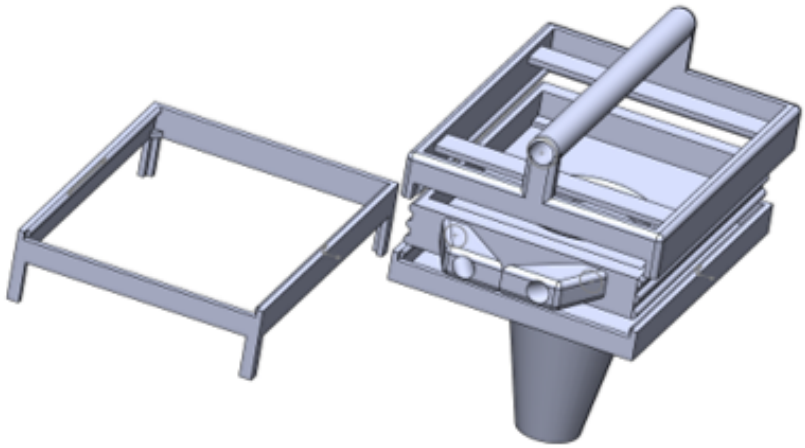

Figure V.2: CAD model that illustrates possible attachments to the handheld device that separates the actuator from the sample a specific distance or directs the samples.

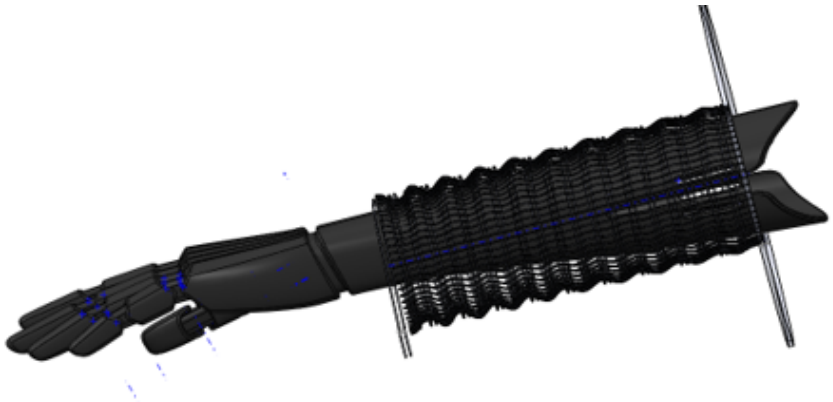

Figure V.3: An extended version of the current cuff. Ideally large enough to wear.

ing can remain something easily 3D manufacturable. Several more iterations will happened before the 'right' form factor is found. The current one material uses a normal black resin from FormLabs, but a transparent resin to look inside the device or high temperature resin to withstand damage over time. The actuator should remain close to the same, Teflon dielectric with copper electrodes covered with a solder mask.

REFERENCES

[1] Masao Akahane, Kazuhide Kanda, and Kichinosuke Yahagi, *Effect of dielectric constant on surface discharge of polymer insulators in vacuum*, Journal of Applied Physics **44** (1973), no. 6, 2927–2927.

[2] Meltem Y. Akbas and Murat Ozdemir, *Effect of gaseous ozone on microbial inactivation and sensory of flaked red peppers*, International Journal of Food Science and Technology **43** (2008), no. 9, 1657–1662.

[3] A. Aleinik, A. Baikov, G. Dambaev, E. Semichev, and P. Bushlanov, *Liver hemostasis by using cold plasma*, Surg Innov **24** (2017), no. 3, 253–258.

[4] J. J. Allen and M. S. Chong, *Vortex formation in front of a piston moving through a cylinder*, Journal of Fluid Mechanics **416** (2000), 1–28.

[5] M. R. Amini, M. Sheikh Hosseini, S. Fatollah, S. Mirpour, M. Ghoranneviss, B. Larijani, M. R. Mohajeri-Tehrani, and M. R. Khorramizadeh, *Beneficial effects of cold atmospheric plasma on inflammatory phase of diabetic foot ulcers; a randomized clinical trial*, J Diabetes Metab Disord **19** (2020), no. 2, 895–905.

[6] C. A. Arias and B. E. Murray, *Antibiotic-resistant bugs in the 21st century–a clinical super-challenge*, N Engl J Med **360** (2009), no. 5, 439–43.

[7] Ender H. Arserim, Deepti Salvi, Gregory Fridman, Donald W. Schaffner, and Mukund V. Karwe, *Microbial inactivation by non-equilibrium short-pulsed atmospheric pressure dielectric barrier discharge (cold plasma): Numerical and experimental studies*, Food Engineering Reviews **13** (2020), no. 1, 136–147.

[8] M. Asadian, K. V. Chan, M. Norouzi, S. Grande, P. Cools, R. Morent, and N. De Geyter, *Fabrication and plasma modification of nanofibrous tissue engineering scaffolds*, Nanomaterials (Basel) **10** (2020), no. 1, 63.

[9] H. K. Ashar, N. C. Mueller, J. M. Rudd, T. A. Snider, M. Achanta, M. Prasanthi, S. Pulavendran, P. G. Thomas, A. Ramachandran, J. R. Malayer, J. W. Ritchey, R. Rajasekhar, V. T. K. Chow, C. T. Esmon, and N. Teluguakula, *The role of extracellular histones in influenza virus pathogenesis*, Am J Pathol **188** (2018), no. 1, 135–148.

[10] N. Y. Babaeva and G. V. Naidis, *Modeling of plasmas for biomedicine*, Trends Biotechnol **36** (2018), no. 6, 603–614.

[11] Qin Bai-Lin, Zhang Qinghua, G. V. Barbosa-Canovas, B. G. Swanson, and P. D. Pedrow, *Inactivation of microorganisms by pulsed electric fields of different voltage waveforms*, IEEE Transactions on Dielectrics and Electrical Insulation **1** (1994), no. 6, 1047–1057.

[12] Tae-Yeong Bak, Min-Suk Kook, Sang-Chul Jung, and Byung-Hoon Kim, *Biological effect of gas plasma treatment on co2gas foaming/salt leaching fabricated porous polycaprolactone scaffolds in bone tissue engineering*, Journal of Nanomaterials **2014** (2014), 1–6.

[13] Orianne Bastin, Max Thulliez, Jean Servais, Antoine Nonclercq, Alain Delchambre, Alia Hadefi, Jacques Devière, and François Reniers, *Optical and electrical characteristics of an endoscopic dbd plasma jet*, Plasma Medicine **10** (2020), no. 2, 71–90.

[14] K. W. Bayles, *Bacterial programmed cell death: making sense of a paradox*, Nat Rev Microbiol **12** (2014), no. 1, 63–9.

[15] Sander Bekeschus, Anke Schmidt, Klaus-Dieter Weltmann, and Thomas von Woedtke, *The plasma jet kinpen – a powerful tool for wound healing*, Clinical Plasma Medicine **4** (2016), no. 1, 19–28.

[16] N. Bellakhal and M. Dachraoui, *Study of the benzotriazole efficiency as a corrosion inhibitor for copper in humid air plasma*, Materials Chemistry and Physics **85** (2004), no. 2-3, 366–369.

[17] T. Bernhardt, M. L. Semmler, M. Schafer, S. Bekeschus, S. Emmert, and L. Boeckmann, *Plasma medicine: Applications of cold atmospheric pressure plasma in dermatology*, Oxid Med Cell Longev **2019** (2019), 3873928.

[18] Annemie Bogaerts, *Glow discharge mass spectrometry, methods*, pp. 669–676, Wiley Analytical Science, 1999.

[19] Michael Bolitho and Jamey Jacob, *Thrust vectoring flow control using plasma synthetic jet actuators*, 2008.

[20] D. Bolliger, M. D. Seeberger, and K. A. Tanaka, *Principles and practice of thromboelastography in clinical coagulation management and transfusion practice*, Transfus Med Rev **26** (2012), no. 1, 1–13.

[21] Corina Bradu, Kinga Kutasi, Monica Magureanu, Nevena Puač, and Suzana Živković, *Reactive nitrogen species in plasma-activated water: generation, chemistry and application in agriculture*, Journal of Physics D: Applied Physics **53** (2020), no. 22, 1.

[22] R. N. Franklin Braithwaite and N. St J, *80 years of plasma*, Plasma Sources Science and Technology **18** (2009), no. 1, 4.

[23] Roy H. Burdon, *Superoxide and hydrogen peroxide in relation to mammalian cell proliferation*, Free Radical Biology and Medicine **18** (1995), no. 4, 775–794.

[24] J.B. Calvert, *Electrical discharges*, 2005.

[25] John A. Carlisle and Orlando Auciello, *Ultrananocrystalline diamond properties and applications in biomedical devices*, The Electrochemical Society Interface **12** (2003), no. 1, 28–31.

[26] Armando J. Castro, Gustavo V. Barbosa-CÁNovas, and Barry G. Swanson, *Microbial inactivation of foods by pulsed electric fields*, Journal of Food Processing and Preservation **17** (1993), no. 1, 47–73.

[27] V. Cech, R. Prikryl, R. Balkova, A. Grycova, and J. Vanek, *Plasma surface treatment and modification of glass fibers*, Composites Part A: Applied Science and Manufacturing **33** (2002), no. 10, 1367–1372.

[28] The Tu Chau, Kwan Chi Kao, Gregory Blank, and Francisco Madrid, *Microwave plasmas for low-temperature dry sterilization*, Biomaterials **17** (1996), no. 13, 1273–1277.

[29] Thomas C. Corke, C. Lon Enloe, and Stephen P. Wilkinson, *Dielectric barrier discharge plasma actuators for flow control*, Annual Review of Fluid Mechanics **42** (2010), no. 1, 505–529.

[30] P. Cornejo-Juarez, D. Vilar-Compte, C. Perez-Jimenez, S. A. Namendys-Silva, S. Sandoval-Hernandez, and P. Volkow-Fernandez, *The impact of hospital-acquired infections with multidrug-resistant bacteria in an oncology intensive care unit*, Int J Infect Dis **31** (2015), 31–4.

[31] M. E. de Kraker, A. J. Stewardson, and S. Harbarth, *Will 10 million people die a year due to antimicrobial resistance by 2050?*, PLoS Med **13** (2016), no. 11, e1002184.

[32] M. de la Guardia and S. Armenta, *Avoiding sample treatments*, Comprehensive Analytical Chemistry, pp. 59–86, Wiley, 2011.

[33] Danil Dobrynin, Kimberly Wasko, Gary Friedman, Alexander A. Fridman, and Gregory Fridman, *Fast blood coagulation of capillary vessels by cold plasma: A rat ear bleeding model*, Plasma Medicine **1** (2011), no. 3-4, 241–247.

[34] Chang Ming Du, Jing Wang, Lu Zhang, Hong Xia Li, Hui Liu, and Ya Xiong, *The application of a non-thermal plasma generated by gas–liquid gliding arc discharge in sterilization*, New Journal of Physics **14** (2012), no. 1, 19.

[35] Sunil Kumar Dubey, Shraddha Parab, Amit Alexander, Mukta Agrawal, Vaishnav Pavan Kumar Achalla, Udit Narayan Pal, Murali Monohar Pandey, and Prashant Kesharwani, *Cold atmospheric plasma therapy in wound healing*, Process Biochemistry **112** (2022), 112–123.

[36] Alan H. Duong, Thomas C. Corke, and Flint O. Thomas, *Characteristics of drag-reduced turbulent boundary layers with pulsed-direct-current plasma actuation*, Journal of Fluid Mechanics **915** (2021), –.

[37] S. Eliezer and Y. Eliezer, *The fourth state of matter: an introduction to plasma science*, CRC Press, 2001.

[38] C. L. Enloe, Thomas E. McLaughlin, Robert D. VanDyken, K. D. Kachner, Eric J. Jumper, and Thomas C. Corke, *Mechanisms and responses of a single dielectric barrier plasma actuator: Plasma morphology*, AIAA Journal **42** (2004), no. 3, 589–594.

[39] J. Espinel-Ruperez, M. D. Martin-Rios, V. Salazar, M. R. Baquero-Artigao, and G. Ortiz-Diez, *Incidence of surgical site infection in dogs undergoing soft tissue surgery: risk factors and economic impact*, Vet Rec Open **6** (2019), no. 1, e000233.

[40] A. Filipic, I. Gutierrez-Aguirre, G. Primc, M. Mozetic, and D. Dobnik, *Cold plasma, a new hope in the field of virus inactivation*, Trends Biotechnol **38** (2020), no. 11, 1278–1291.

[41] Christophe Fleury, Bernard Mignotte, and Jean-Luc Vayssière, *Mitochondrial reactive oxygen species in cell death signaling*, Biochimie **84** (2002), no. 2-3, 131–141.

[42] T. J. Foster, *Plasmid-determined resistance to antimicrobial drugs and toxic metal ions in bacteria*, Microbiol Rev **47** (1983), no. 3, 361–409.

[43] Alexander Fridman and Gary Friedman, *Plasma medicine*, 1 ed., Wiley, 2013.

[44] R. G. Frykberg and J. Banks, *Challenges in the treatment of chronic wounds*, Adv Wound Care (New Rochelle) **4** (2015), no. 9, 560–582, Frykberg, Robert G Banks, Jaminelli eng Review 2015/09/05 Adv Wound Care (New Rochelle). 2015 Sep 1;4(9):560-582. doi: 10.1089/wound.2015.0635.

[45] L. Gan, J. Jiang, J. W. Duan, X. J. Z. Wu, S. Zhang, X. R. Duan, J. Q. Song, and H. X. Chen, *Cold atmospheric plasma applications in dermatology: A systematic review*, J Biophotonics **14** (2021), no. 3, e202000415.

[46] Mohsen Gavahian, Yan-Hwa Chu, Amin Mousavi Khaneghah, Francisco J. Barba, and N. N. Misra, *A critical analysis of the cold plasma induced lipid oxidation in foods*, Trends in Food Science and Technology **77** (2018), 32–41.

[47] Valentin I. Gibalov and Gerhard J. Pietsch, *The development of dielectric barrier discharges in gas gaps and on surfaces*, Journal of Physics D: Applied Physics **33** (2000), no. 20, 2618–2636.

[48] M. T. Gillespie, J. W. May, and R. A. Skurray, *Plasmid-encoded resistance to acriflavine and quaternary ammonium compounds in methicillin-*

resistantstaphylococcus aureus, FEMS Microbiology Letters **34** (1986), no. 1, 47–51.

[49] B. F. Gilmore, P. B. Flynn, S. O'Brien, N. Hickok, T. Freeman, and P. Bourke, *Cold plasmas for biofilm control: Opportunities and challenges*, Trends Biotechnol **36** (2018), no. 6, 627–638.

[50] G. G. Ginsberg, A. N. Barkun, J. J. Bosco, J. S. Burdick, G. A. Isenberg, N. L. Nakao, B. T. Petersen, W. B. Silverman, A. Slivka, P. B. Kelsey, and Endoscopy American Society for Gastrointestinal, *The argon plasma coagulator: February 2002*, Gastrointest Endosc **55** (2002), no. 7, 807–10.

[51] Monireh Golpour, Mina Alimohammadi, Alireza Mohseni, Ehsan Zaboli, Farshad Sohbatzadeh, Sander Bekeschus, and Alireza Rafiei, *Lack of adverse effects of cold physical plasma-treated blood from leukemia patients: A proof-of-concept study*, Applied Sciences **12** (2021), no. 1, 1.

[52] E. Gonzalez, F. M. Pieracci, E. E. Moore, and J. L. Kashuk, *Coagulation abnormalities in the trauma patient: the role of point-of-care thromboelastography*, Semin Thromb Hemost **36** (2010), no. 7, 723–37.

[53] David B. Graves, *Reactive species from cold atmospheric plasma: Implications for cancer therapy*, Plasma Processes and Polymers **11** (2014), no. 12, 1120–1127.

[54] David Greenblatt, Berkant Goksel, Ingo Rechenberg, Chan Yong Schule, Daniel Romann, and Christian O. Paschereit, *Dielectric barrier discharge flow control at very low flight reynolds numbers*, AIAA Journal **46** (2008), no. 6, 1528–1541.

[55] Kenneth Grossman, Cybyk Bohdan, and David VanWie, *Sparkjet actuators for flow control*, 2003.

[56] B. Haertel, T. von Woedtke, K. D. Weltmann, and U. Lindequist, *Non-thermal atmospheric-pressure plasma possible application in wound healing*, Biomol Ther (Seoul) **22** (2014), no. 6, 477–90.

[57] J. Richard Hall, Carolyn A. L. Westerdahl, Andrew T. Devine, and Michael J. Bodnar, *Activated gas plasma surface treatment of polymers for adhesive bonding*, Journal of Applied Polymer Science **13** (1969), no. 10, 2085–2096.

[58] G. Han and R. Ceilley, *Chronic wound healing: A review of current management and treatments*, Adv Ther **34** (2017), no. 3, 599–610.

[59] L. Han, S. Patil, D. Boehm, V. Milosavljevic, P. J. Cullen, and P. Bourke, *Mechanisms of inactivation by high-voltage atmospheric cold plasma differ for escherichia coli and staphylococcus aureus*, Appl Environ Microbiol **82** (2016), no. 2, 450–8.

[60] Ronald Hanson, Joel Kimelman, and Philippe Lavoie, *Effect of dielectric degradation on dielectric barrier discharge plasma actuator performance*, 2013.

[61] Liming He, Yi Chen, Jun Deng, Jianping Lei, Li Fei, and Pengfei Liu, *Experimental study of rotating gliding arc discharge plasma-assisted combustion in an aero-engine combustion chamber*, Chinese Journal of Aeronautics **32** (2019), no. 2, 337–346.

[62] Mengwen He, Jiangwei Duan, Jialu Xu, Mingyu Ma, Bao Chai, Guangyuan He, Lu Gan, Song Zhang, Xiaoru Duan, Xinpei Lu, and Hongxiang Chen, *Candida albicans biofilm inactivated by cold plasma treatment in vitro and in vivo*, Plasma Processes and Polymers **17** (2020), no. 4, 1.

[63] Dirk Hegemann, Herwig Brunner, and Christian Oehr, *Plasma treatment of polymers for surface and adhesion improvement*, Nuclear Instruments and

Methods in Physics Research Section B: Beam Interactions with Materials and Atoms **208** (2003), 281–286.

[64] B. Hota, *Contamination, disinfection, and cross-colonization: are hospital surfaces reservoirs for nosocomial infection?*, Clin Infect Dis **39** (2004), no. 8, 1182–9.

[65] U.S. Inan and M. Golkowski, *Principles of plasma physics for engineers and scientists*, Cambridge University Press, 2011.

[66] A. L. Isaac, *Addressing complications with negative pressure wound therapy use*, 2019.

[67] G. Isbary, G. Morfill, H. U. Schmidt, M. Georgi, K. Ramrath, J. Heinlin, S. Karrer, M. Landthaler, T. Shimizu, B. Steffes, W. Bunk, R. Monetti, J. L. Zimmermann, R. Pompl, and W. Stolz, *A first prospective randomized controlled trial to decrease bacterial load using cold atmospheric argon plasma on chronic wounds in patients*, British Journal of Dermatology **163** (2010), no. 1, 78–82.

[68] J. Jeong, J. Y. Kim, and J. Yoon, *The role of reactive oxygen species in the electrochemical inactivation of microorganisms*, Environ Sci Technol **40** (2006), no. 19, 6117–22.

[69] Kenth S. Johansson, *Surface modification of plastics*, pp. 443–487, Wiley Analytical Science, 2017.

[70] S. G. Joshi, M. Paff, G. Friedman, G. Fridman, A. Fridman, and A. D. Brooks, *Control of methicillin-resistant staphylococcus aureus in planktonic form and biofilms: a biocidal efficacy study of nonthermal dielectric-barrier discharge plasma*, Am J Infect Control **38** (2010), no. 4, 293–301.

[71] Tim Jukes, Kwing-So Choi, Graham Johnson, and Simon Scott, *Turbulent boundary-layer control for drag reduction using surface plasma*, 2004.

[72] A. Jurov, S. Kos, T. Blagus, I. Sremacki, G. Filipic, N. Hojnik, A. Nikiforov, C. Leys, M. Cemazar, G. Sersa, and U. Cvelbar, *Atmospheric pressure plasma jet-mouse skin interaction: Mitigation of damages by liquid interface and gas flow control*, Biointerphases **17** (2022), no. 2, 021004, Jurov, Andrea Kos, Spela Blagus, Tanja Sremacki, Ivana Filipic, Gregor Hojnik, Natasa Nikiforov, Anton Leys, Christophe Cemazar, Maja Sersa, Gregor Cvelbar, Uros eng Research Support, Non-U.S. Gov't 2022/04/02 Biointerphases. 2022 Mar 31;17(2):021004. doi: 10.1116/6.0001596.

[73] S. L. Kaplan and P. W. Rose, *Plasma surface treatment of plastics to enhance adhesion*, International Journal of Adhesion and Adhesives **11** (1991), no. 2, 109–113.

[74] M. Keidar, R. Walk, A. Shashurin, P. Srinivasan, A. Sandler, S. Dasgupta, R. Ravi, R. Guerrero-Preston, and B. Trink, *Cold plasma selectivity and the possibility of a paradigm shift in cancer therapy*, Br J Cancer **105** (2011), no. 9, 1295–301.

[75] Michael Keidar, *Plasma for cancer treatment*, Plasma Sources Science and Technology **24** (2015), no. 3, 1.

[76] Hassan Ahmed Khan, Fatima Kanwal Baig, and Riffat Mehboob, *Nosocomial infections: Epidemiology, prevention, control and surveillance*, Asian Pacific Journal of Tropical Biomedicine **7** (2017), no. 5, 478–482.

[77] T. C. Killian, T. Pattard, T. Pohl, and J. M. Rost, *Ultracold neutral plasmas*, Physics Reports **449** (2007), no. 4-5, 77–130.

[78] J. G. Kim, A. E. Yousef, and S. Dave, *Application of ozone for enhancing the microbiological safety and quality of foods: a review*, J Food Prot **62** (1999), no. 9, 1071–87.

[79] B. Kleineidam, M. Nokhbehsaim, J. Deschner, and G. Wahl, *Effect of cold plasma on periodontal wound healing-an in vitro study*, Clin Oral Investig **23** (2019), no. 4, 1941–1950.

[80] S. Kos, T. Blagus, M. Cemazar, G. Filipic, G. Sersa, and U. Cvelbar, *Safety aspects of atmospheric pressure helium plasma jet operation on skin: In vivo study on mouse skin*, PLoS One **12** (2017), no. 4, e0174966, Kos, Spela Blagus, Tanja Cemazar, Maja Filipic, Gregor Sersa, Gregor Cvelbar, Uros eng 2017/04/06 PLoS One. 2017 Apr 5;12(4):e0174966. doi: 10.1371/journal.pone.0174966. eCollection 2017.

[81] A. Kramer, I. Schwebke, and G. Kampf, *How long do nosocomial pathogens persist on inanimate surfaces? a systematic review*, BMC Infect Dis **6** (2006), 130.

[82] Ya E. Krasik, A. Dunaevsky, and J. Felsteiner, *Formation of discharge plasma on the surface of cathodes with different dielectric constants*, Journal of Applied Physics **85** (1999), no. 11, 7946–7951.

[83] Jochen Kriegseis, Benjamin Möller, Sven Grundmann, and Cameron Tropea, *Capacitance and power consumption quantification of dielectric barrier discharge (dbd) plasma actuators*, Journal of Electrostatics **69** (2011), no. 4, 302–312.

[84] K. Krishnamurthy, A. Demirci, and J. Irudayaraj, *Inactivation of staphylococcus aureus by pulsed uv-light sterilization*, J Food Prot **67** (2004), no. 5, 1027–30.

[85] Spencer P. Kuo, *Air plasma for medical applications*, Journal of Biomedical Science and Engineering **05** (2012), no. 09, 481–495.

[86] M. Kurosawa, T. Takamatsu, H. Kawano, Y. Hayashi, H. Miyahara, S. Ota, A. Okino, and M. Yoshida, *Endoscopic hemostasis in porcine gastrointestinal tract using co(2) low-temperature plasma jet*, J Surg Res **234** (2019), 334–342.

[87] Jiangnan Lai, Bob Sunderland, Jianming Xue, Sha Yan, Weijiang Zhao, Melvyn Folkard, Barry D. Michael, and Yugang Wang, *Study on hydrophilicity of polymer surfaces improved by plasma treatment*, Applied Surface Science **252** (2006), no. 10, 3375–3379.

[88] Mounir Laroussi, *Plasma medicine: A brief introduction*, Plasma **1** (2018), no. 1, 47–60.

[89] Kyu-Hang Lee, Sichan Kim, Hyun Jo, Byung-Koo Son, Myung-Sun Shin, and Guangsup Cho, *Plasma skincare device based on floating electrode dielectric barrier discharge*, Plasma Science and Technology **21** (2019), no. 12, 1.

[90] Kyung Ha Lee, Hyun-Joo Kim, Koan Sik Woo, Cheorun Jo, Jae-Kyung Kim, Sae Hun Kim, Hye Young Park, Sea-Kwan Oh, and Wook Han Kim, *Evaluation of cold plasma treatments for improved microbial and physicochemical qualities of brown rice*, Lwt **73** (2016), 442–447.

[91] D. Lendeckel, C. Eymann, P. Emicke, G. Daeschlein, K. Darm, S. O'Neil, A. G. Beule, T. von Woedtke, U. Volker, K. D. Weltmann, M. Junger, W. Hosemann, and C. Scharf, *Proteomic changes of tissue-tolerable plasma treated airway epithelial cells and their relation to wound healing*, Biomed Res Int **2015** (2015), 506059.

[92] Z. Li and A. Yu, *Complications of negative pressure wound therapy: a mini review*, Wound Repair Regen **22** (2014), no. 4, 457–61.

[93] X. Liao, A. I. Muhammad, S. Chen, Y. Hu, X. Ye, D. Liu, and T. Ding, *Bacterial spore inactivation induced by cold plasma*, Crit Rev Food Sci Nutr **59** (2019), no. 16, 2562–2572.

[94] M.A. Lieberman and A.J. Lichtenberg, *Principles of plasma discharges and materials processing*, John Wiley and Sons, Hoboken, New Jersey, 2005.

[95] S. P. Lin, D. Khumsupan, Y. J. Chou, K. C. Hsieh, H. Y. Hsu, Y. Ting, and K. C. Cheng, *Applications of atmospheric cold plasma in agricultural, medical, and bioprocessing industries*, Appl Microbiol Biotechnol (2022), 14.

[96] D. M. Livermore, *Multiple mechanisms of antimicrobial resistance in pseudomonas aeruginosa: Our worst nightmare?*, Clinical Infectious Diseases **34** (2002), no. 5, 634–640.

[97] R. P. Lopes, M. J. Mota, A. M. Gomes, I. Delgadillo, and J. A. Saraiva, *Application of high pressure with homogenization, temperature, carbon dioxide, and cold plasma for the inactivation of bacterial spores: A review*, Compr Rev Food Sci Food Saf **17** (2018), no. 3, 532–555.

[98] Ante S. Lundberg, William C. Hahn, Piyush Gupta, and Robert A. Weinberg, *Genes involved in senescence and immortalization*, Current Opinion in Cell Biology **12** (2000), no. 6, 705–709.

[99] N. Mahanta, V. Saxena, L. M. Pandey, P. Batra, and U. S. Dixit, *Performance study of a sterilization box using a combination of heat and ultraviolet light irradiation for the prevention of covid-19*, Environ Res **198** (2021), 111309.

[100] A. Mai-Prochnow, M. Clauson, J. Hong, and A. B. Murphy, *Gram positive and gram negative bacteria differ in their sensitivity to cold plasma*, Sci Rep **6** (2016), 38610, Mai-Prochnow, Anne Clauson, Maryse Hong, Jungmi Mur-

phy, Anthony B eng England 2016/12/10 Sci Rep. 2016 Dec 9;6:38610. doi: 10.1038/srep38610.

[101] Danik Martirosyan, Hamid Ghomi, Mohammad Reza Ashoori, Alireza Rezaeinezhad, Afsaneh Seyed Mikaeili, Fahimeh Jahanbakhshi, and Hossein Mirmiranpour, *Study of the effect of gallic acid and cold plasma on the levels of inflammatory factors and antioxidants in the serum sample of subjects with type 2 diabetes mellitus*, Bioactive Compounds in Health and Disease **4** (2021), no. 8, 1.

[102] Sabah N. Mazhir, Alyaa H. Ali, Nisreen Kh Abdalameer, and Farah W. Hadi, *Studying the effect of cold plasma on the blood using digital image processing and images texture analysis*, 2016, pp. 909–914.

[103] J. M. Meek and J. D. Craggs, *Electrical breakdown of gases*, Oxford at the Claredon Press, 1978.

[104] Hans-Robert Metelmann, Christian Seebauer, Vandana Miller, Alexander Fridman, Georg Bauer, David B. Graves, Jean-Michel Pouvesle, Rico Rutkowski, Matthias Schuster, Sander Bekeschus, Kristian Wende, Kai Masur, Sybille Hasse, Torsten Gerling, Masaru Hori, Hiromasa Tanaka, Eun Ha Choi, Klaus-Dieter Weltmann, Philine Henriette Metelmann, Daniel D. Von Hoff, and Thomas von Woedtke, *Clinical experience with cold plasma in the treatment of locally advanced head and neck cancer*, Clinical Plasma Medicine **9** (2018), 6–13.

[105] Hans-Robert Metelmann, Thi Thom Vu, Hoang Tung Do, Thi Nguyen Binh Le, Thi Ha Anh Hoang, Thi Thu Trang Phi, Tran My Linh Luong, Van Tien Doan, Thi Trang Huyen Nguyen, Thi Hong Minh Nguyen, Thuy Linh Nguyen, Dinh Quyen Le, Thi Kim Xuan Le, Thomas von Woedtke, René Bussiahn,

Klaus-Dieter Weltmann, Roya Khalili, and Fred Podmelle, *Scar formation of laser skin lesions after cold atmospheric pressure plasma (cap) treatment: A clinical long term observation*, Clinical Plasma Medicine **1** (2013), no. 1, 30–35.

[106] Sea C. Min, Si Hyeon Roh, Brendan A. Niemira, Joseph E. Sites, Glenn Boyd, and Alison Lacombe, *Dielectric barrier discharge atmospheric cold plasma inhibits escherichia coli o157:h7, salmonella, listeria monocytogenes, and tulane virus in romaine lettuce*, International Journal of Food Microbiology **237** (2016), 114–120.

[107] N. N. Misra, Sonal Patil, Tamara Moiseev, Paula Bourke, J. P. Mosnier, K. M. Keener, and P. J. Cullen, *In-package atmospheric pressure cold plasma treatment of strawberries*, Journal of Food Engineering **125** (2014), 131–138.

[108] N. N. Misra, B. K. Tiwari, K. S. M. S. Raghavarao, and P. J. Cullen, *Nonthermal plasma inactivation of food-borne pathogens*, Food Engineering Reviews **3** (2011), no. 3-4, 159–170.

[109] Ankit Moldgy, Gaurav Nayak, Hamada A. Aboubakr, Sagar M. Goyal, and Peter J. Bruggeman, *Inactivation of virus and bacteria using cold atmospheric pressure air plasmas and the role of reactive nitrogen species*, Journal of Physics D: Applied Physics **53** (2020), no. 43, 1.

[110] P. Monika, M. N. Chandraprabha, A. Rangarajan, P. V. Waiker, and K. N. Chidambara Murthy, *Challenges in healing wound: Role of complementary and alternative medicine*, Front Nutr **8** (2021), 791899.

[111] G. J. Moran, A. Krishnadasan, R. J. Gorwitz, G. E. Fosheim, L. K. McDougal, R. B. Carey, D. A. Talan, and E. MERGEncy ID Net Study Group, *Methicillin-resistant s. aureus infections among patients in the emergency department*, N Engl J Med **355** (2006), no. 7, 666–74.

[112] T. Narasaraju, E. Yang, R. P. Samy, H. H. Ng, W. P. Poh, A. A. Liew, M. C. Phoon, N. van Rooijen, and V. T. Chow, *Excessive neutrophils and neutrophil extracellular traps contribute to acute lung injury of influenza pneumonitis*, Am J Pathol **179** (2011), no. 1, 199–210.

[113] Nasruddin, Yukari Nakajima, Kanae Mukai, Heni Setyowati Esti Rahayu, Muhammad Nur, Tatsuo Ishijima, Hiroshi Enomoto, Yoshihiko Uesugi, Junko Sugama, and Toshio Nakatani, *Cold plasma on full-thickness cutaneous wound accelerates healing through promoting inflammation, re-epithelialization and wound contraction*, Clinical Plasma Medicine **2** (2014), no. 1, 28–35.

[114] Gabriele Neretti, Andrea Cristofolini, Carlo A. Borghi, Alessandro Gurioli, and Roberto Pertile, *Experimental results in dbd plasma actuators for air flow control*, IEEE Transactions on Plasma Science **40** (2012), no. 6, 1678–1687.

[115] G. Nersisyan and W. G. Graham, *Characterization of a dielectric barrier discharge operating in an open reactor with flowing helium*, Plasma Sources Science and Technology **13** (2004), no. 4, 582–587.

[116] Alvin Ngo, Kedar Pai, and Jamey D. Jacob, *Investigation of scaling effects due to varying dielectric materials in asymmetric surface dielectric barrier discharge*, 2017.

[117] Alvin D. Ngo, Kedar Pai, Christopher Timmons, Li Maria Ma, and Jamey Jacob, *Evaluation of cylindrical asymmetric surface dielectric barrier discharge actuators for surface decontamination and mixing*, Plasma **4** (2021), no. 4, 755–763.

[118] João Nunes-Pereira, Frederico Freire Rodrigues, Mohammadmahdi Abdollahzadehsangroudi, José Carlos Páscoa, and Senentxu Lanceros-Mendez, *Improved performance of polyimide cirlex-based dielectric barrier discharge plasma*

actuators for flow control, Polymers for Advanced Technologies **33** (2021), no. 4, 1278–1290.

[119] Yuji Okita, Timothy Jukes, Kwing-So Choi, and Katsutaka Nakamura, *Flow reattachment over an airfoil using surface plasma actuator*, 2008.

[120] K. Pai, *Asymmetric surface dielectric barrier discharge as a novel method for biological decontamination*, Thesis, Oklahoma State University, 2015.

[121] K. Pai, C. Timmons, K. D. Roehm, A. Ngo, S. S. Narayanan, A. Ramachandran, J. D. Jacob, L. M. Ma, and S. V. Madihally, *Investigation of the roles of plasma species generated by surface dielectric barrier discharge*, Sci Rep **8** (2018), no. 1, 16674.

[122] Shashi K. Pankaj and Kevin M. Keener, *Cold plasma: background, applications and current trends*, Current Opinion in Food Science **16** (2017), 49–52.

[123] H. J. Park, T. T. Nguyen, J. Yoon, and C. Lee, *Role of reactive oxygen species in escherichia coli inactivation by cupric ion*, Environ Sci Technol **46** (2012), no. 20, 11299–304.

[124] S. Patil, T. Moiseev, N. N. Misra, P. J. Cullen, J. P. Mosnier, K. M. Keener, and P. Bourke, *Influence of high voltage atmospheric cold plasma process parameters and role of relative humidity on inactivation of bacillus atrophaeus spores inside a sealed package*, J Hosp Infect **88** (2014), no. 3, 162–9, Patil, S Moiseev, T Misra, N N Cullen, P J Mosnier, J P Keener, K M Bourke, P eng Research Support, Non-U.S. Gov't England 2014/10/14 J Hosp Infect. 2014 Nov;88(3):162-9. doi: 10.1016/j.jhin.2014.08.009. Epub 2014 Sep 19.

[125] Stanislav Pekárek, *Experimental study of surface dielectric barrier discharge in air and its ozone production*, Journal of Physics D: Applied Physics **45** (2012), no. 7, 10.

[126] S. Petti, M. De Giusti, C. Moroni, and A. Polimeni, *Long-term survival curve of methicillin-resistant staphylococcus aureus on clinical contact surfaces in natural-like conditions*, Am J Infect Control **40** (2012), no. 10, 1010–2.

[127] Jérôme Pons, Eric Moreau, and Gérard Touchard, *Asymmetric surface dielectric barrier discharge in air at atmospheric pressure: electrical properties and induced airflow characteristics*, Journal of Physics D: Applied Physics **38** (2005), no. 19, 3635–3642.

[128] A. Popelka, I. Novak, M. Lehocky, I. Chodak, J. Sedliacik, M. Gajtanska, M. Sedliacikova, A. Vesel, I. Junkar, A. Kleinova, M. Spirkova, and F. Bilek, *Anti-bacterial treatment of polyethylene by cold plasma for medical purposes*, Molecules **17** (2012), no. 1, 762–85.

[129] M.L. Post, *Plasma actuators for separation control on stationary and oscillating airfoils*, Thesis, University of Notre Dame, 2004.

[130] S. Pulavendran, J. M. Rudd, P. Maram, P. G. Thomas, R. Akhilesh, J. R. Malayer, V. T. K. Chow, and N. Teluguakula, *Combination therapy targeting platelet activation and virus replication protects mice against lethal influenza pneumonia*, Am J Respir Cell Mol Biol **61** (2019), no. 6, 689–701.

[131] Y.P. Raizer, *Gas discharge physics*, Springer, 1991.

[132] Martin C. Robson, *Wound infection*, Surgical Clinics of North America **77** (1997), no. 3, 637–650.

[133] N. C. Roy, M. M. Hasan, A. H. Kabir, M. A. Reza, M. R. Talukder, and A. N. Chowdhury, *Atmospheric pressure gliding arc discharge plasma treatments for improving germination, growth and yield of wheat*, Plasma Science and Technology **20** (2018), no. 11, 12.

[134] J. M. Rudd, S. Pulavendran, H. K. Ashar, J. W. Ritchey, T. A. Snider, J. R. Malayer, M. Marie, V. T. K. Chow, and T. Narasaraju, *Neutrophils induce a novel chemokine receptors repertoire during influenza pneumonia*, Front Cell Infect Microbiol **9** (2019), 108.

[135] Arvind Santhanakrishnan and Jamey Jacob, *On plasma synthetic jet actuators*, 2006.

[136] C. Scharf, C. Eymann, P. Emicke, J. Bernhardt, M. Wilhelm, F. Gorries, J. Winter, T. von Woedtke, K. Darm, G. Daeschlein, L. Steil, W. Hosemann, and A. Beule, *Improved wound healing of airway epithelial cells is mediated by cold atmospheric plasma: A time course-related proteome analysis*, Oxid Med Cell Longev **2019** (2019), 7071536.

[137] Jürgen Schlegel, Julia Köritzer, and Veronika Boxhammer, *Plasma in cancer treatment*, Clinical Plasma Medicine **1** (2013), no. 2, 2–7.

[138] A. Schmidt, G. Liebelt, J. Striesow, E. Freund, T. von Woedtke, K. Wende, and S. Bekeschus, *The molecular and physiological consequences of cold plasma treatment in murine skin and its barrier function*, Free Radic Biol Med **161** (2020), 32–49, Schmidt, Anke Liebelt, Grit Striesow, Johanna Freund, Eric von Woedtke, Thomas Wende, Kristian Bekeschus, Sander eng 2020/10/05 Free Radic Biol Med. 2020 Dec;161:32-49. doi: 10.1016/j.freeradbiomed.2020.09.026. Epub 2020 Oct 1.

[139] K. Schröder, A. Meyer-Plath, D. Keller, W. Besch, G. Babucke, and A. Ohl, *Plasma-induced surface functionalization of polymeric biomaterials in ammonia plasma*, Contributions to Plasma Physics **41** (2001), no. 6, 562–572.

[140] I. V. Schweigert, A. L. Alexandrov, and Dm E. Zakrevsky, *Self-organization of touching-target current with ac voltage in atmospheric pressure plasma jet*

for medical application parameters, Plasma Sources Science and Technology **29** (2020), no. 12, 1.

[141] Takehiko Segawa, Hirohide Furutani, Hiro Yoshida, Timothty Jukes, and Kwing-So Choi, *Wall normal jet under elevated temperatures produced by surface plasma actuator*, 2007.

[142] Shawn C. Shadden, John O. Dabiri, and Jerrold E. Marsden, *Lagrangian analysis of fluid transport in empirical vortex ring flows*, Physics of Fluids **18** (2006), no. 4, 1.

[143] P. Shaw, N. Kumar, H. S. Kwak, J. H. Park, H. S. Uhm, A. Bogaerts, E. H. Choi, and P. Attri, *Bacterial inactivation by plasma treated water enhanced by reactive nitrogen species*, Sci Rep **8** (2018), no. 1, 11268.

[144] D. C. Shoults and N. J. Ashbolt, *Decreased efficacy of uv inactivation of staphylococcus aureus after multiple exposure and growth cycles*, Int J Hyg Environ Health **222** (2019), no. 1, 111–116.

[145] A. Simmons, *Future trends for the sterilisation of biomaterials and medical devices*, Sterilisation of Biomaterials and Medical Devices (2012), 11.

[146] Mario G. Sobacchi, Alexei V. Saveliev, A. A. Fridman, A. F. Gutsol, and Lawrence A. Kennedy, *Experimental assessment of pulsed corona discharge for treatment of voc emissions*, Plasma Chemistry and Plasma Processing **23** (2003), no. 2, 347–370.

[147] I. Sremacki, S. Kos, M. Bosnjak, A. Jurov, G. Sersa, M. Modic, C. Leys, U. Cvelbar, and A. Nikiforov, *Plasma damage control: From biomolecules to cells and skin*, ACS Appl Mater Interfaces **13** (2021), no. 39, 46303–46316, Sremacki, Ivana Kos, Spela Bosnjak, Masa Jurov, Andrea Sersa, Gregor Modic, Martina

Leys, Christophe Cvelbar, Uros Nikiforov, Anton eng 2021/09/28 ACS Appl Mater Interfaces. 2021 Oct 6;13(39):46303-46316. doi: 10.1021/acsami.1c12232. Epub 2021 Sep 26.

[148] Zhi Su, Haohua Zong, Hua Liang, Jun Li, and Xiancong Chen, *Characteristics of a dielectric barrier discharge plasma actuator driven by pulsed-dc high voltage*, Journal of Physics D: Applied Physics **55** (2021), no. 7, 16.

[149] Toshihiro Takamatsu, Kodai Uehara, Yota Sasaki, Hidekazu Miyahara, Yuriko Matsumura, Atsuo Iwasawa, Norihiko Ito, Takeshi Azuma, Masahiro Kohno, and Akitoshi Okino, *Investigation of reactive species using various gas plasmas*, RSC Adv. **4** (2014), no. 75, 39901–39905.

[150] Y. Tanouchi, A. J. Lee, H. Meredith, and L. You, *Programmed cell death in bacteria and implications for antibiotic therapy*, Trends Microbiol **21** (2013), no. 6, 265–70.

[151] Claire Tendero, Christelle Tixier, Pascal Tristant, Jean Desmaison, and Philippe Leprince, *Atmospheric pressure plasmas: A review*, Spectrochimica Acta Part B: Atomic Spectroscopy **61** (2006), no. 1, 2–30.

[152] Flint O. Thomas, Thomas C. Corke, Muhammad Iqbal, Alexey Kozlov, and David Schatzman, *Optimization of dielectric barrier discharge plasma actuators for active aerodynamic flow control*, AIAA Journal **47** (2009), no. 9, 2169–2178.

[153] Flint O. Thomas, Alexey Kozlov, and Thomas C. Corke, *Plasma actuators for cylinder flow control and noise reduction*, AIAA Journal **46** (2008), no. 8, 1921–1931.

[154] Chris Timmons, Kedar Pai, Jamey Jacob, Guodong Zhang, and Li Maria Ma, *Inactivation of salmonella enterica, shiga toxin-producing escherichia coli, and*

listeria monocytogenes by a novel surface discharge cold plasma design, Food Control **84** (2018), 455–462.

[155] R. S Tipa, B. Boekema, E. Middelkoop, and G. M. W. Kroesen, *Cold plasma for bacteria inactivation*, 2012.

[156] Roxana Silvia Tipa and Gerrit M. W. Kroesen, *Plasma-stimulated wound healing*, IEEE Transactions on Plasma Science **39** (2011), no. 11, 2978–2979.

[157] B. K. Tiwari, C. S. Brennan, T. Curran, E. Gallagher, P. J. Cullen, and C. P. O' Donnell, *Application of ozone in grain processing*, Journal of Cereal Science **51** (2010), no. 3, 248–255.

[158] Muhammad Umair, Saqib Jabbar, Zubaria Ayub, Rana Muhammad Aadil, Muhammad Abid, Jianhao Zhang, and Zhao Liqing, *Recent advances in plasma technology: Influence of atmospheric cold plasma on spore inactivation*, Food Reviews International (2021), 1–23.

[159] F. Vatansever, W. C. de Melo, P. Avci, D. Vecchio, M. Sadasivam, A. Gupta, R. Chandran, M. Karimi, N. A. Parizotto, R. Yin, G. P. Tegos, and M. R. Hamblin, *Antimicrobial strategies centered around reactive oxygen species–bactericidal antibiotics, photodynamic therapy, and beyond*, FEMS Microbiol Rev **37** (2013), no. 6, 955–89.

[160] P. Vos, G. Garrity, D. Jones, W. Ludwig, F. A. Rainey, K. Schleifer, and W. B. Whitman, *Bergey's manual of systematic bacteriology*, vol. 3, Springer, 2009.

[161] Kazuaki Wagatsuma, *Emission characteristics of mixed gas plasmas in low-pressure glow discharges*, Spectrochimica Acta Part B: Atomic Spectroscopy **56** (2001), no. 5, 465–486.

[162] Jin-Jun Wang, Kwing-So Choi, Li-Hao Feng, Timothy N. Jukes, and Richard D. Whalley, *Recent developments in dbd plasma flow control*, Progress in Aerospace Sciences **62** (2013), 52–78.

[163] X. F. Wang, Q. Q. Fang, B. Jia, Y. Y. Hu, Z. C. Wang, K. P. Yan, S. Y. Yin, Z. Liu, and W. Q. Tan, *Potential effect of non-thermal plasma for the inhibition of scar formation: a preliminary report*, Sci Rep **10** (2020), no. 1, 1064.

[164] Richard D. Whalley and Kwing-So Choi, *The starting vortex in quiescent air induced by dielectric-barrier-discharge plasma*, Journal of Fluid Mechanics **703** (2012), 192–203.

[165] Nicholas D. Wilde, Haofeng Xu, Nicolas Gomez-Vega, and Steven R. H. Barrett, *A model of surface dielectric barrier discharge power*, Applied Physics Letters **118** (2021), no. 15, 8.

[166] H. N. Wilkinson and M. J. Hardman, *Wound healing: cellular mechanisms and pathological outcomes*, Open Biol **10** (2020), no. 9, 200223.

[167] A. M. Wróbel, M. Kryszewski, W. Rakowski, M. Okoniewski, and Z. Kubacki, *Effect of plasma treatment on surface structure and properties of polyester fabric*, Polymer **19** (1978), no. 8, 908–912.

[168] S. C. Wu, W. Marston, and D. G. Armstrong, *Wound care: the role of advanced wound healing technologies*, J Vasc Surg **52** (2010), no. 3 Suppl, 59S–66S.

[169] Y. Wu, Y. Liang, K. Wei, W. Li, M. Yao, J. Zhang, and S. A. Grinshpun, *Ms2 virus inactivation by atmospheric-pressure cold plasma using different gas carriers and power levels*, Appl Environ Microbiol **81** (2015), no. 3, 996–1002.

[170] D. Xiao, *Gas discharge and gas insulation*, Shanghai Jiao Tong University Press, 2016.

[171] H. Xu, Y. He, K. L. Strobel, C. K. Gilmore, S. P. Kelley, C. C. Hennick, T. Sebastian, M. R. Woolston, D. J. Perreault, and S. R. H. Barrett, *Flight of an aeroplane with solid-state propulsion*, Nature **563** (2018), no. 7732, 532–535.

[172] Haofeng Xu, Nicolas Gomez-Vega, Nicholas D. Wilde, Jayaprakash D. Kambhampaty, and Steven R. H. Barrett, *Electrical characteristics of wire-to-wire dielectric barrier discharges*, Plasma Sources Science and Technology **30** (2021), no. 8, 9.

[173] Mitsuo Yamamoto, Masateru Nishioka, and Masayoshi Sadakata, *Sterilization by h2o2 droplets under corona discharge*, Journal of Electrostatics **55** (2002), no. 2, 173–187.

[174] T. Yamamoto, Y. Tamura, and T. Yokota, *Antiseptic and antibiotic resistance plasmid in staphylococcus aureus that possesses ability to confer chlorhexidine and acrinol resistance*, Antimicrob Agents Chemother **32** (1988), no. 6, 932–5.

[175] Keping Yan, Qikang Jin, Chao Zheng, Guanlei Deng, Shengyong Yin, and Zhen Liu, *Pulsed cold plasma-induced blood coagulation and its pilot application in stanching bleeding during rat hepatectomy*, Plasma Science and Technology **20** (2018), no. 4, 1.

[176] Shuiliang Yao, Zuliang Wu, Jingyi Han, Xiujuan Tang, Boqiong Jiang, Hao Lu, Sin Yamamoto, and Satoshi Kodama, *Study of ozone generation in an atmospheric dielectric barrier discharge reactor*, Journal of Electrostatics **75** (2015), 35–42.

[177] S. Zhang, Z. Chen, B. Zhang, and Y. Chen, *Numerical investigation on the effects of dielectric barrier on a nanosecond pulsed surface dielectric barrier discharge*, Molecules **24** (2019), no. 21, 1.

[178] Xing Zheng, Huimin Song, Dongliang Bian, Hua Liang, Haohua Zong, Zhengyong Huang, Yaogong Wang, and Wenjie Xu, *A hybrid plasma de-icing actuator by using sic hydrophobic coating-based quartz glass as barrier dielectric*, Journal of Physics D: Applied Physics **54** (2021), no. 37, 1.

[179] Yulin Zhu, Changzhu Li, Haiying Cui, and Lin Lin, *Feasibility of cold plasma for the control of biofilms in food industry*, Trends in Food Science and Technology **99** (2020), 142–151.

[180] D. B. Zorov, M. Juhaszova, and S. J. Sollott, *Mitochondrial reactive oxygen species (ros) and ros-induced ros release*, Physiol Rev **94** (2014), no. 3, 909–50.

APPENDIX

Matlab Codes:

Dabiri Lab, LCS Calculations: "LCS MATLAB Kit Version

https://dabirilab.com/software

Software List:

- 'DaVis - LaVision': Software solution for laser imaging. Used for PIV analysis.
- 'MotionStudio': Software used to capture raw images for PIV analysis.
- 'Eagle': PCB design and electrical schematic software. Used to design plasma actuators.
- 'MATLAB': Programming language used to perform LCS analysis and plot data.
- 'Arduino': Programming language specific for Arduino microcontroller programming. Used to control actuator pulse and duty cycle.
- 'SOLIDWORKS': Solid modeling computer-aided design application. Used to make CAD models of actuators, setups, and housing devices.

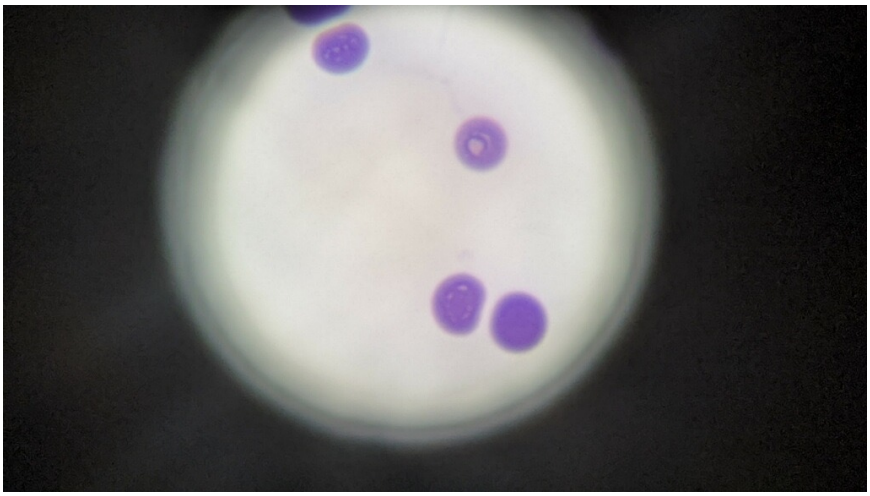

Figure 4: Platelets

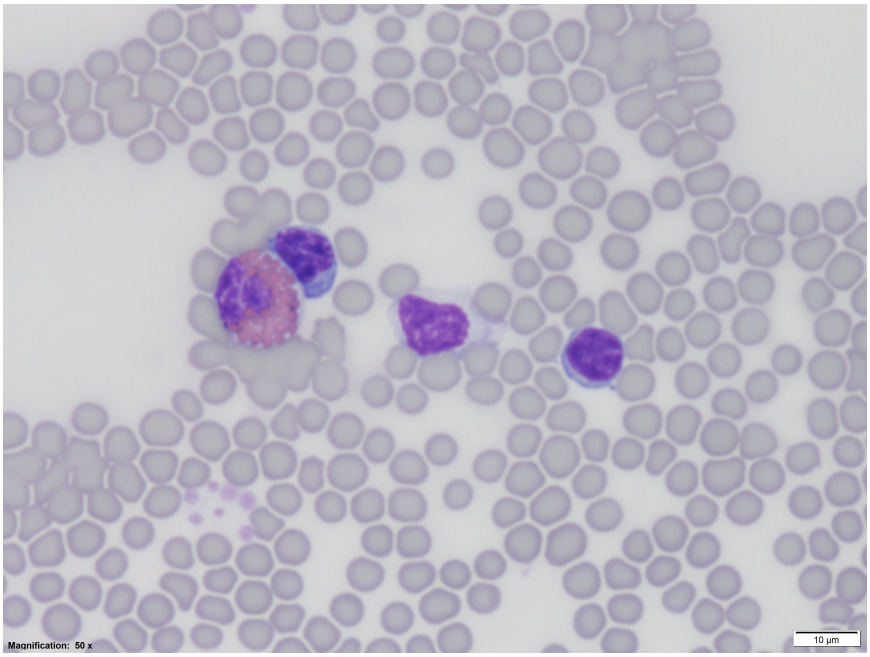

Figure 5: T-0 Control

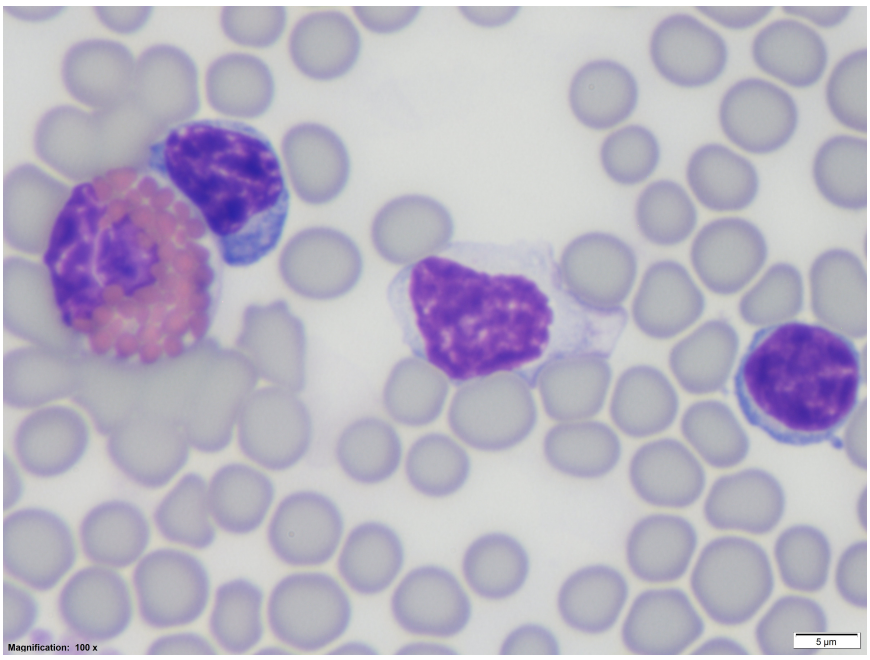

Figure 6: T-0 Control

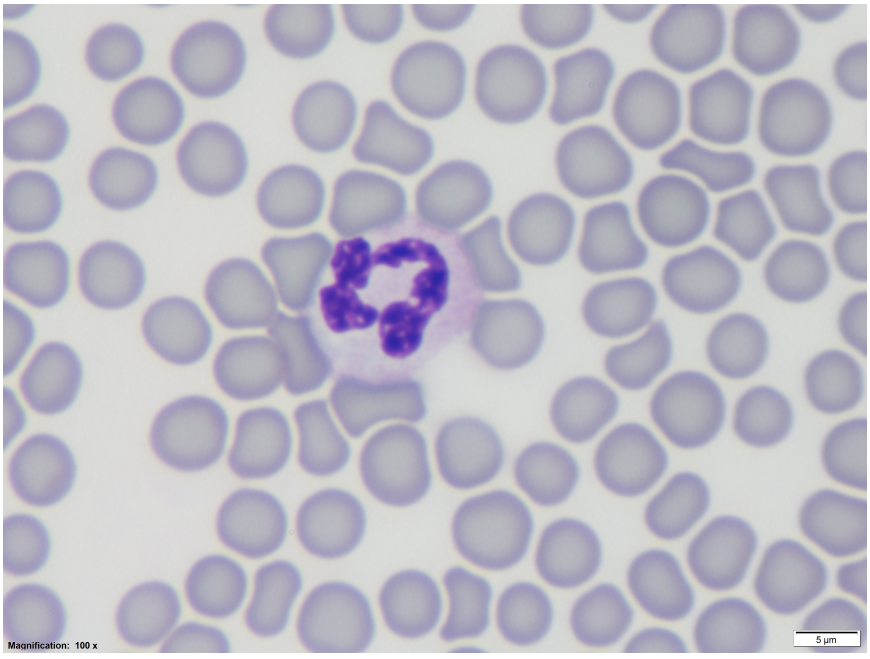

Figure 7: T-0 Control

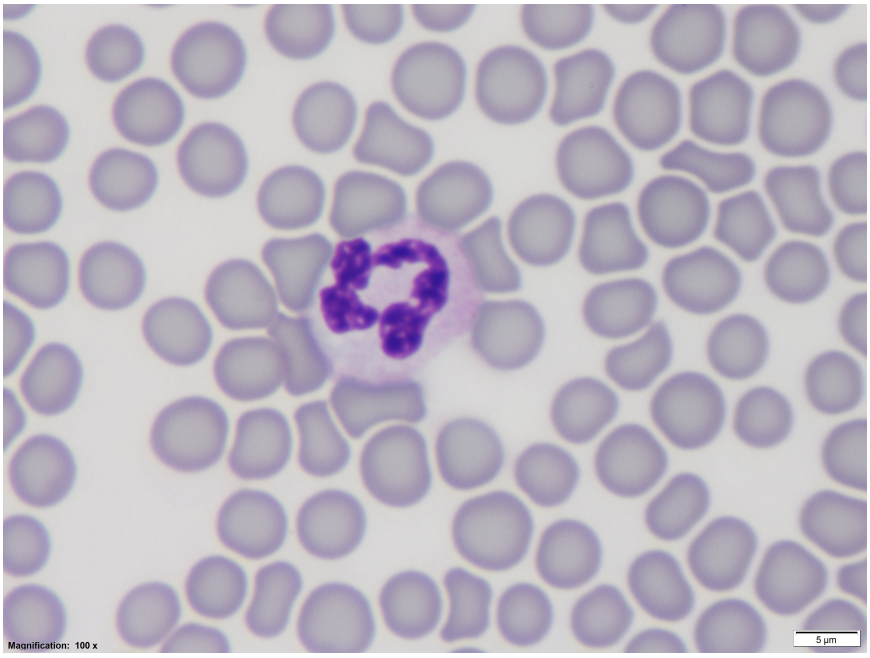

Figure 8: T-0 Control

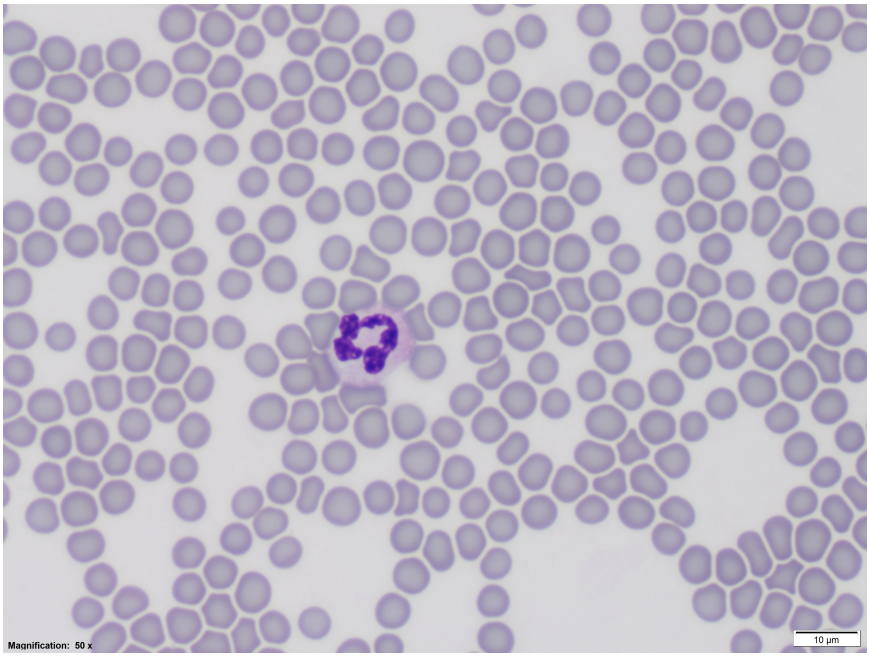

Figure 9: T-0 Control

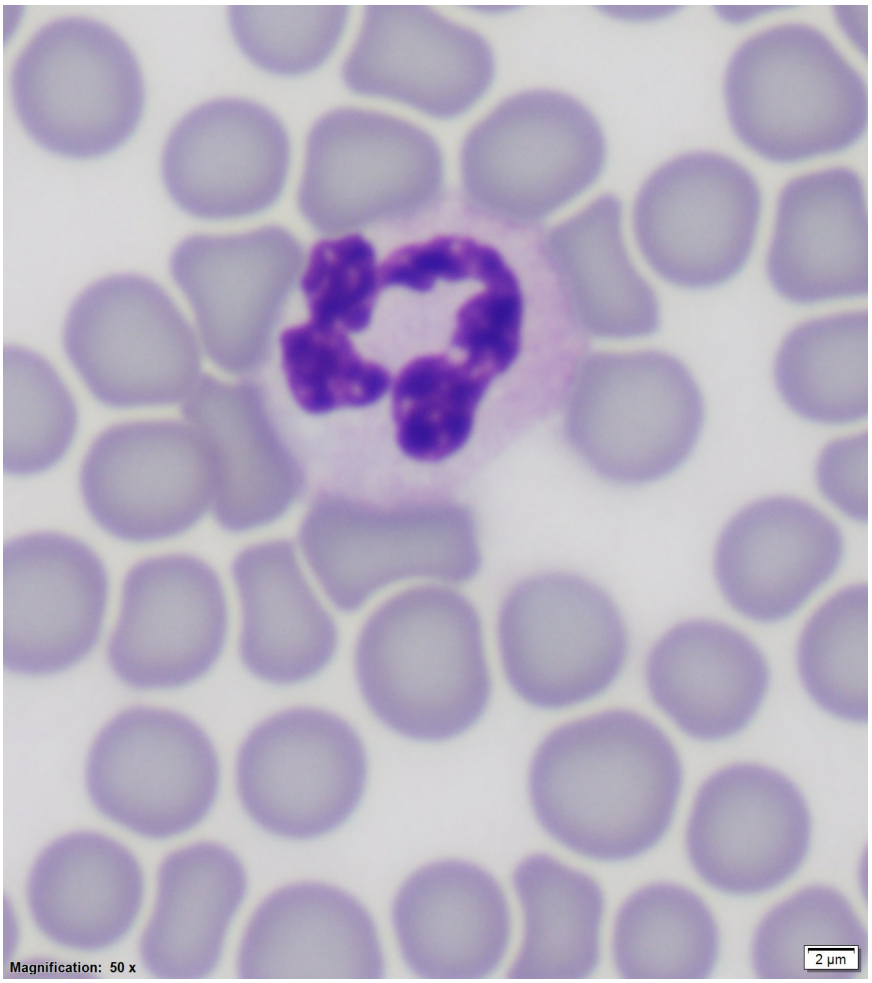

Figure 10: T-0 Control

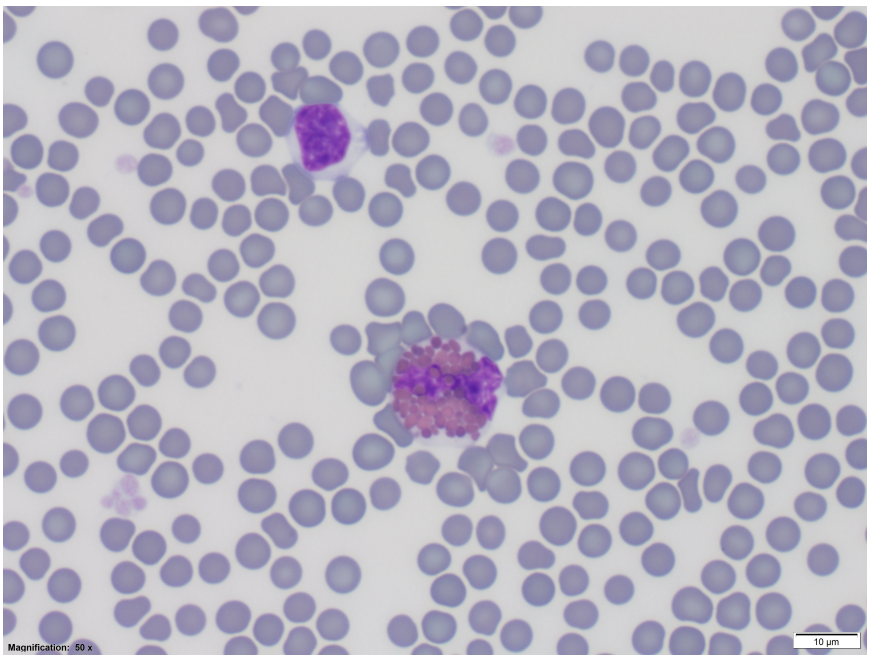

Figure 11: T-1 min plasma treatment

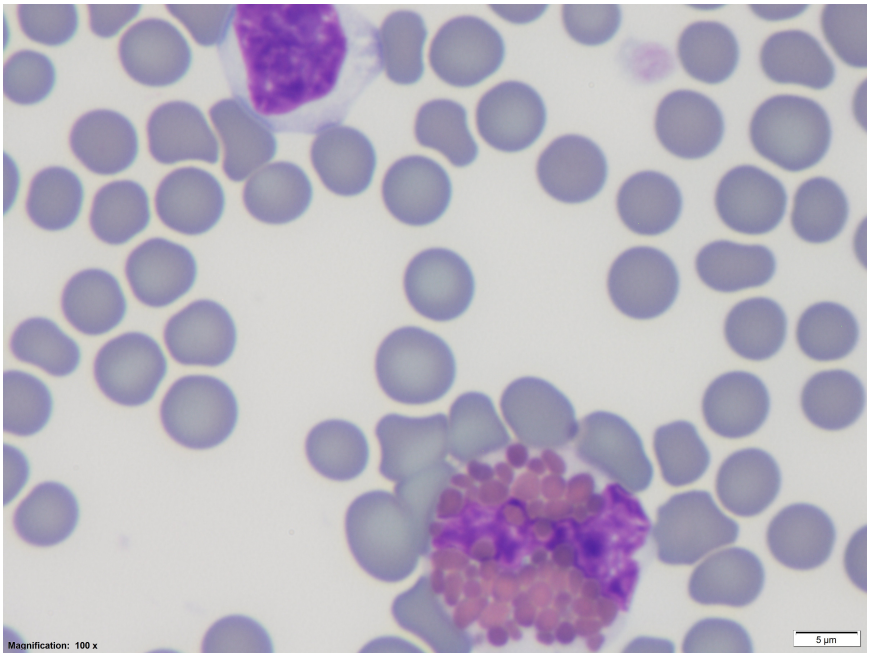

Figure 12: T-1 min plasma treatment

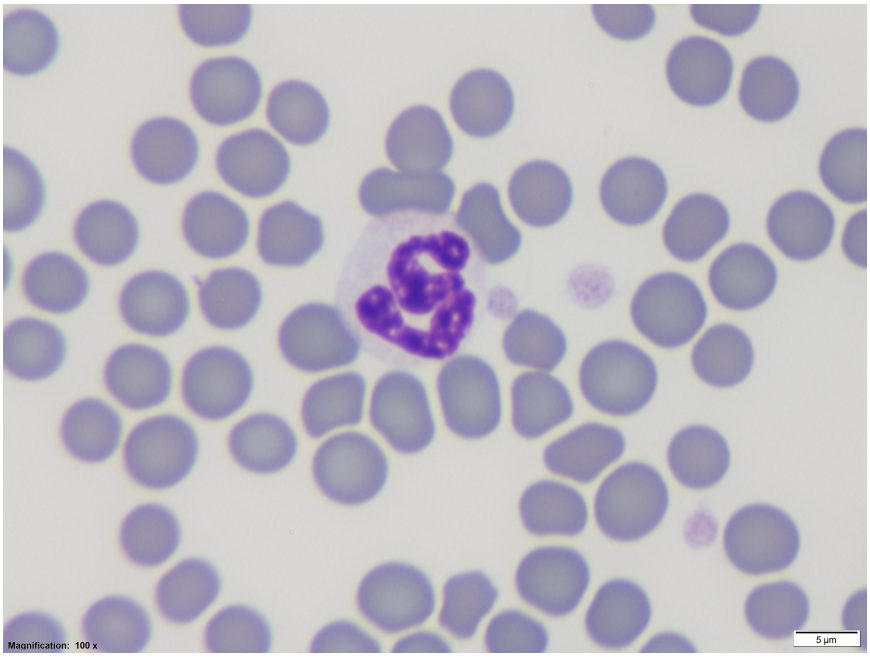

Figure 13: T-1 min plasma treatment

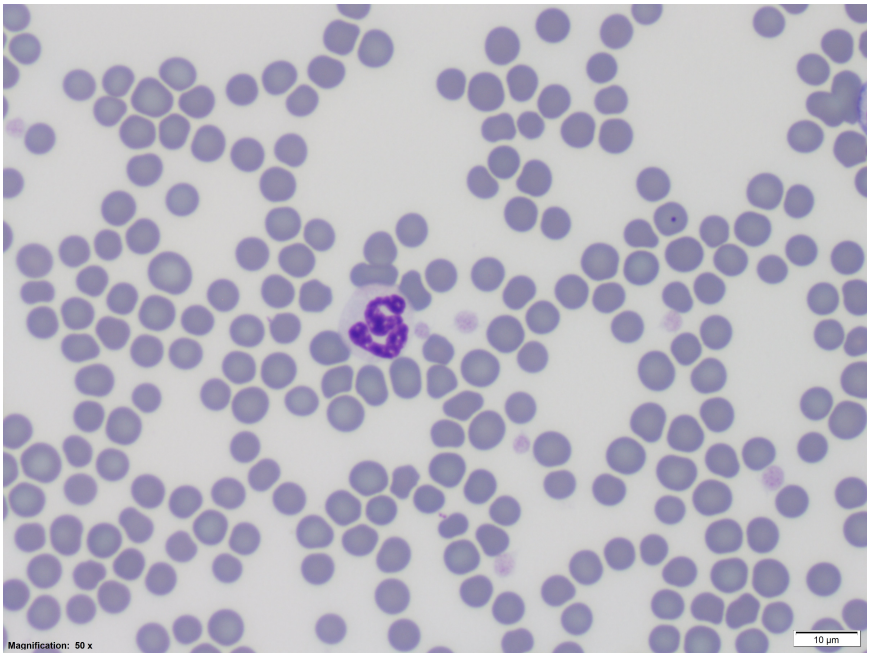

Figure 14: T-1 min plasma treatment

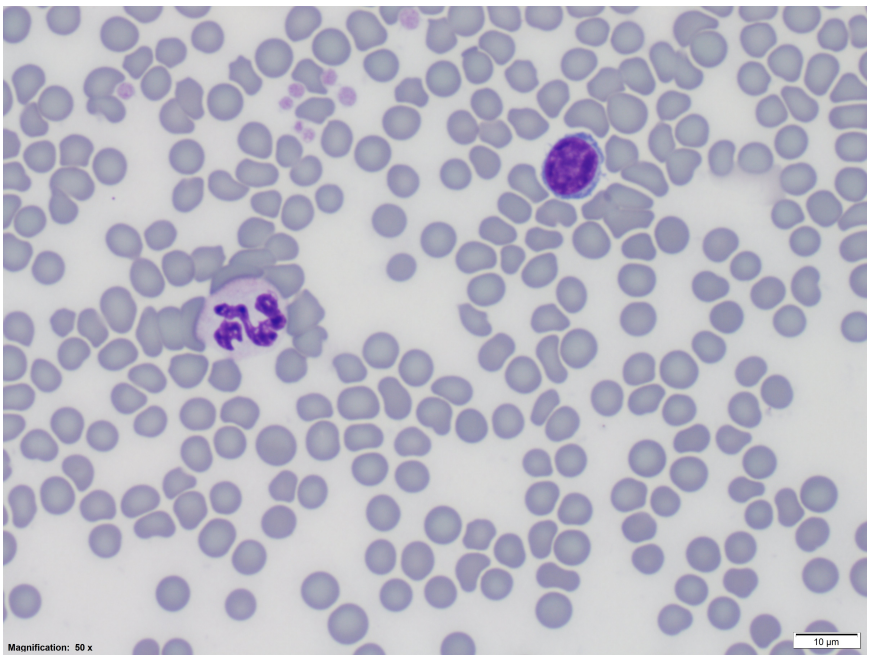

Figure 15: T-2 min plasma treatment

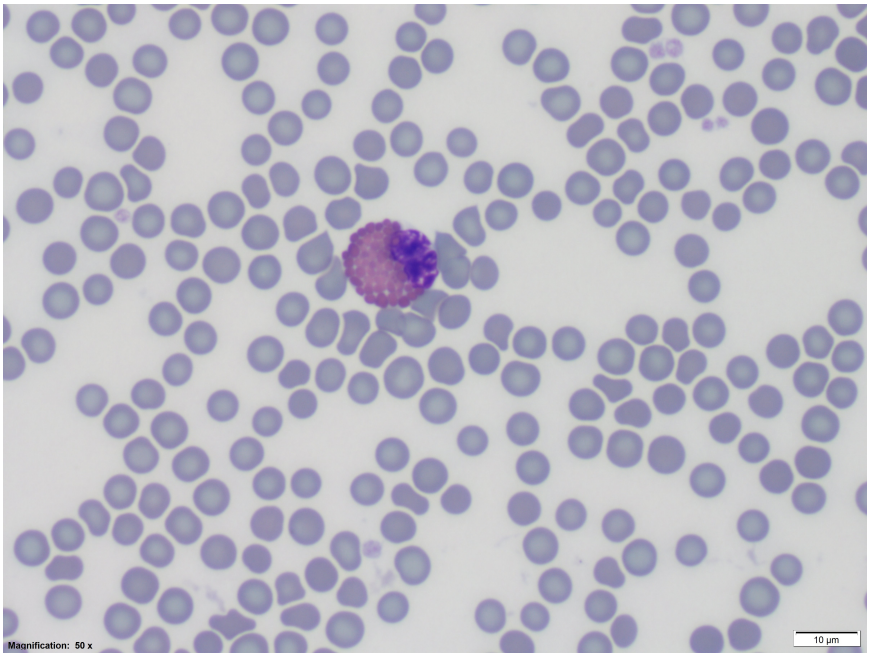

Figure 16: T-2 min plasma treatment

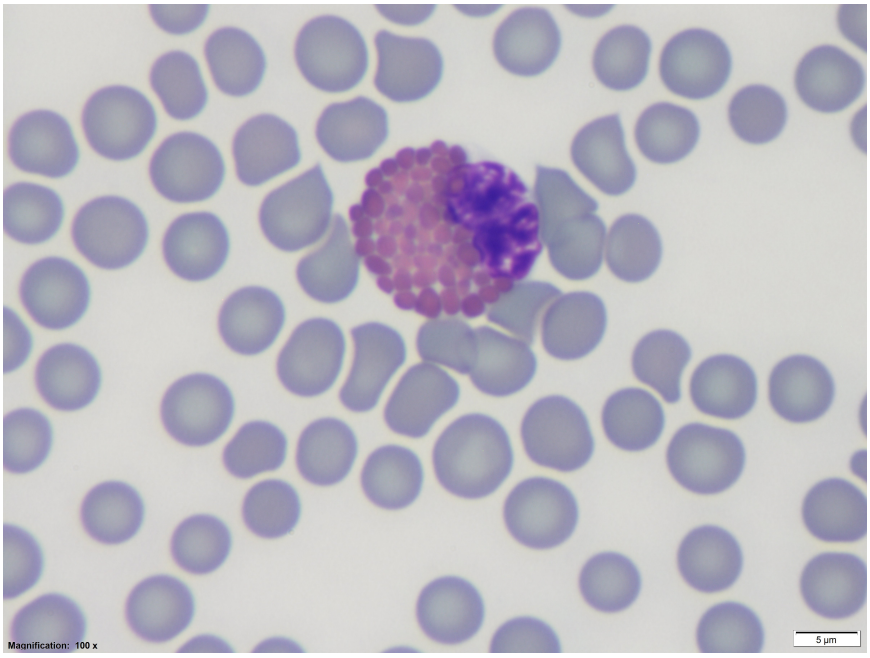

Figure 17: T-2 min plasma treatment

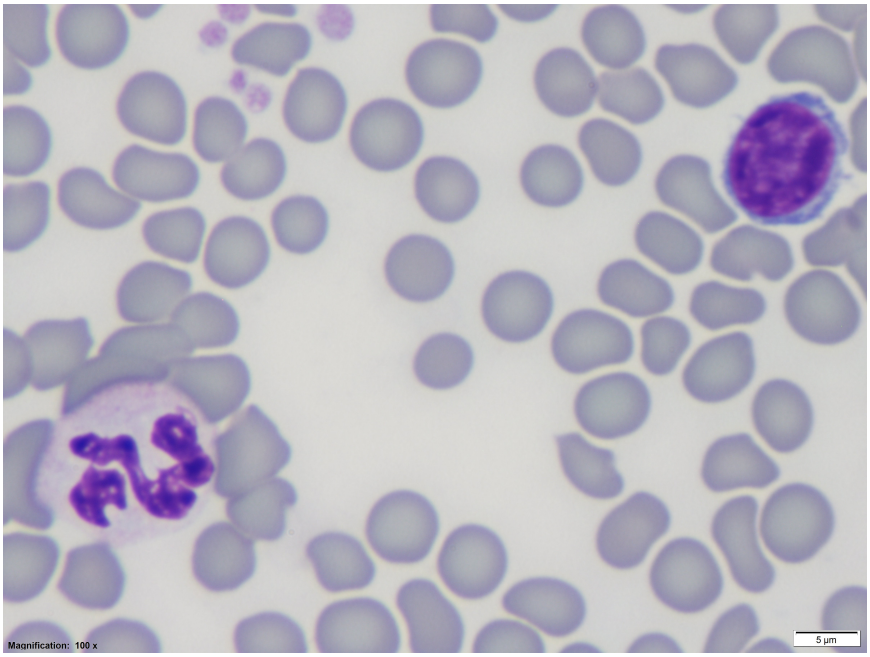

Figure 18: T-2 min plasma treatment

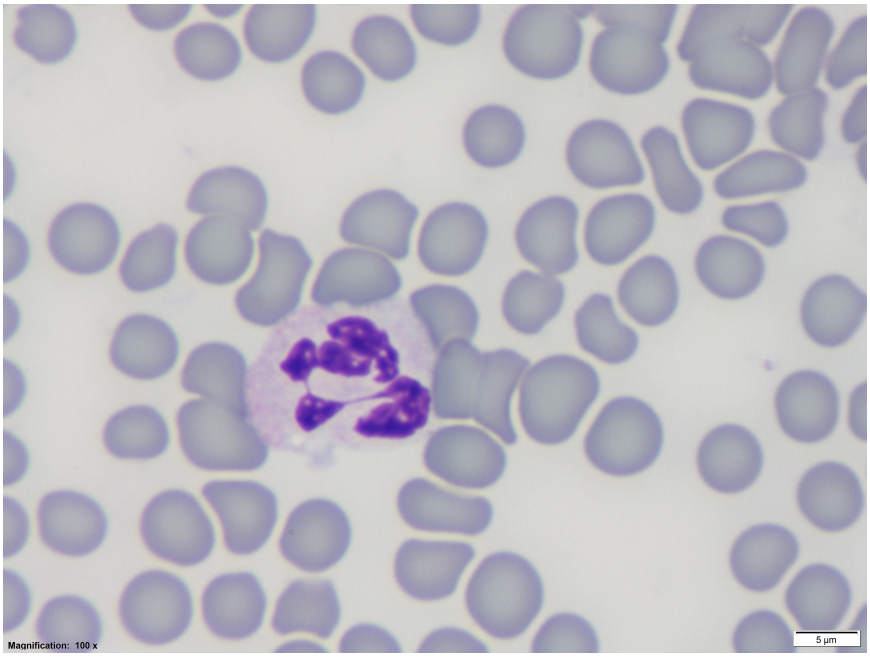

Figure 19: T-2 min plasma treatment

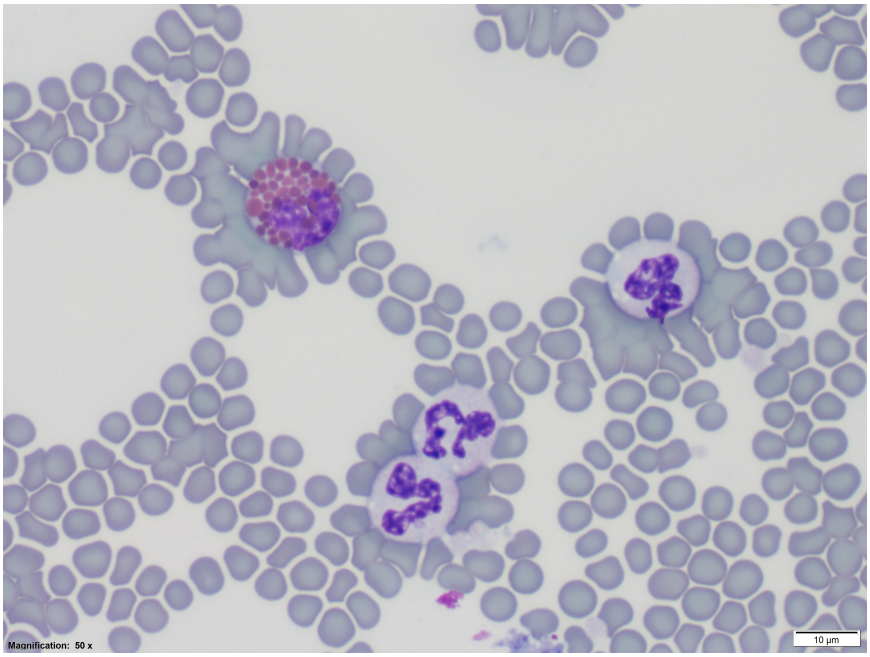

Figure 20: T-2 min plasma treatment

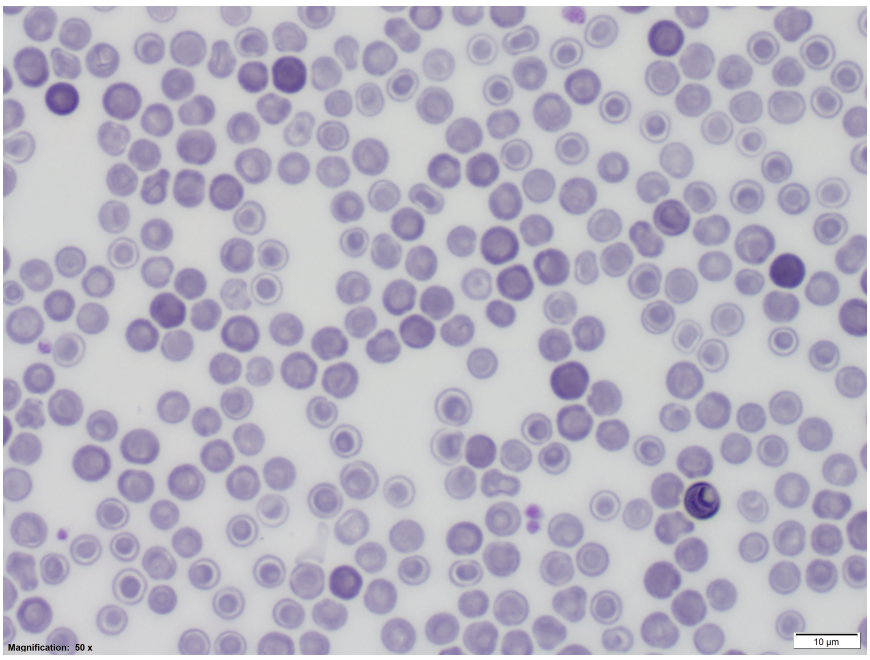

Figure 21: T-5 min plasma treatment

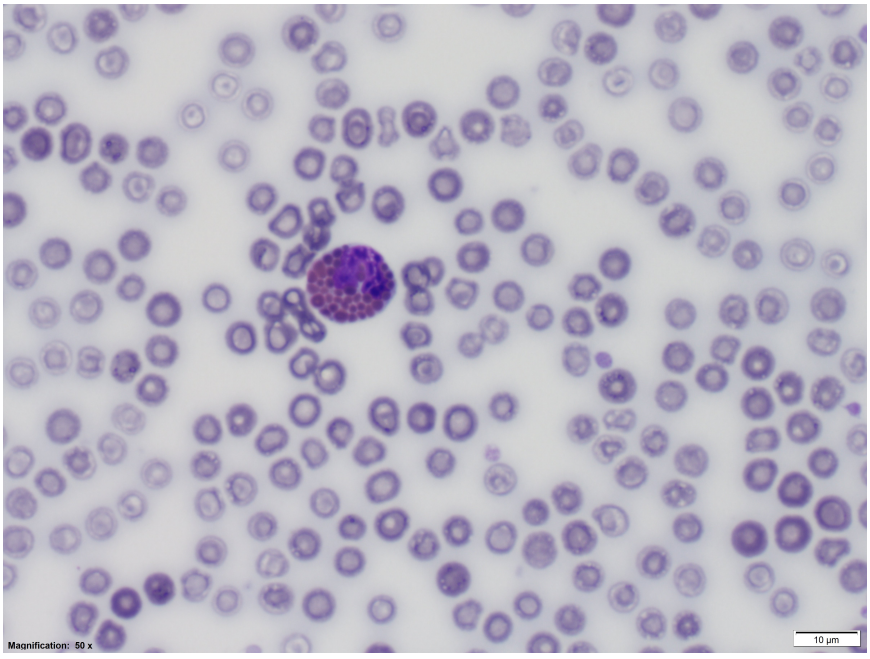

Figure 22: T-5 min plasma treatment

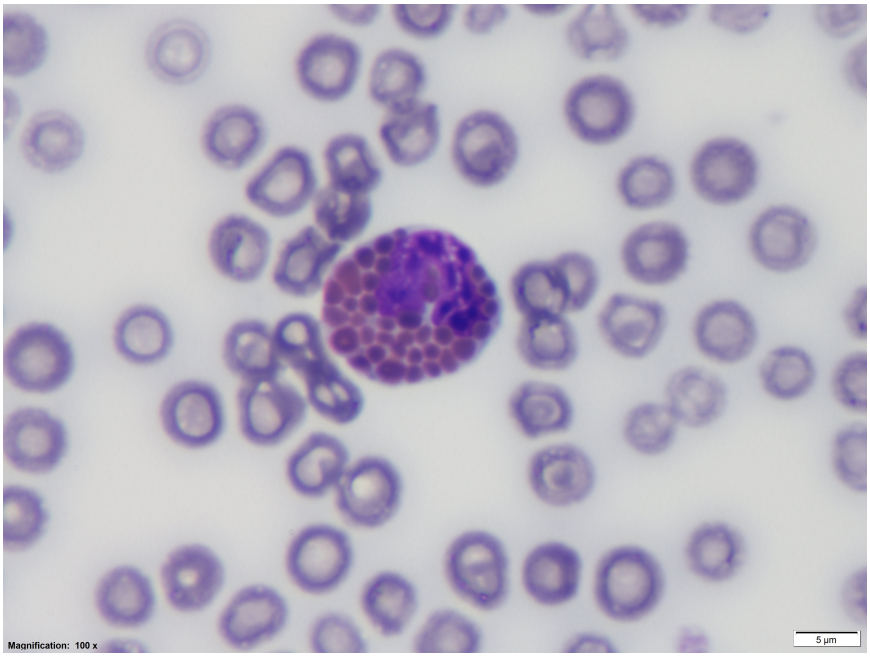

Figure 23: T-5 min plasma treatment

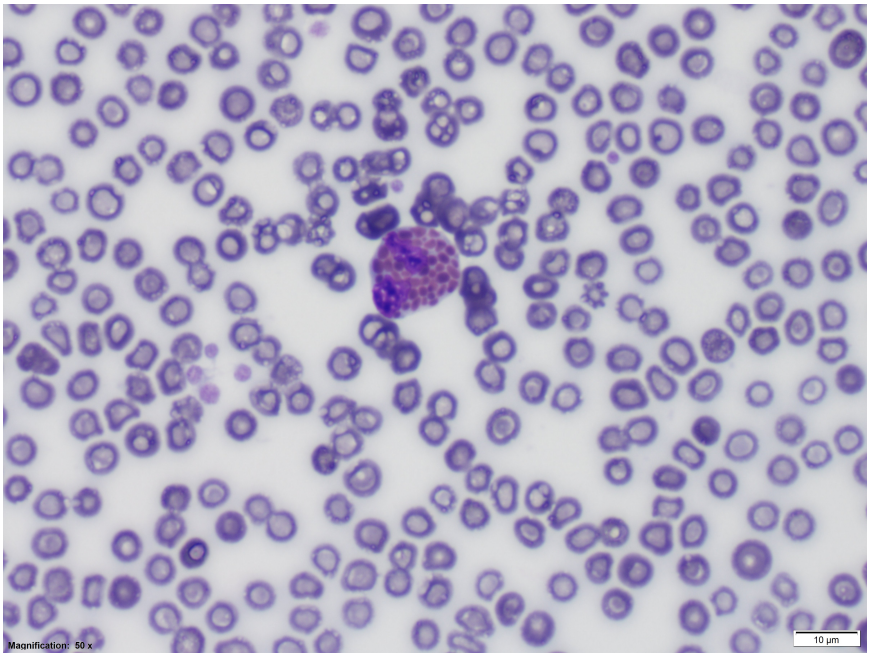

Figure 24: T-5 min plasma treatment

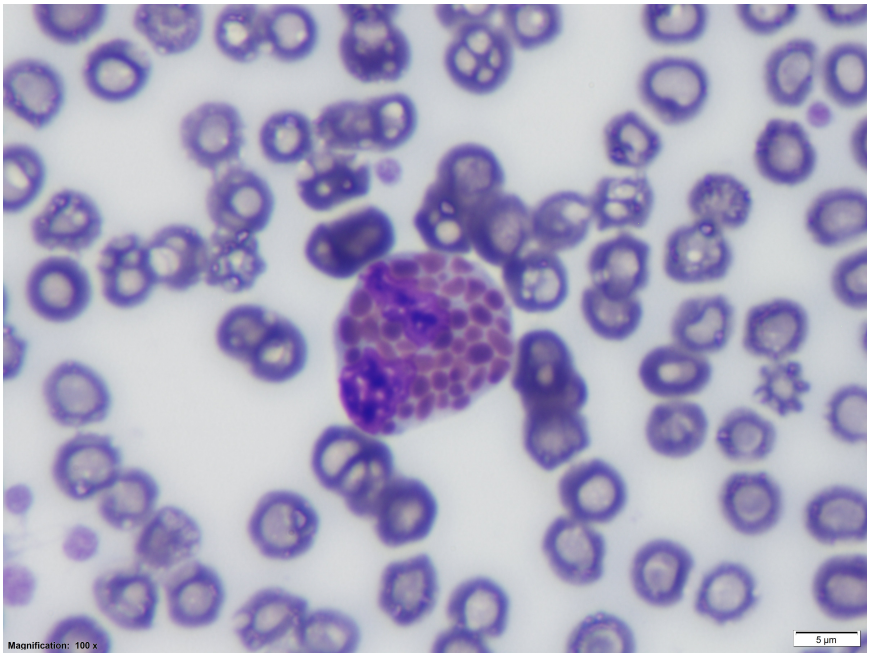

Figure 25: T-5 min plasma treatment

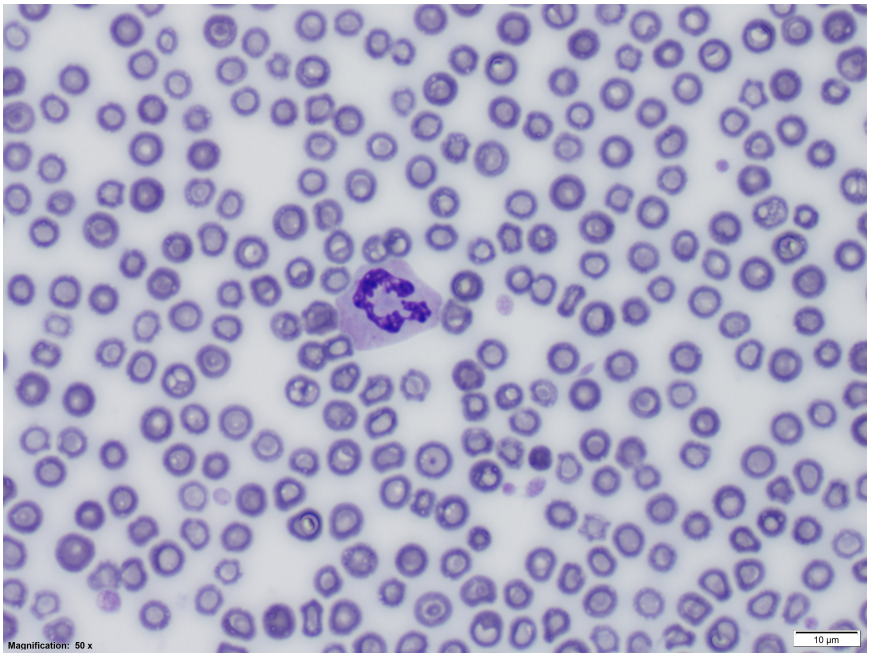

Figure 26: T-5 min plasma treatment

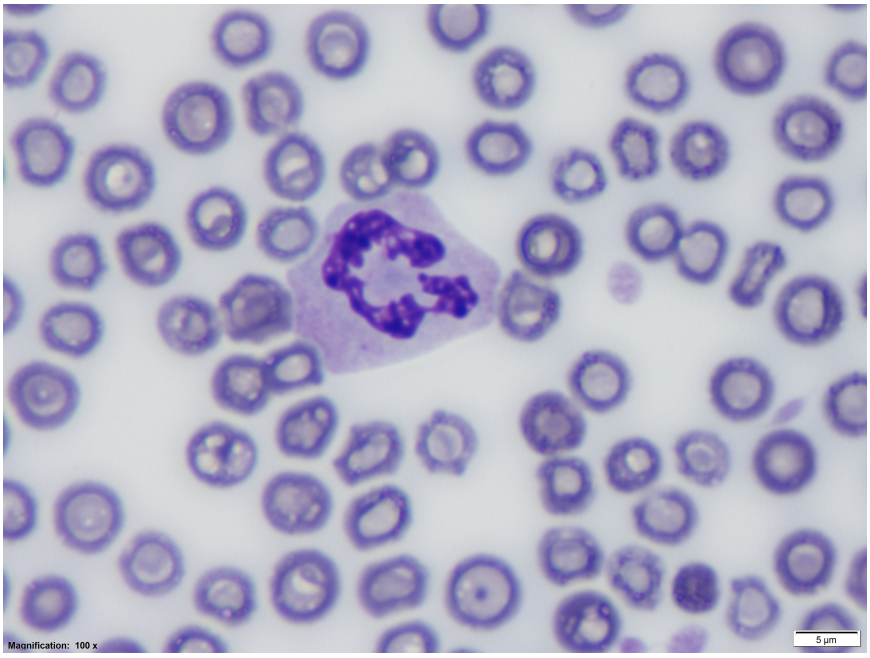

Figure 27: T-5 min plasma treatment

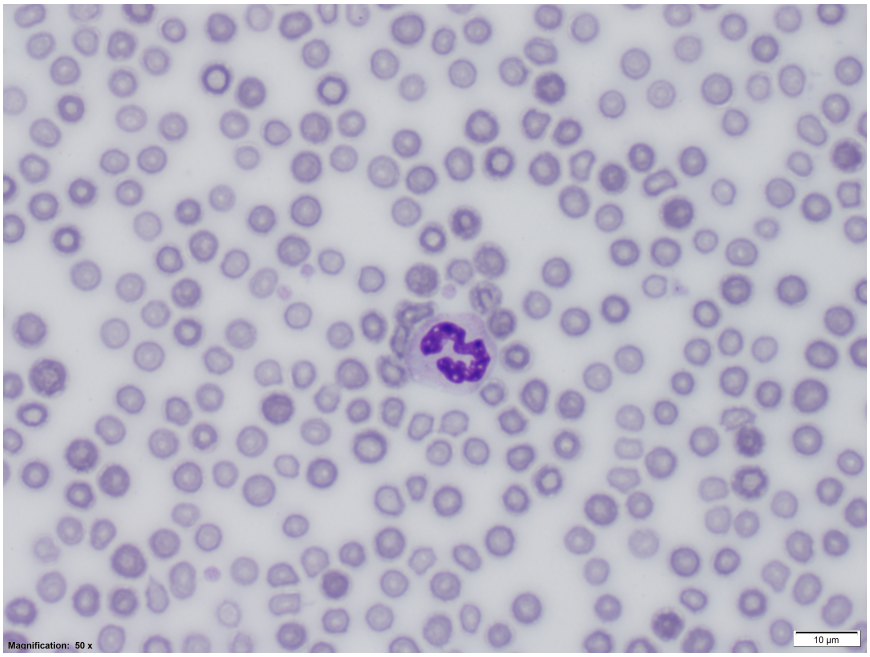

Figure 28: T-5 min plasma treatment

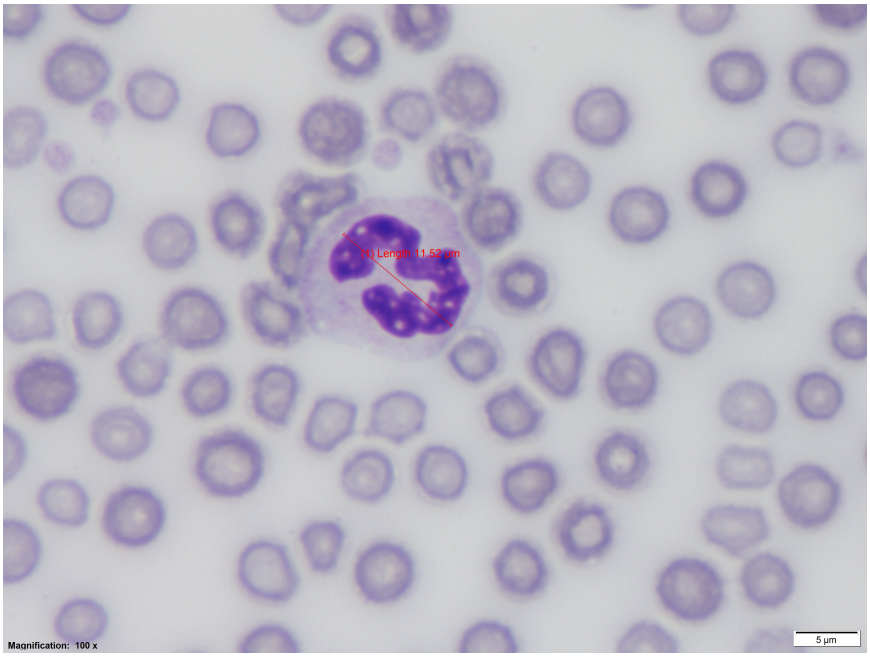

Figure 29: T-5 min plasma treatment

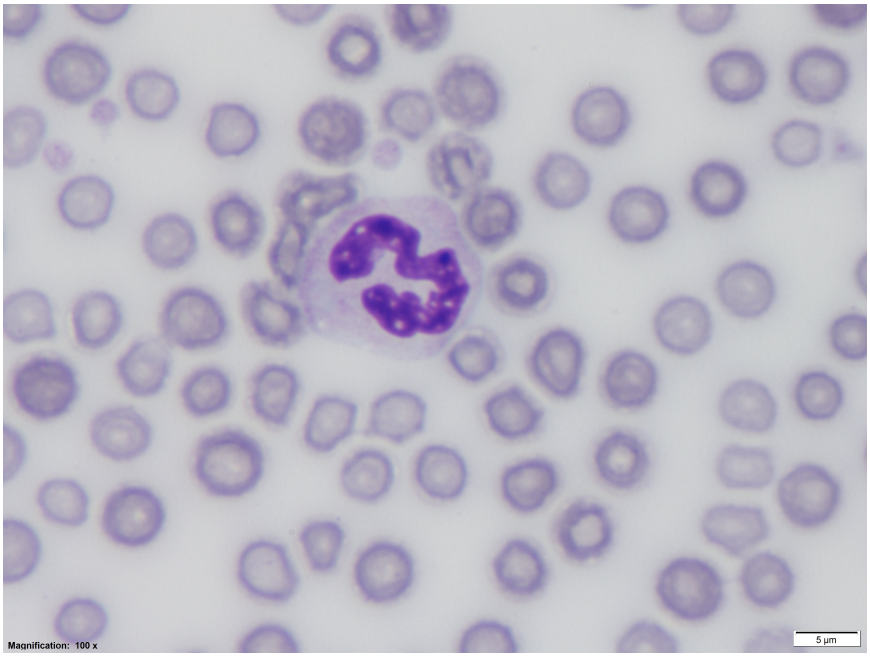

Figure 30: T-5 min plasma treatment

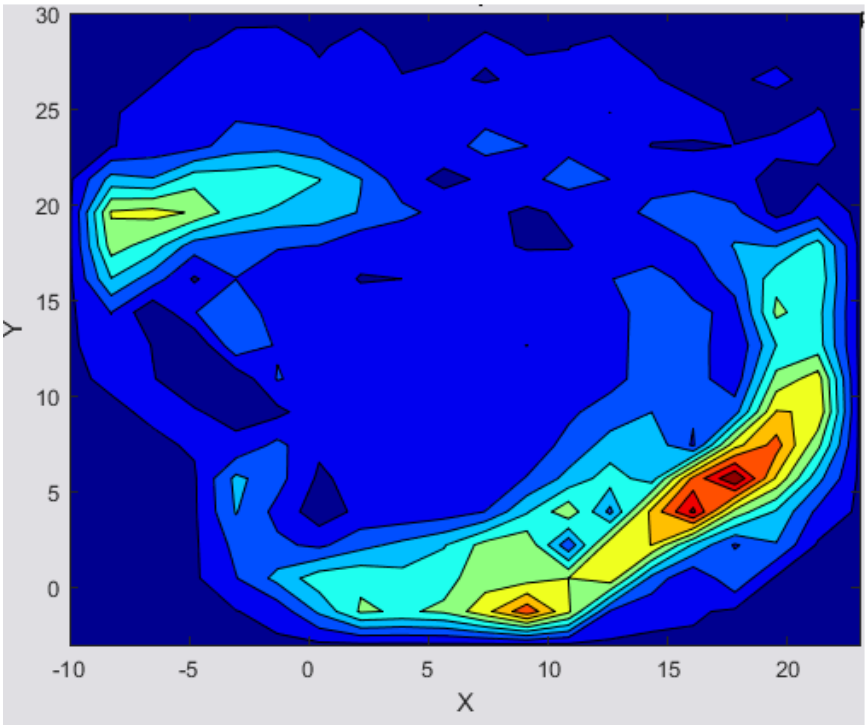

Figure 31: 1E FTLE Plot 20x20

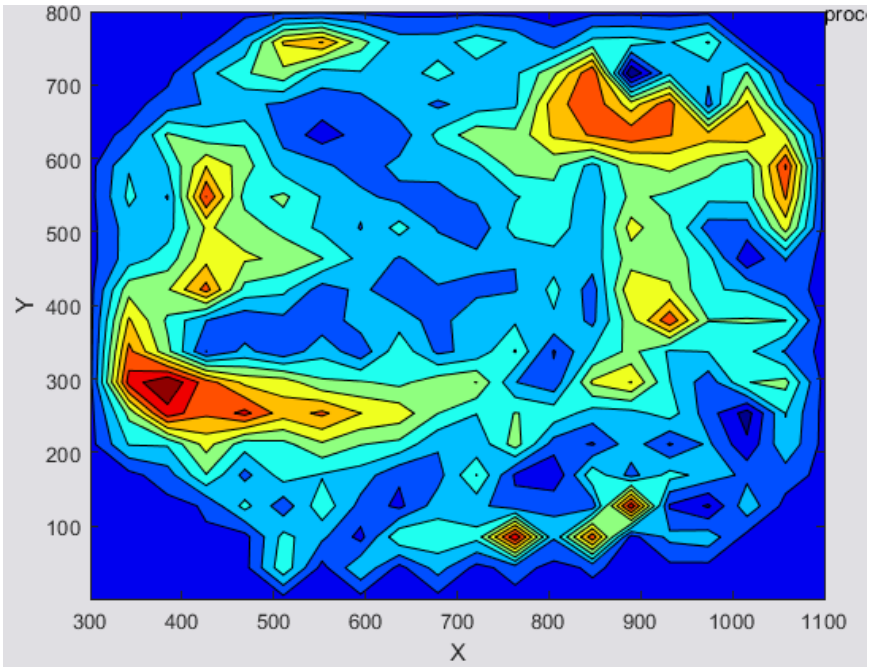

Figure 32: 1E FTLE Plot 20x20

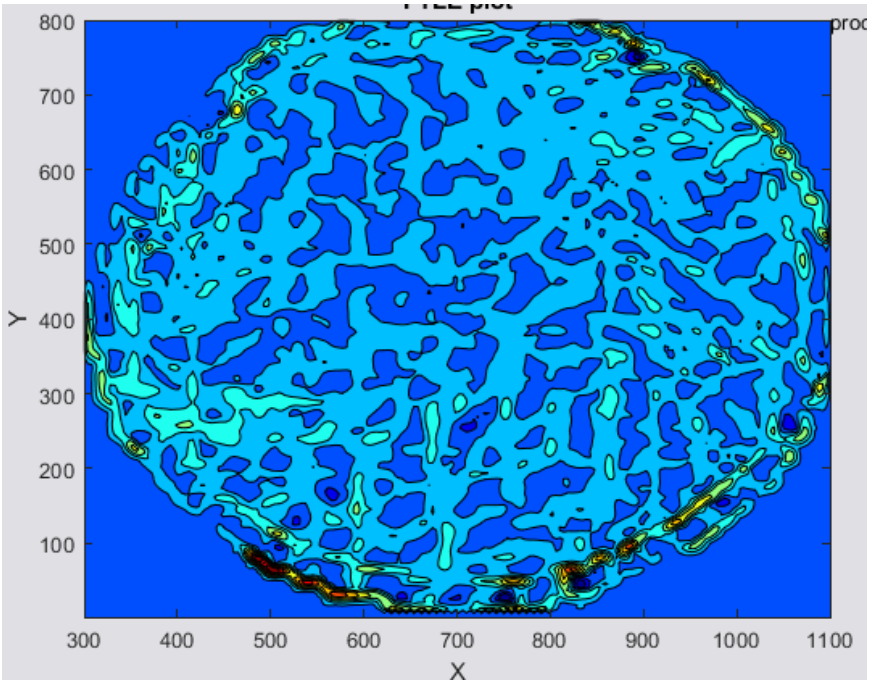

Figure 33: 1E FTLE Plot 200x200

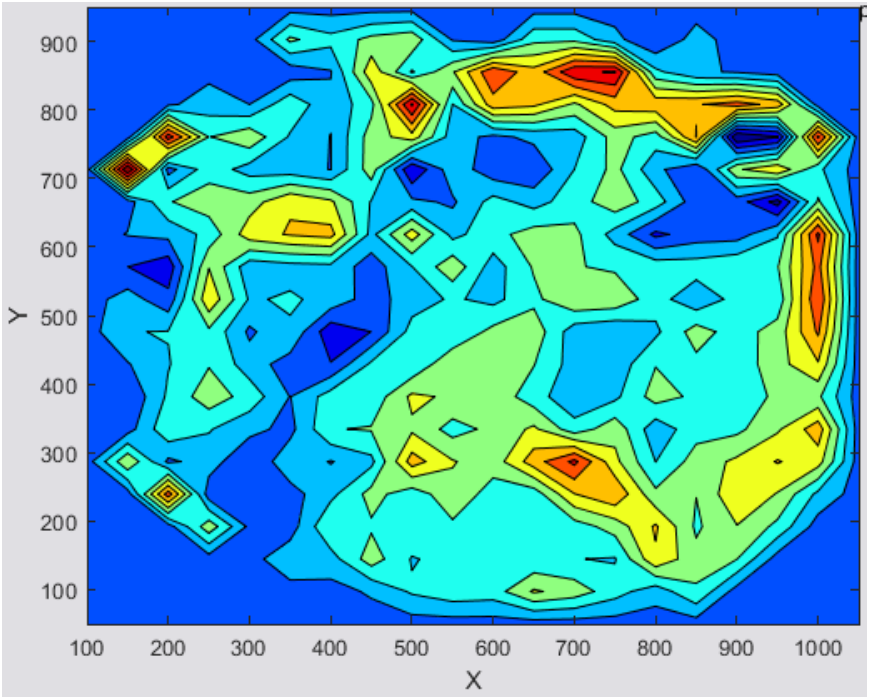

Figure 34: 2E FTLE Plot 20x20

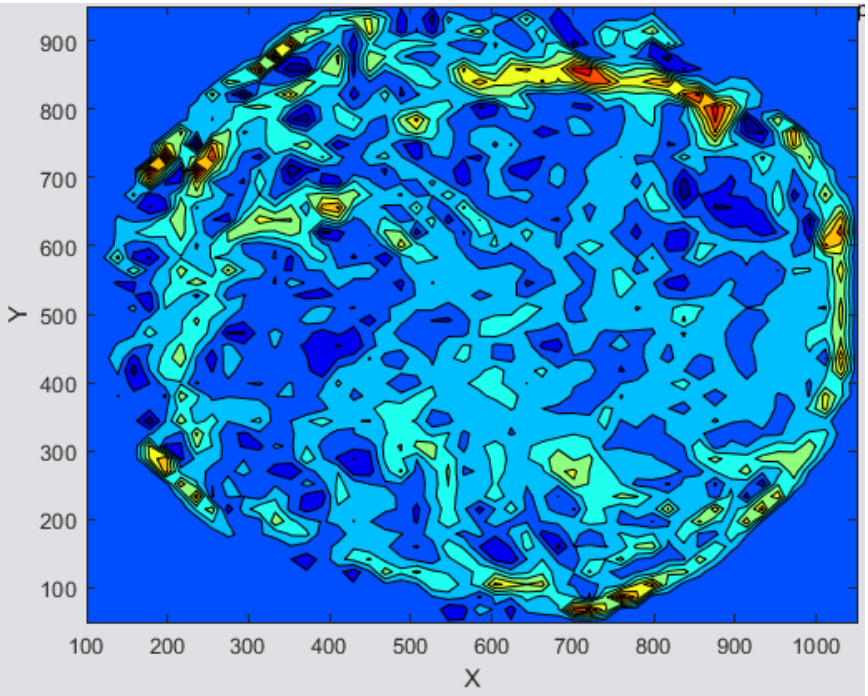

Figure 35: 2E FTLE Plot 50x50

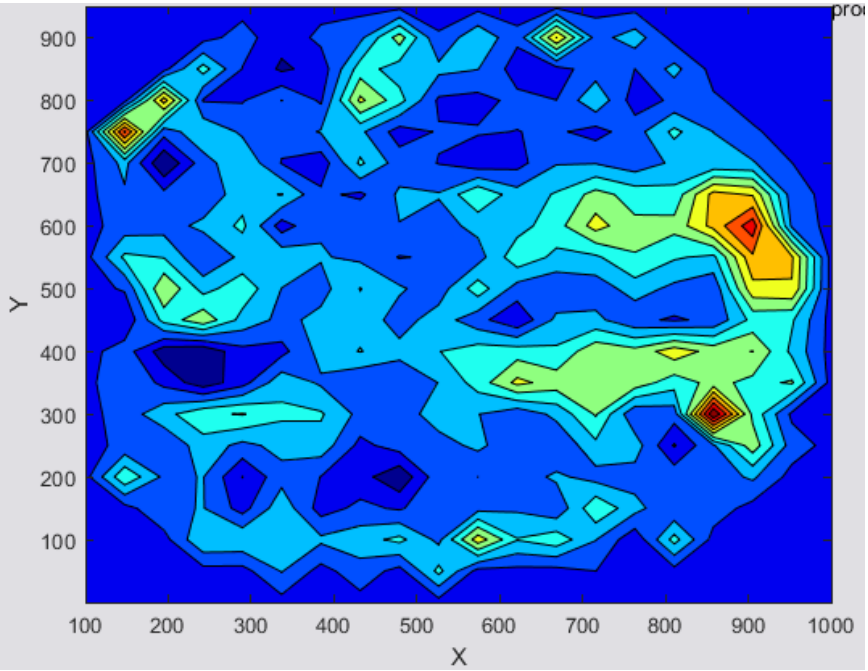

Figure 36: 3E FTLE Plot 20x20

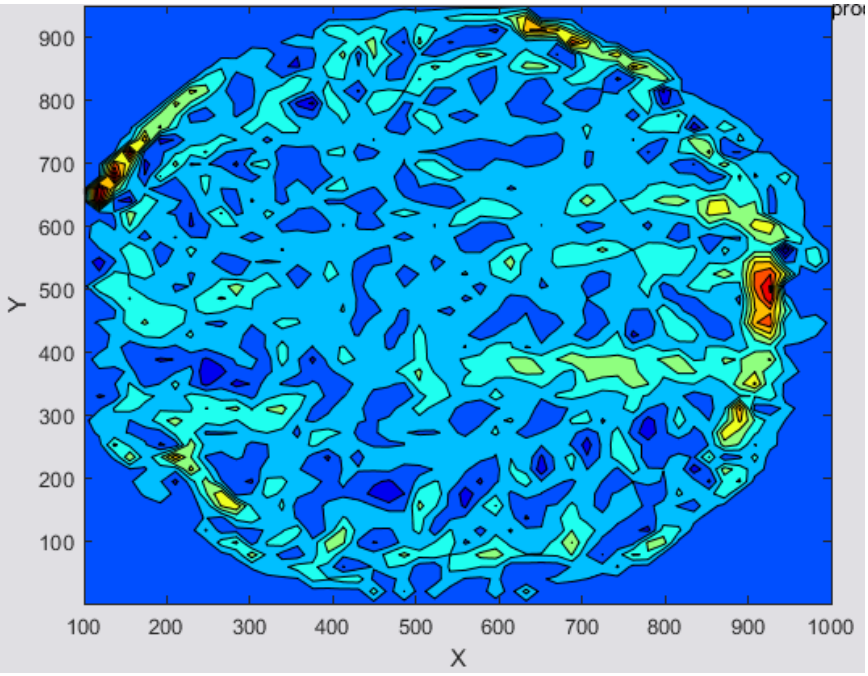

Figure 37: 3E FTLE Plot 50x50

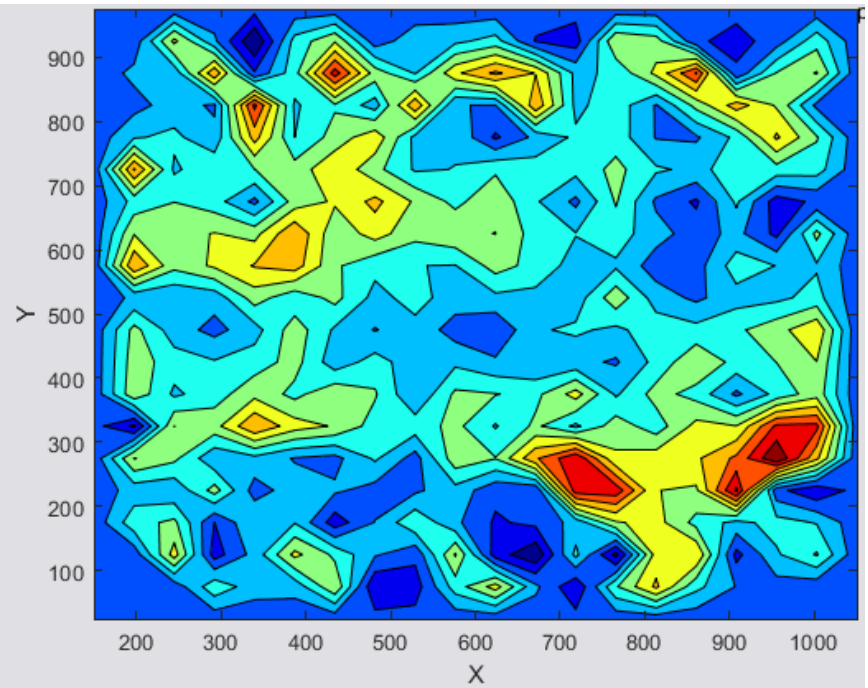

Figure 38: 6E FTLE Plot 20x20

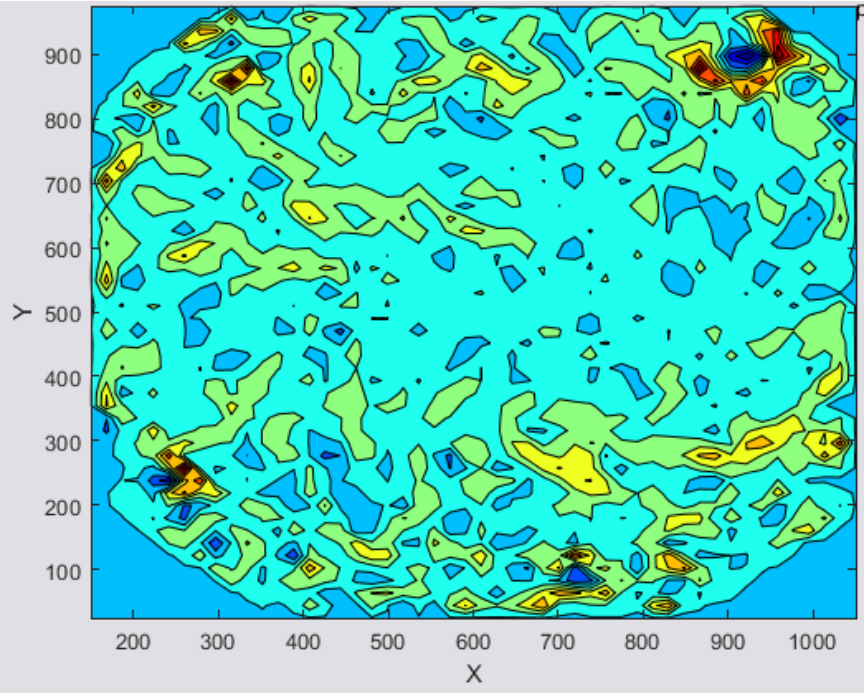

Figure 39: 6E FTLE Plot 50x50

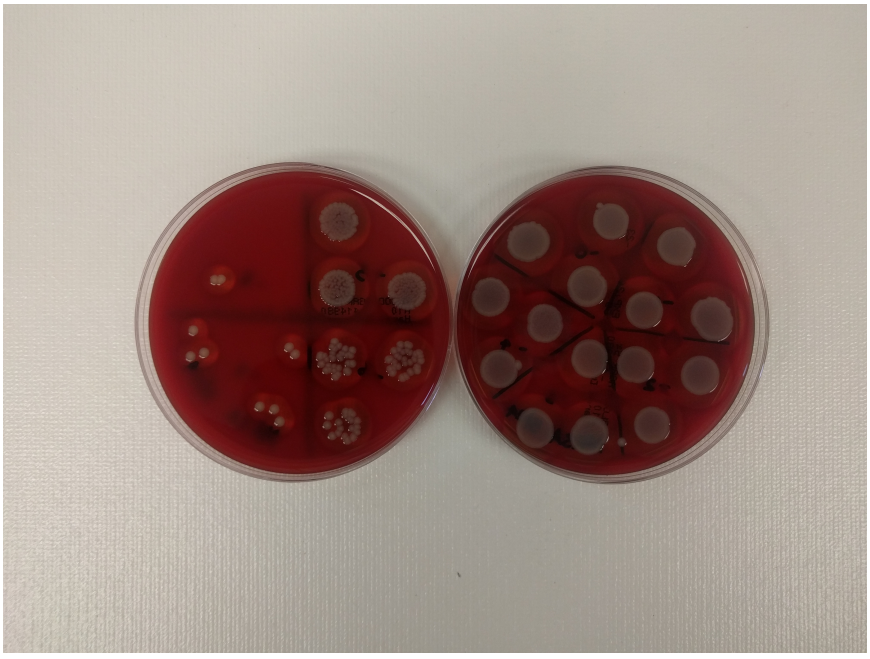

Figure 40: Base agar growth plate.

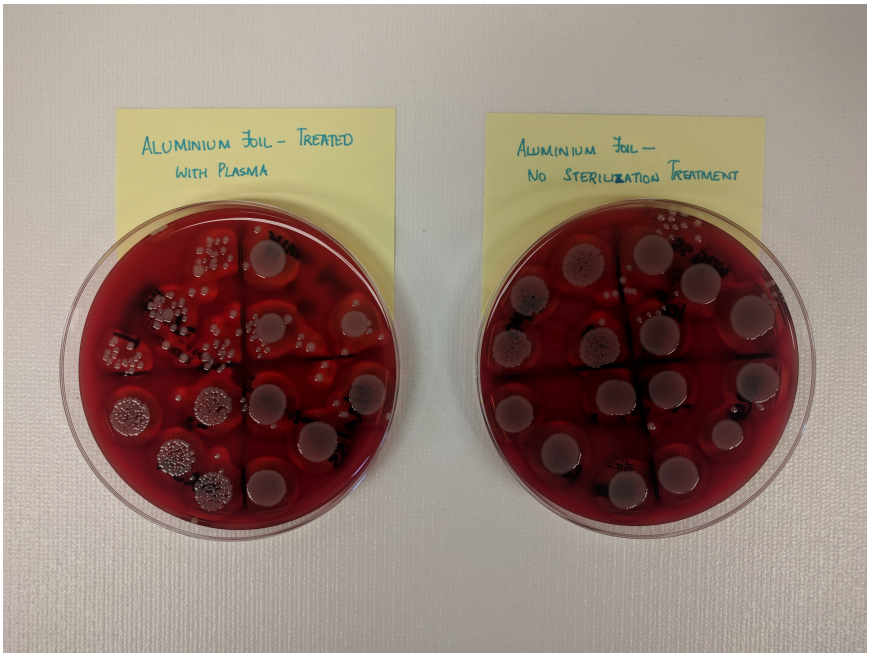

Figure 41: Aluminum foil treated and untreated.

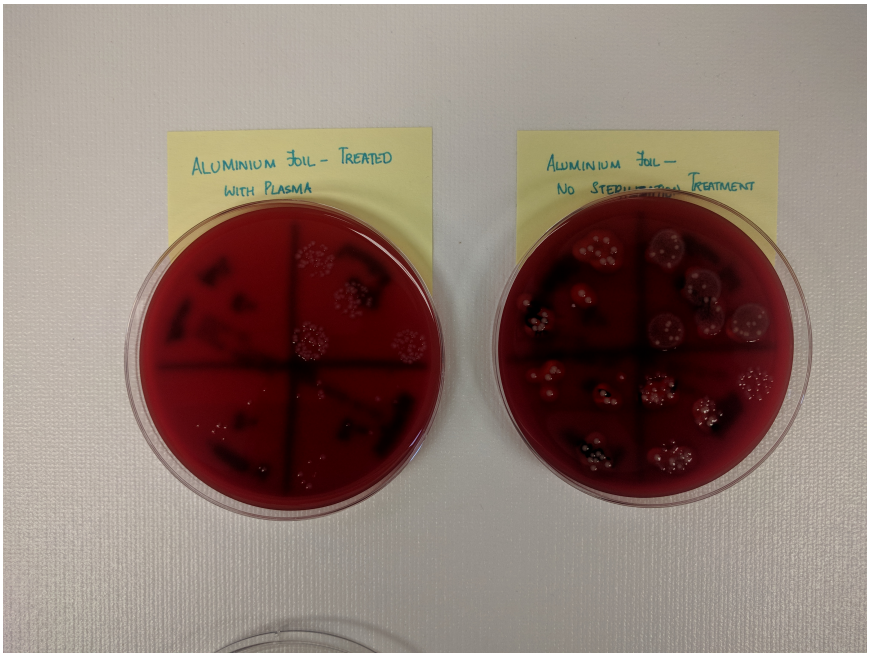

Figure 42: Aluminum foil treated and untreated.

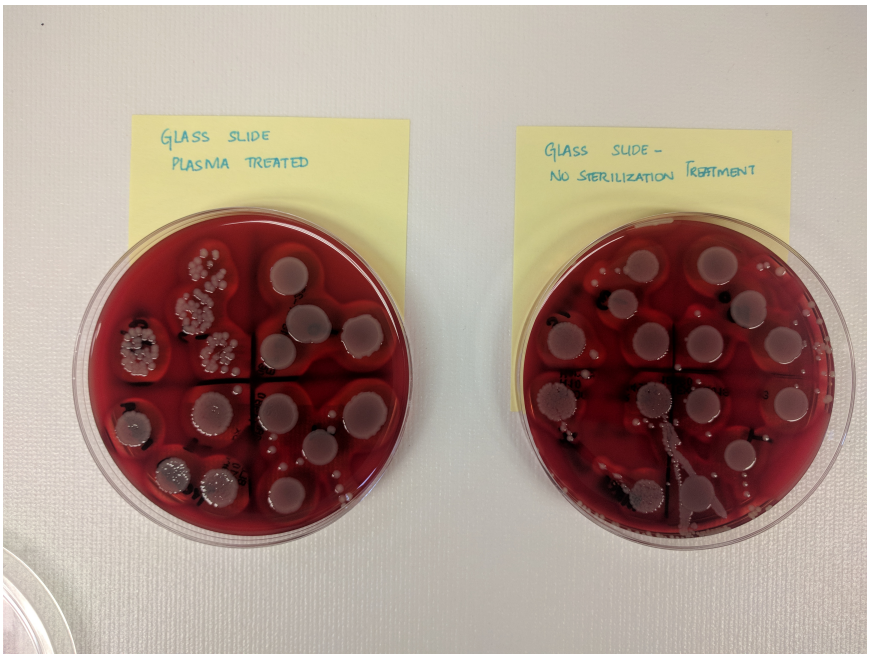

Figure 43: Glass slide treated and untreated.

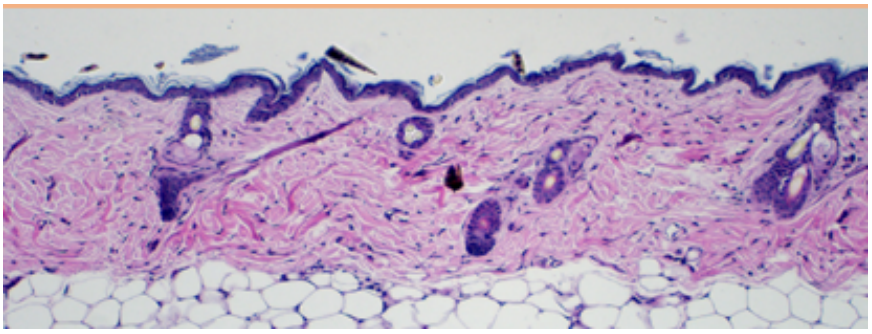

Figure 44: Albino mouse skin untreated.

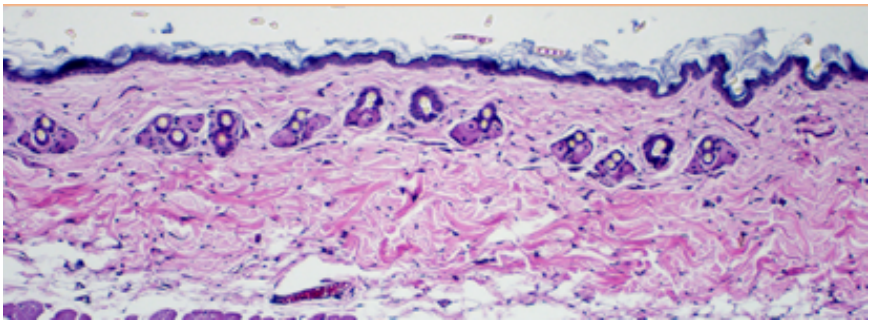

Figure 45: Albino mouse skin treated with plasma.

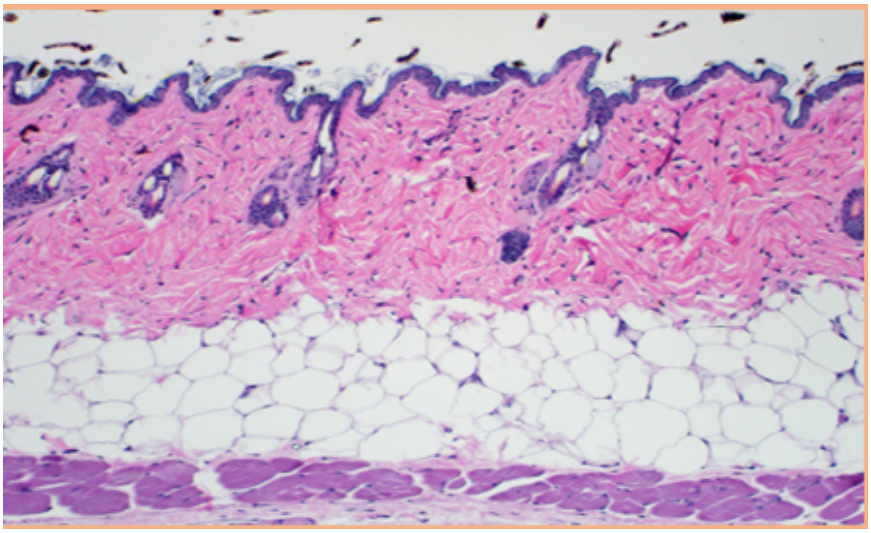

Figure 46: Black mouse skin untreated.

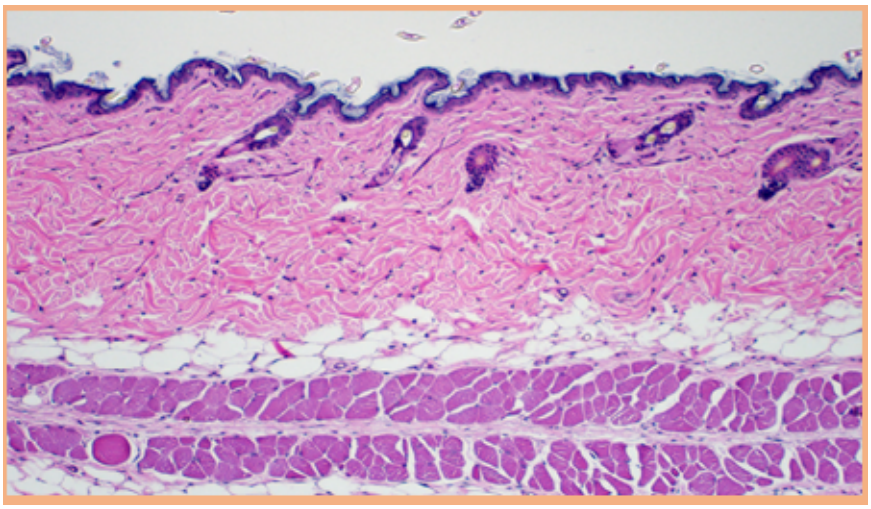

Figure 47: Black mouse skin treated with plasma.

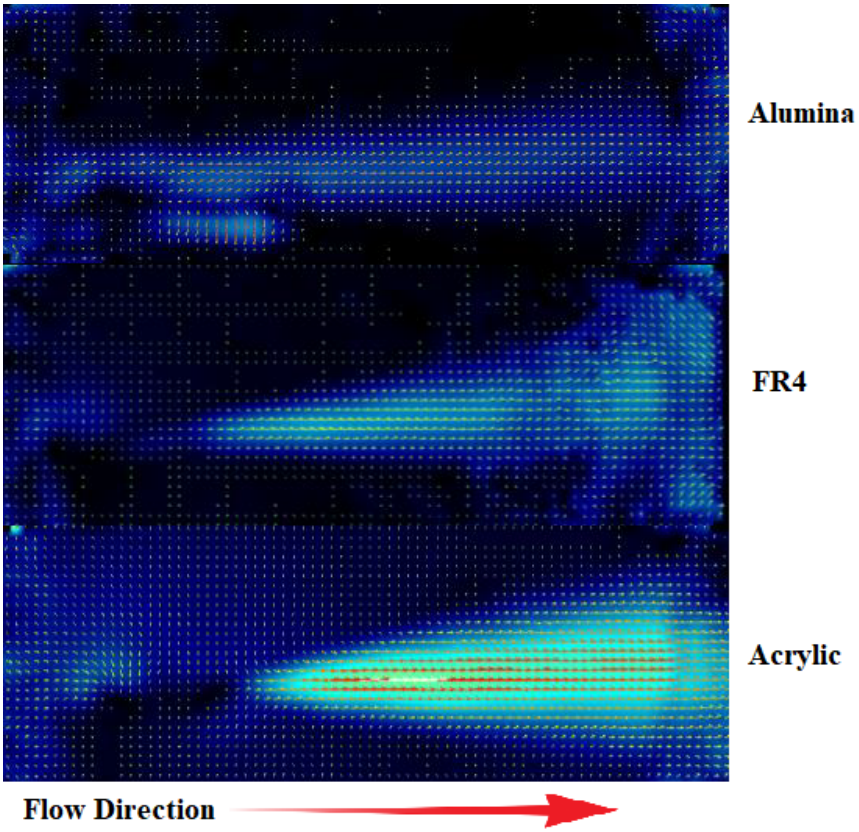

Figure 48: PIV flow visualization of different dielectric materials.

VITA

Alvin Dinh Ngo

Candidate for the Degree of

Doctor of Philosophy

Thesis: INVESTIGATION OF COLD ATMOSPHERIC PLASMA FOR WOUND CARE

Major Field: Mechanical and Aerospace Engineering

Biographical:

Education:
Completed the requirements for the Doctor of Philosophy in Mechanical and Aerospace Engineering at Oklahoma State University, Stillwater, Oklahoma in May, 2023.

Completed the requirements for the Master of Science in Mechanical and Aerospace Engineering at Oklahoma State University, Stillwater, Oklahoma in 2017.

Completed the requirements for the Bachelor of Science in Aerospace Engineering at University of Oklahoma, Norman, Oklahoma in 2015.

Experience:
- Internship: NASA Planetary Science Summer School (May 2022 – Aug 2022)
- Graduate Research Assistant, Oklahoma State University (Aug 2015 – Present)
    - Mechanical and Aerospace Engineering Department
- Graduate Teaching Associate, Oklahoma State University (Aug 2016 – Present)
    - Mechanical and Aerospace Engineering Department

Professional Membership:
- Sigma Gamma Tau
- Pi Tau Sigma
- American Institute of Aeronautics and Astronautics
- American Physical Society